1971

Optimum synthesis of three-dimensional structures

Richard Joseph Polo
Iowa State University

Optimum synthesis of three-dimensional structures

by

Richard Joseph Polo

A Dissertation Submitted to the

Graduate Faculty in Partial Fulfillment of

The Requirement for the Degree of

DOCTOR OF PHILOSOPHY

Major Subject: Structural Engineering

Approved:

Signature was redacted for privacy.

In Charge of Major Work

Signature was redacted for privacy.

Head of Major Department

Signature was redacted for privacy.

Dean of Graduate College

Iowa State University
Of Science and Technology
Ames, Iowa

1971

TABLE OF CONTENTS

LIST OF SYMBOLS USED

A, A_R	cross-sectional area of member, compression ring, respectively.
A, B, C	points in a structure or graph.
$\bar{F}_i$, F_i, F_R	force vector acting at point i, scalar magnitude of $\bar{F}_i$, force resultant in shell compression ring, respectively.
K_i	constant.
L_i, L_c, L_t	length of member i, of compression member, of tension member, respectively.
L_R, L_T, L_Z	projections of L in radial, tangential and vertical directions, respectively.
N_i	shell traction per unit length in direction i
N_H, N_V	components of N in horizontal and vertical directions, respectively.
P_i, P_S	load at point i, line load per unit length on a shell, respectively.
Q_i	force resultant of σ_i on face i of a differential element of volume.
R_i	radius of curvature of a shell in i direction.
S	shell traction constant in all directions.
S_H, S_V	horizontal and vertical components of S, respectively.
T, T_c, T_t	force in a member, in a compression member, in a tension member, respectively.
T_R, T_T, T_V	components of T in radial, tangential and vertical directions, respectively.
T_x, T_y, T_z	components of T in x, y and z directions, respectively.
$\bar{U}_a$	absolute potential energy.

V, V_T	volume, total volume, respectively.
V^u, V^b, V^t	volume of uniaxially, biaxially, triaxially stressed portions of a structure, respectively.
V_c, V_t	volume of compression, tensile stressed portions of a structure, respectively.
V_D, V_L, V_P, V_R, V_S	volume of dome, lattice, plate, ring, shell, respectively.
V_{S+P}, V_{S+R}	volume of shell-plate, shell-ring structure, respectively.
V_S^*, V_{S+R}^*	volume of shell optimized without considering, considering volume of tension ring, respectively.
$\bar{V}_e$, $\bar{V}_i$	work of external, internal forces, respectively.
W	load.
X_i, Y_i, Z_i	components of $\bar{F}_i$ in x, y and z directions respectively; components of reactions at point i in x, y and z directions respectively.
Z	load intensity per unit area acting perpendicular to middle surface of shell.
a, b_i	lengths of bar fields.
c	constant.
d	length.
$d\ell$	differential element of length along a meridian.
e	magnitude of a hypothetical dilatation.
f, f_c, f_t	allowable stress, allowable stress in compression, tension, respectively.
$g(\ )$, $h(\ )$	function of ( ).
i, j, k, m, n	indexing integers.
$k(\ )$	function of ( ).
k_m	Owen's statical constant $k_m = \sum \bar{F}_i . \bar{r}_i$.

p	intensity of load per horizontal unit area acting in a vertical direction.
$p(\ )$	function of ( ).
$\bar{r}_i$, r_i	position vector of point i, scalar magnitude of $\bar{r}_i$ respectively.
r, r_j	radius, radius at point j, respectively.
t, t_r	thickness of shell, thickness of shell when a function of r, respectively.
x, y, z	coordinates.
z, z_i	component of $\bar{r}_i$ in z direction, component of $\bar{r}_i$ in z direction evaluated at i, respectively.
α	angle.
α_i	dimensional variable (length, area, thickness).
β	angle.
γ	angle.
δ_i	deformation; deflection.
ε	a small number.
ζ_i	unsigned magnitude of σ_i.
θ	angle; coordinate angle.
λ_i	spacing of grid lines in i direction in a rectangular grid lattice.
σ_i	normal stress on i face in i direction.
σ_R	normal stress on cross-sectional area of shell compression ring.
τ_{ij}	shear stress on i face in j direction.
ϕ_i	angle; coordinate angle; tangent angle of a meridian.
Φ_i	angle ϕ evaluated at support point i.

CHAPTER ONE - INTRODUCTION AND LITERATURE SURVEY

General

The purpose of structural design is to develop a structure which will safely perform its intended functions at an acceptable cost. For structural purposes, these functions are ultimately expressed in terms of forces or loads which the structure must support. However, other considerations such as esthetics and cost may restrict the general form of acceptable structures.

Safety is assured by insisting that the structure should function without excessive deformations and that either 1) the stresses do not exceed a certain fraction of the ultimate strength of the material, or 2) the loads do not exceed a certain fraction of the ultimate loads for the structure.

The determination of what constitutes an acceptable cost varies greatly. Even the definitions of the terms by which the costs are to be assessed (such as monetary expenditure, construction effort, time required for construction, weight, volume, special materials or constructional techniques required, and possibly, operating expenditures) are likely to vary from time to time for each location, and for structures of different purposes.

The process of arriving at a simultaneous statement of the form of the structure and the loads to be supported is more of an art than a science on account of their mutual influence. Little has been written about this process. Torroja (39) has written what is probably one of the finest philosophical expositions of the process. Otto (23) has gone

deeper into a discussion of the very reasons which motivate man to build.

After the general form of the structure and the loads are defined, the design process is still complex and requires great experience as the loads are still affected by variations in the design. Finally, experience is also required in judging the structure and its costs as acceptable.

Optimum structural design techniques assist the designer by allowing him to determine directly the form of the structure that will support the loads with the minimum cost. Such knowledge, when available, is invaluable in deciding if the additional cost of alternative designs is warranted in view of their additional features.

The purpose of this dissertation is to explore the conditions under which three-dimensional structures achieve their least volume, and culminate in the development of methods suitable for the structural optimization synthesis of nonplanar latticed roof structures.

It is necessary, for proper development of the theory, to contrast conventional structural design and optimum structural design procedures, and to review at some length certain concepts to be used later.

Conventional Structural Design

As opposed to the elusiveness of the art of design as discussed above, the analysis of structures (and stress analysis of structural components) has been developed into a science. There is a considerable body of knowledge available, expressible in useful mathematical equations, in the theory of structural analysis. These mathematical tools allow the structural analyst to determine uniquely and with acceptable accuracy the stresses and the deformations of the structures he analyzes.

It is not surprising then, in view of the mathematical tools available for analysis, that structural design has traditionally been an iterative process where: 1) the geometry of the structure is assumed on the basis of an informed guess and the loads determined, 2) the structure is analyzed, and then, 3) the geometry is modified on the basis of the results of the analysis. This process continues until the structure is deemed to be of an acceptable cost not worthy of further refinement.

The structure resulting from the above process is only as economical as the informed guesses have been. It is almost certainly not the most economical of all possible alternatives.

There is no intent here to slight the great accomplishments of structural designers. The informed guessing is based on the experience of the entire human race. Otto (23) considered this constructional experience as a component of the evolution of man. In addition, he reported that since nature provides, in some organic structure, examples of structural forms of the greatest known efficiencies, these forms are now being studied for possible application in structural design. Prager (27) also commented that the human femur shows a trajectorial system remarkably similar to a pattern developed by using minimum weight optimization techniques. In the past, designers have undoubtedly been using such conscious or unconscious observations of nature to guide their informed guessing.

Still, in the conventional design by iterative process, it is only the designer's experience and that of his predecessors which form the basis for his deciding whether the final structural cost is acceptable.

Optimum Structural Design

In contrast to conventional structural design, optimum structural design methods leave the geometry of the structure as variable (within a class of structures) and formulate the problem in terms of the desired structural behavioral constraints (stresses, buckling, and deformations). There will be a range of possible geometrical solutions that satisfy the constraints. An optimization technique is then used, usually with the objective of minimizing a certain cost, to select the optimum geometry among those possible.

In classical optimum structural design procedures, the behavioral constraints are satisfied only one at a time. Thus, the optimum structural design procedures can be classified, according to Barnett (2), into 1) Strength Designs (elastic or plastic), 2) Stability Designs and 3) Stiffness Designs. He also pointed out that no analytical solution appears feasible for the simultaneous satisfaction of all three kinds of constraints since the problem becomes extremely complex. In addition, it should be noted that analytical methods are used to optimize the structural form only with respect to a single system of loads. The system may consist of a multiplicity of loads, but all must be simultaneously applied.

Stability designs

Stability designs are based on the concept that, if the structural elements to be designed are subject to buckling, then the minimum weight (cost) is obtained when the elements are so proportioned that all the possible buckling modes occur simultaneously. This is a very powerful method

amenable to straight forward solutions for the conditions postulated. For an example, see Gerard (14). The stability design method, however, is not likely to yield an absolute minimum. The very fact that the elements are subject to buckling failure, may in itself indicate that the problem has been too narrowly defined and that some configurational modification, if permissible, may result in a design not limited by buckling and with lesser weight (cost).

Stiffness designs

Stiffness design methods are, as their name implies, particularly well suited when the requirement is to design a structure with one or more deflection limits. These methods are most useful in developing the material properties to be considered in choosing the best material among those available. If the deflections in question are proportional to the loads being considered, then stiffness designs are identically the same as those resulting from strength design methods (Barnett (2)). This is logical and to be expected since, as shown by Cox (10), strength designs provide the least deflection possible under the given loads.

Strength designs

Strength design methods are based on the philosophy that the lightest structure will be one in which all the structural elements are stressed to their maximum allowable values (Barnett (2)). That such is the case for statically determinate structures can be easily verified. It is not so readily apparent that this should be so for statically indeterminate structures optimized with respect to a single system of loads. It

is felt that the difficulty in showing that the optimum is a fully stressed design (even for hyperstatic structures) resides in that the geometry of the structure is usually given in terms of its unloaded configuration. Consequently, the requirements of compatibility of deformations unnecessarily complicate and obscure the optimization process. It has been shown that in many cases the optimization process reduces a hyperstatic structure to a static one as the redundant members vanish (Cox (10)). In other cases, it has been shown that it is possible to replace static structures with statically equivalent hyperstatic structures, also fully stressed, of the same but not lesser volume (cost) (Prager (27)). It is hoped that the theorem to be developed in this dissertation will shed some light on this point.

In plastic strength design, the optimum structure is achieved when designed to be just at the point of collapse, through a continuous collapse mode such that the dissipation of energy per unit volume is constant throughout the entire structure (Barnett(2)).

Numerical solutions

No review of structural optimization methods would be complete without discussing at some length the numerical procedures that have become possible with the advent of computers.

Any structural design problem can be formulated as a generalized optimization problem in which a certain objective function is to be optimized subject to a certain set of constraints. Because of the nature of the constraint equations, structural optimization problems are usually nonlinear. Therefore, the development of suitable structural optimization methods has

closely followed the development of nonlinear programming methods in operations research. Conceptually, each constraint equation describes a surface in an N-dimensional space that corresponds to the N parameters to be varied. The global optimum occurs where the surface described by the objective function has its minimum (maximum) value and just touches (or is tangent to) the surface of the solid bounded by all the constraint surfaces. Schmit and Kicher (31) applied this concept to the structural optimization problem. Their formulation is general enough to be applicable to structures subject to multiple systems of loads and to the use of different materials.

Since linear programming problems are readily solved, many structural optimization methods seek to linearize the constraint equations. Anderheggen and Thurlimann (1) linearized the constraints in the optimization of a skew highway bridge, continuous over several spans, by expressing them in terms of the moment at each section rather than in terms of the stresses as is more often done, and by assuming the cost to be proportional to the resistance required of each member. Moses (21), amd Romstad and Wang (28) linearized the constraints by approximating each parameter by a single term of its Taylor series expansion. This has also been called the "cutting plane method".

Another approach to deal with the nonlinear programming problem has been to develop certain algorithms for directed iterative search procedures in the feasible space, and for accelerating the convergence of such procedures. Among the algorithms used are the alternate steps method of Schmit and Kicher (31), the gradient projection method used by Brown and Ang (6), and the steepest descent and side-step procedure of Dobbs and

Felton (12). Crockett (11) used a sequential unconstrained minimization technique, developed by Fiacco and McCormick (13), which combines the constraint equations with the objective function to generate a new function. A computer program for the solution of the general nonlinear programming problem, based on the same technique, has been written by Sposito and Soults (35).

Distinct advantages of numerical optimization procedures are that they permit the satisfaction of the three constraints (strength, stability, stiffness) simultaneously, as well as the optimization of a structure with respect to multiple systems of loads. Using these methods, Schmit (30), Kicher (16), and Romstad and Wang (28), proved that the optimum structure for multiple systems of loads need not be fully stressed. Soosaar and Cornell (34) used numerical methods to optimize, topologically as well as geometrically, multistorey buildings for minimum monetary cost. The sensitivity of the results to changes of material-to-fixed-cost ratios is also investigated therein.

Two difficulties exist with numerical optimization procedures. First, there is often a loss of grasp of what is happening in the optimization process. Thus, the designer is apt to feel ill at ease as he no longer has a clear "feel" for the way in which changes in design parameters affect the behavior or the cost of the structure. (The sensitivity analysis of Soosaar and Cornell mentioned above is an attempt to restore this "feeling", while Kicher (16) advocates the use of Lagrangian multipliers so that the designer can at least know which constraint or constraints are operative at the optimum solution.) Secondly, because of the nature of the

constraint equations, it is not possible, in most practical cases, to provide clear proof that the optimum found is a global optimum and not merely a local optimum. The most usual way to provide some assurance that the global minimum has been found is to start the optimization process at different points in the feasible space and verify that subsequent trials either, converge to the solution already considered to be the global optimum, or else, to other local optima no better than the global.

A limitation of numerical optimization techniques is that the structural form whose geometry is to be optimized must be very explicitly defined. The optimum found will apply only within that class, and there may be no indication that an acceptable change in structural class may result in large changes in the value of the optimization objective function. To guard against the possibility of excluding from consideration a particularly efficient class of structures, it is best to define the class as broadly as possible. This requires an increase in the number of variables. Consequently, the complexity of the problem and the computational demands grow rapidly, while the assurance of having found a global optimum decreases.

Optimization objective

While it is obvious that the functional requirements of a structure should not be compromised in optimization, surely no designer will insist that there is no range of variations possible in meeting the needs. Nor will he insist that the fulfillment of the needs, and even the beauty of the structure is completely unrelated to its structural concept or its efficiency. Torroja (39) commented that a properly designed structure

should convey the feeling that the loads are supported in a clear, uncomplicated manner and "without discomforts". Although he pointed out that the most beautiful structure is not necessarily the most efficient structurally, he did say:

> "There are exceptional cases, but in general it can be stated that in any given circumstances, the condition of the least cost or the greatest economy should always be observed and respected." (Torroja (39)).

Even if the least cost structure is not to be selected, it would be desirable to know what its form is and what its cost is. This information serves as a standard in judging the cost to be paid in deviating from the least cost form.

In this dissertation, the quantity of material will be the sole criterion by which relative structural merit will be judged. Volume will be the measure of the quantity thereby eliminating the need to consider material properties. If least weight rather than least volume is desired as an optimization objective, it is a simple matter to modify the basic equations by making use of the material properties. The use of least volume as the optimization objective is consistent with usual objectives in strength design methods, and there are a number of reasons which justify it.

Other measures of efficiency or cost, such as monetary expenditure, although important, are likely to change. Otto (23) pointed out that costs are likely to be higher for new structural systems through lack of experience in the design and construction techniques and in estimating. He stated that consequently, total energy consumption (material, man-hours, erection time, maintenance, etc.) is a better yardstick since in

the long run the structure requiring the lesser energy expenditure will probably be more economical. He also considered lighter structures preferable as being more adaptable, with structures thought of as massless being the ideal. Smith and Wilson (32) pointed out that large, massive structures usually imply high cost, and that in some cases such as dams the quantity of material is the critical factor in determining the economic cost. Cox (10) stated that least weight is the obvious criterion there being no point in using more material than is required, and since normally other costs follow weight when even the operating cost is usually less for lighter structures. In some structures, such as aerospace structures, the weight may in fact be the critical factor.

Conceptual Review of Strength Optimization Design

This dissertation will develop a theory that is more closely related to strength design methods. It is thus necessary to review some concepts and theorems of strength design methods to be referred to later.

Galileo's studies

It is generally accepted that the theory of elasticity had its origin with the studies of Galileo, in 1638, into the configuration of beams of constant strength (Barnett (2), Wasiutynski and Brandt (40)). Thus, the conceptual basis of strength design optimization methods is as old as the theory of elasticity itself, and as old as

> "... the notion of force and the laws of mechanics as a foundation for designing structures." (Wasiutynski and Brandt (40)).

Maxwell's theorem

In 1869, Maxwell (19) developed from statics (and also through the use of a hypothetical dilatation of space) what has come to be known as Maxwell's theorem, applicable to framed structures. Mathematically, and in the notation used in this dissertation, the theorem can be expressed as follows:

$$\sum_t T_t L_t - \sum_c T_c L_c = \sum_i \bar{F}_i . \bar{r}_i \qquad (1.1)$$

where T_c and T_t are the numerical values of the forces in typical compression and tension members, respectively; L_c and L_t are the lengths of such members; $\bar{F}_i$ is a typical external force vector (reaction inclusive) acting on the structure at point i; and $\bar{r}_i$ is the position vector of the point i with respect to an arbitrary origin.

If each strut or tie is proportioned so that it is stressed to its allowable limit f_c or f_t, then considering that in general, if A is the area of the member,

$$T = fA ,$$

equation 1.1 can be written as

$$f_t V_t - f_c V_c = \sum \bar{F}_i . \bar{r}_i \qquad (1.2)$$

where V_c and V_t are the total volumes of all the compression members and all the tension members, respectively.

The significance of Maxwell's theorem, and, in particular, of the ensuing equation 1.2 has been amply discussed by Owen (25). Noting that the total volume of a structure, V_T, is

$$V_T = V_t + V_c , \qquad (1.3)$$

use of equation 1.2 can be made to express V_T as follows,

$$\left.\begin{aligned} V_T &= V_c\ (1 + f_c/f_t) + k_m/f_t\ , \\ \text{or,}\quad V_T &= V_t\ (1 + f_t/f_c) - k_m/f_c \end{aligned}\right\} \qquad (1.4)$$

where, following Owen's notation, k_m is used to denote $\sum \bar{F}_i . \bar{r}_i$. Since the volume cannot be negative, equations 1.4 indicate that, if k_m is positive, the minimum volume structure will be one with no compression members, i.e. $V_c = 0$, if this is geometrically possible. Then $V_t \equiv V_T = k_m/f_t$. Conversely, when k_m is negative the minimum volume structure would be an all compressive structure, if this is possible. When k_m is zero, equation 1.2 indicates that an all tension or all compression structure is not possible. In such a case,

$f_c V_c = f_t V_t$, and, if $f_c = f_t$, $V_c = V_t$.

Thus, when k_m (or $\sum \bar{F}_i . \bar{r}_i$) is zero, Maxwell's theorem does not help in determining V_T of the least volume structure.

Michell structures

In 1904, Michell (20), recognizing the limitations of Maxwell's theorem, developed the conditions to be fulfilled for the volume of a tension-compression framework to be a minimum. Equations 1.2 and 1.3 can be used to yield the expression

$$2f_t f_c V_T = (f_c + f_t)\{f_t V_t + f_c V_c\} + (f_c - f_t) \sum \bar{F}_i . \bar{r}_i \qquad (1.5)$$

Michell noted that, for any given value of $\sum \bar{F}_i . \bar{r}_i$, the minimum total volume, V_T, will be obtained by insisting that the quantity within the

brackets be a minimum. Thus, since $fV = \sum TL$,

$$V_{T_{min}} \Rightarrow \{\sum T_t L_t + \sum T_c L_c\}|_{min} \tag{1.6}$$

To develop the conditions that must be fulfilled by a structure for its volume to be a minimum, Michell then postulated a virtual deformation of the domain occupied by the structure such that, while the supports are not displaced, the domain is dilated by +e along tension members and by -e (a contraction) along compression members. Furthermore, he postulated that nowhere in the domain is the dilatation greater than +e or less than -e. By computing the change in strain energy under such a virtual deformation, Michell proved that, if the structure is such that it can be subjected to a deformation as described above, then no other statically equivalent structure can have a lesser volume, provided, of course, that all members are fully stressed.

It is obvious then, that in a Michell structure, the members must lie along lines of principal strains ±e in the virtual deformation strain field. Compression members must be orthogonal to tension members. Members carrying stresses of the same sign may meet at any angle since the deformation in that portion of the domain is then an isotropic expansion or contraction.

Michell considered the structures resulting from the application of Maxwell's theorem as special cases wherein the geometry of the loads is such that all compression or all tension structures are possible and thus the Michell strain field is then an isotropic expansion or contraction.

Some examples of Maxwell structures are shown in Fig. 1.1 and of Michell structures in Fig. 1.2.

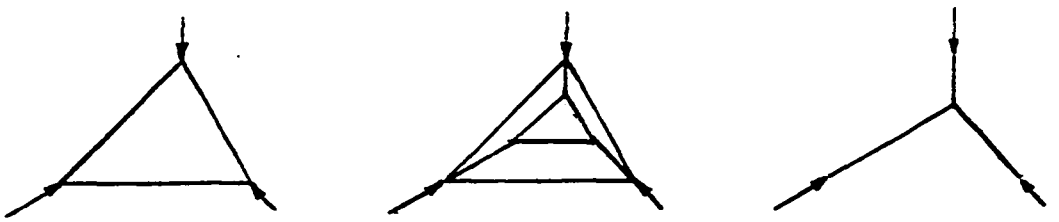

a. Static. b. Hyperstatic. c. Mechanism.

Fig. 1.1. Maxwell structures of equal volume.

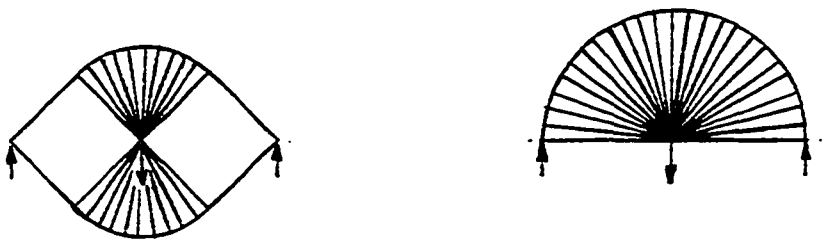

a. Least volume for central load.

b. Structure restricted to lie entirely above supports.

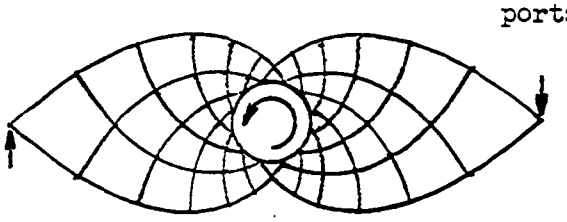

c. Cantilevers.

Fig. 1.2. Michell structures.

Cox (10) has made a detailed study of Michell strain fields and concluded that they can all be generated by a single kernel, and, that it is very probable that no Michell strain fields exist in three-dimensional space.

Templeman's note

In 1966, Templeman (36) suggested that the lower limits on the volume of Maxwell/Michell structures holds only in the case of structures made up of uniaxially stressed members. If the structure can be made of a combination of uniaxially stressed members and of sheets stressed biaxially by stresses of like sign, and, if maximum shear is the criterion of failure, then, according to Templeman,

$$V_T = \frac{1}{f} \sum \bar{F}_i . \bar{r}_i - V^b \tag{1.7}$$

where V^b is the volume of the amount of material stressed biaxially. Templeman pointed out that this is true, from a philosophical point of view, because the biaxially stressed material is now being utilized twice. He demonstrated that it is feasible, in some cases, to add loads to a structure (accepting a change in $\sum \bar{F}_i . \bar{r}_i$) to make possible the use of biaxially loaded sheets and thereby reduce the volume of the original structure. He concludes that, potentially,,

$$V_T \equiv V_T^b = \frac{1}{2f} \sum \bar{F}_i . \bar{r}_i \tag{1.8}$$

in a fully biaxially loaded structure, and, potentially,

$$V_T \equiv V_T^t = \frac{1}{3f} \sum \bar{F}_i . \bar{r}_i \tag{1.9}$$

in a fully triaxially loaded structure.

Scope of the Dissertation

This dissertation will include:

1. the derivation of a new unifying theorem for three-dimensional bodies (the generalized counterpart of Maxwell's theorem for frameworks) which underlies and links the observations of Maxwell and Templeman, and from which it is possible to deduce the conditions for least volume structures with respect to a single system of loads (chapter two),
2. the detailed development of methods suitable for the optimum structural synthesis of nonplanar lattice type structures, and the development of general methods for the optimum structural synthesis of shells with suggestions of the lines along which detailed procedures could be developed (chapter three),
3. the presentation of several examples which illustrate the applicability of the methods, namely, the optimum structural synthesis of rectangular grid lattices, of network domes, of Schwedler-like domes, and of a paraboloidal shell, with and without tension rings (chapter four), and
4. the presentation of a sequence of alternate structures synthesized for the support of the same loads to illustrate the relationship between uniaxially stressed and biaxially stressed structures and the transitions between them (chapter five).

CHAPTER TWO - THEORETICAL DEVELOPMENT

Theorem of Zero Absolute Potential Energy

Mathematical derivation

Let a generalized, three-dimensional structure be subjected to a single system of loads, F_i, which is in external static equilibrium. See Fig. 2.1. A small differential element of volume of size dx, dy and dz can be depicted in a generalized state of stress as shown in Fig. 2.2.

Let the structure be replaced by an equivalent system of molecules, each concentrated at the center point of the corresponding differential element of volume. For the system of points to be statically equivalent to the original structure, each point will be considered to be held fixed in space by forces of attraction or repulsion between it and the adjacent points. Such forces will be equal to the resultant of the normal stress acting on the face (of the differential element of volume) that separates the two points. Thus, if Q_x is the force in the x direction,

$$Q_x = \sigma_x \, dy \, dz \tag{2.1}$$

Similar relations apply to the other faces and normal stresses. In addition, each point or molecule is acted upon by three twisting couples, each equal in magnitude to the resultant of the shear stresses acting on opposite faces multiplied by their separation distance.

Assume now that the space occupied by the equivalent system of points undergoes an imaginary dilatation of magnitude e which is constant in all directions. Assume further that all forces in the system remain constant throughout the dilatation. Because the dilatation is constant in all directions, the structure and all its parts are not distorted and remain

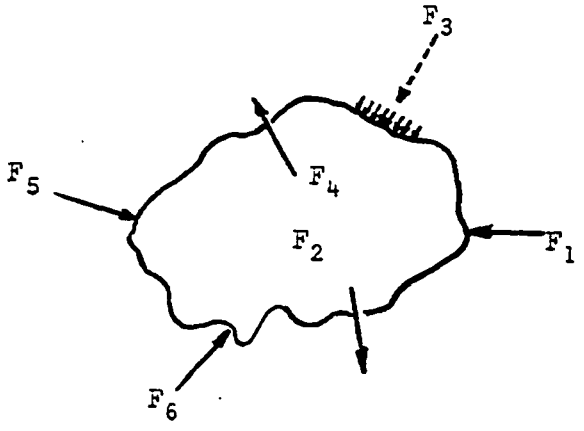

Fig. 2.1. Generalized structure.

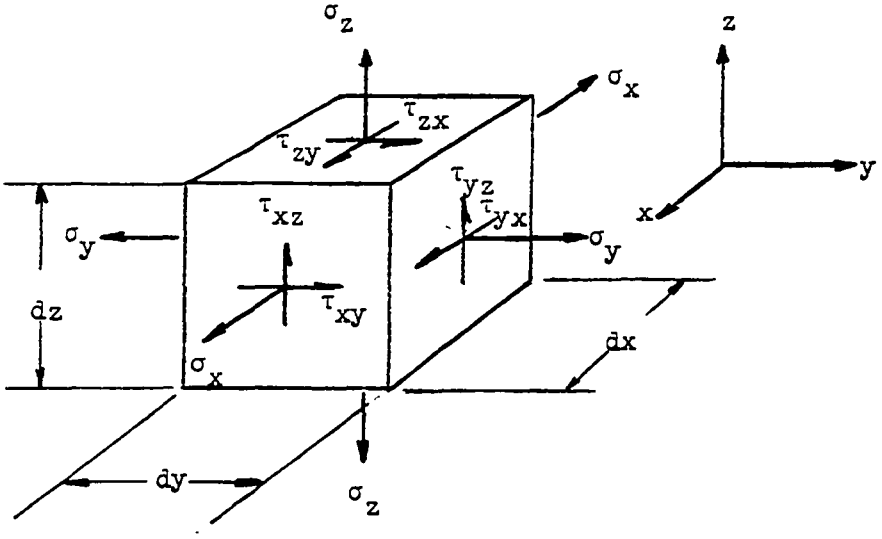

Fig. 2.2. Differential element.

always similar to their original configuration, having changed only in size. Since the forces remain of constant magnitude, and their relative orientations remain unchanged by the dilatation, the statical equilibrium of the external system of forces is not disturbed. Similarly, the internal equilibrium of all the points is not disturbed, and the forces acting on all the molecules remain constant. Only the relative distances between the molecules are changed.

If the dilatation is assumed to have occurred adiabatically so that no energy enters or leaves the system, then the internal work done by the forces acting between the points plus the work done by the external force system, F_i, during the dilatation must be equal to zero.

In computing the work done by the internal system of forces the couples need not be considered because the relative orientation of each point with respect to the others is not disturbed and therefore the couples do no work. Noting that the original distances between the points are dx, dy and dz, the center to center distances of the elements, the differential element of work, $d\bar{V}_i$, done by the forces between the points is

$$d\bar{V}_i = -(Q_x \, e \, dx + Q_y \, e \, dy + Q_z \, e \, dz). \qquad (2.2)$$

where Q_x, Q_y and Q_z are assumed to be positive if tensile, and e is assumed to be positive if causing expansion of the space. Using expressions similar to expression 2.1, equation 2.2 becomes

$$d\bar{V}_i = -e(\sigma_x + \sigma_y + \sigma_z) \, dx \, dy \, dz \, . \qquad (2.3)$$

The total work done by all the internal forces between all the points of the entire equivalent structure is

$$\bar{V}_i = -e \int_z \int_y \int_x (\sigma_x + \sigma_y + \sigma_z) \, dx \, dy \, dz \, , \qquad (2.4)$$

or, with a change of variables,

$$\bar{V}_i = -e \int_V (\sigma_x + \sigma_y + \sigma_z) dV, \tag{2.5}$$

where V is the volume of the structure.

In the derivation of equation 2.5, body forces were assumed to be non-existent. If there are body forces present, they give rise to terms in equation 2.5 which are similar to those presently to be derived for the work done by the external forces. Consequently, the body forces, if present, may be assumed to be part of the load system F_i.

Now consider the work done by the system of loads, F_i, during the dilatation. A single force of the system is shown in Fig. 2.3. Such a force can be represented by its three components X_i, Y_i and Z_i parallel to the x, y and z axes respectively.

For computational convenience assume that the origin is so selected that it does not move during the dilatation. Then the displacements of i, the point at which F_i acts, in the x, y and z directions are ex_i, ey_i and ez_i, respectively.

Thus, the work done by the single force, F_i, during the dilatation is

$$X_i ex_i + Y_i ey_i + Zez_i$$

or,

$$e \{X_i x_i + Y_i y_i + Z_i z_i\},$$

and the total work done by the external system of forces, $\bar{V}_e$, is

$$\bar{V}_e = \sum_i e \{ X_i x_i + Y_i y_i + Z_i z_i \} \tag{2.6}$$

In vector notation, equation 2.6 can be written as

$$\bar{V}_e = \sum_i e \bar{F}_i \cdot \bar{r}_i \tag{2.7}$$

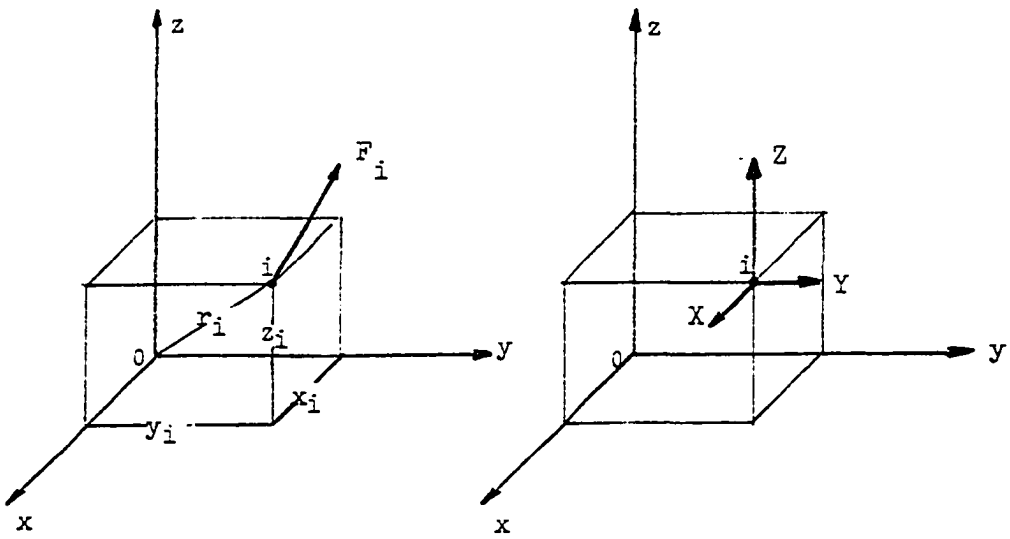

a. Force, F_i.

b. Components of force, F_i.

Fig. 2.3. Single force of the F_i system.

Either equation 2.6 or 2.7 can be used as convenience dictates when actual computations are to be made. For computational ease, equation 2.7 can also be expressed as

$$\bar{V}_e = \sum_i e F_i r_i \cos\theta \qquad (2.8)$$

where F_i and r_i are the scalar magnitudes of the vectors $\bar{F}_i$ and $\bar{r}_i$, (r_i is the radial distance between the origin and point i), and θ is the angle between the two vectors.

It can easily be shown that $\bar{F}_i.\bar{r}_i$ is positive for all forces directed away from the origin and negative for all forces directed towards the origin regardless of their position in space.

Equating to zero the sum of the right-hand sides of equations 2.5 and 2.7, and rearranging,

$$\int_V (e\,\sigma_x + e\,\sigma_y + e\,\sigma_z)\,dV = \sum_i e\,\bar{F}_i.\bar{r}_i \qquad (2.9)$$

or, cancelling the constant e

$$\int_V (\sigma_x + \sigma_y + \sigma_z)\,dV = \sum_i \bar{F}_i.\bar{r}_i,$$

or

$$\int_V \sigma_x\,dV + \int_V \sigma_y\,dV + \int_V \sigma_z\,dV = \sum_i \bar{F}_i.\bar{r}_i \qquad (2.10)$$

Equation 2.10 is the mathematical expression of a new theorem proposed here for the first time. The theorem will be called the "Theorem of Zero Absolute Potential Energy" for reasons to be discussed after a discussion of the general validity of expression 2.10.

General validity of the theorem

The mathematical derivation of the theorem required four assumptions:

1. that the system is in external and internal equilibrium

2. that a constant dilatation of the space takes place,

3. that the forces remain constant, and

4. that the dilatation is an adiabatic process.

Assumptions 2 and 3 are consistent with assumption 1, the preservation of equilibrium, as was shown in the derivation. Neither of assumptions 2 and 3 place any restrictions on the applicability of the theorem. The dilatation was merely a device to derive the theorem. The validity of the theorem does not depend on the dilatation. In assumption 4 the term adiabatic is used advisedly because the requirement is that no energy enter or leave the total system during the dilatation. Thus, all four assumptions reduce to a single one, the preservation of statical equilibrium, as the only condition that must be met for equation 2.10 to be valid. The mathematical statement of the theorem is derived in the appendix directly from the equations of equilibrium and without any other assumptions. Equation 2.10 is considered to be a different statement of but equivalent to the equations of equilibrium.

Since $\sigma_x + \sigma_y + \sigma_z$ is a constant for any point and invariant with respect to the coordinate system chosen, it follows that the left hand side of the equation is invariant with respect to the axes or origin chosen. Obviously the same is true for $\sum \bar{F}_i . \bar{r}_i$, as can be quickly verified by computation of $\sum \bar{F}_i . \bar{r}_i$, with respect to different origins, for any conveniently simple system of loads in equilibrium. This invariancy of each of the two sides of equation 2.10 can be used to computational advantage since, if convenient, different origins and coordinate systems may be chosen for their separate evaluation. Furthermore, if convenient,

the structure may be subdivided into several segments and the terms computed by using a different coordinate system for each segment. In such a case the equation could be rewritten as

$$\sum_{j}^{n} \left(\int_j \sigma_x \, dV_j + \int_j \sigma_y \, dV_j + \int_j \sigma_z \, dV_j \right) = \sum_i \bar{F}_i . \bar{r}_i \qquad (2.11)$$

where the integrations are to be carried over each element, j, of the n elements of the structure. For computation of $\sum \bar{F}_i . \bar{r}_i$ different origins can be used for each set of loads which is by itself in equilibrium (as for example one for all the vertical force components and another for the horizontal force components).

Conceptual Physical Meaning of the Theorem

General

The mathematical expression of the theorem (equation 2.10) has an interesting form in which the terms involved have units of work, or more generally, of energy. The earliest uses of energy principles in structural engineering, in the form of the principle of virtual work, can be traced back to Jean Bernoulli. But Charlton (9) reported that it was also used implicitly by Jordanus de Nemore in the thirteenth century. Energy principles have been, in one form or another, the starting points for the solution of an innumerable host of important structural and mechanical problems. A good historical review of energy principles in elastomechanics is given by Gunhard AE. Oravas in the introduction to a recent, translated edition of Castigliano's principal work (Castigliano (8)). The physical significance of many of these theorems is sometimes not well defined, and sometimes no physical meaning can be ascribed to their indisputably correct

mathematical definition. It is well known, for example, that complementary energy has no physical meaning (even though in the case of linearly elastic structures it is mathematically but not conceptually equivalent to internal work). Neal (22) reported that the exact nature of the principle of virtual work itself is subject to debate, and he considered its usually given physical meaning as an aid to memory. Thus, it is not uncommon that a useful and correct mathematical expression is found first, and its meaning, in physical terms, is sought only after its derivation. Such conceptualization is most useful as it usually reveals remarkable similarities among until then unrelated phenomena and thus permits advances to be made in one field of knowledge by analogy with another. This section will develop a conceptual physical meaning of equation 2.10 and thus explain the reason for the title chosen for it.

Zero absolute potential energy

All the terms of equation 2.10 have units of energy. Conceptually then, they can be considered to be a measure of some kind of energy. This energy will be given the name of "absolute potential energy". The total absolute potential energy of the system is composed of that of the structure and that of the system of loads. If $\bar{U}_a$ is used to denote this total absolute potential energy of the system, then

$$\bar{U}_a = \int \sigma_1 \, dV + \int \sigma_2 \, dV + \int \sigma_3 \, dV - \sum \bar{F}_i . \bar{r}_i ,$$

and, if the system is in static equilibrium,

$$\bar{U}_a \equiv 0 .$$

It is this last equality that expresses what is considered to be the conceptual physical significance of the theorem which can be stated as follows.

THEOREM: The absolute potential energy of a structure-load system in internal and external static equilibrium is always zero.

The word absolute is used to distinguish this conception of potential energy from its more common meaning. For the structure, it is not a measure of energy stored through deformation but rather can be thought of as the energy equivalent of the stressed material itself. For the forces, the potential energy is referred to a single point, the origin selected, and with respect to the selection of which such absolute potential energy is invariant.

Observations with respect to shear

An interesting feature of equation 2.10 is that it does not include any terms with units of energy arising out of shear stresses. A possible explanation may be found in the observation that a shear stress pattern can always be expressed in terms of the corresponding normal principal stresses at the point. In addition, it is interesting to reflect on the fact that although shear stresses cannot exist without normal stresses on some other plane through the same point, the reverse is possible. Thus, it may be hypothesized that in general the shear pattern is dependent on the normal stress pattern which is in turn dictated by the system of loads on the structure. Conceptually then, shear stresses may be regarded as arising out of a geometric deficiency of the structure that prevents the structure from supporting the loads by purely normal stresses. In that case, shear must arise to preserve internal equilibrium and to "bend" the stress trajectories. It could then be expected that shear stressed struc-

tures are less efficient than structures which support the load system purely by normal stresses.

Shear stresses must be present whenever $\sum \bar{F}_i.\bar{r}_i$ is zero by itself since then, at some point in the body, at least one of the stresses (σ_x, σ_y or σ_z) in the left hand side of equation 2.10 must be of a different sign than the others for the equation to apply. When $\sum \bar{F}_i.\bar{r}_i$ is not zero and an all compression or an all tension structure is possible, equation 2.10 is sufficient to uniquely determine the volume, given the stress pattern (assuming, for example, a fully stressed structure). When $\sum \bar{F}_i.\bar{r}_i$ is zero, however, equation 2.10, although valid, is not sufficient to uniquely determine the volume (given the stresses) since both sides of the equation are separately equal to zero. It is then necessary to know more about its geometry.

Michell structures can be thought of as shear structures (skeleton flexural or torsional structures) where, for efficiency, the material has been concentrated along the lines of principal stress trajectories. It is thus not surprising that to find a Michell structural layout is primarily a geometric exercise which is equivalent to determining the geometry of the principal stress trajectories to carry the loads. This seems to explain the possibility of existence of several Michell structures for the same system of loads, some more efficient than the others in accordance with the relative efficiency of the respective stress trajectories.

Derivation of Maxwell, Michell and Templeman's Results

Since the theorem is generally applicable, it should be possible to derive Maxwell's theorem, the Michell conditions and Templeman's results

from it. This will be done forthwith.

Derivation of Maxwell's theorem

Consider a generalized framework of n bars, which is loaded by a system of m loads (F_i). If the system is in equilibrium, equation 2.11, rewritten for convenience, applies directly to yield:

$$\sum_{j=1}^{n} \left(\int_j \sigma_x \, dV_j + \int_j \sigma_y \, dV_j + \int_j \sigma_z \, dV_j \right) = \sum_{i=1}^{m} \bar{F}_i . \bar{r}_i$$

For each bar, j, select a coordinate system such that the x axis runs along the centerline of the bar. In such a case, assuming constant distribution of stress throughout the cross section,

$$\left. \begin{aligned} \sigma_x|_j &= \frac{T_t}{A}\Big|_j \quad \text{or} \quad \sigma_x|_j = -\frac{T_c}{A}\Big|_j , \\ \text{and} \\ dV_j &= A_j \, d\ell_j , \quad \sigma_y = \sigma_z = 0 \end{aligned} \right\} \tag{2.12}$$

where $d\ell_j$ is the differential element of length, and all other symbols are as previously defined.

Substituting equations 2.12 into 2.11, the result is

$$\sum_{j=1}^{k} \int_j \frac{T_{t_j}}{A_j} A_j \, d\ell_j + \sum_{j=k+1}^{n} \int_j \left(- \frac{T_{c_j}}{A_j} A_j \, d\ell_j \right) = \sum_{i=1}^{n} \bar{F}_i . \bar{r}_i$$

where for convenience the k tension members and the n-k compression numbers have been collected under the appropriate summation signs.

Simplifying and integrating.

$$\sum_t T_t L_t - \sum_c T_c L_c = \sum_i \bar{F}_i . \bar{r}_i \tag{2.13}$$

Equation 2.13 is the mathematical statement of Maxwell's theorem as can be determined by comparison with equation 1.1.

Derivation of Michell conditions

Having derived Maxwell's theorem from the theorem herein presented, it is obvious that it is possible now to proceed in exactly the same manner as Michell, and as outlined in chapter one, to develop his conditions for minimum volume of a structure.

Derivation of Templeman's results

Assume that a structure is under static equilibrium in the face of an external system of loads also in static equilibrium. Assume further that such a structure is composed of uniaxially stressed elements and biaxially stressed sheets. For clarity refer to Fig. 2.4 where a typical structure suggested by Templeman is shown. The structure shown in the illustration is planar, as all of Templeman's examples were, but it is emphasized that the derivation to be made here, using equation 2.11, need not be restricted to planar structures and would apply as well to three-dimensional structures such as a shell. In all the planar structures of Templeman, since the sheet is to be uniformly stressed in all directions, the uniaxially stressed members must always be arcs of circles.

Rewriting equation 2.11 for convenience,

$$\sum_{j=1}^{n} \left(\int_j \sigma_x \, dV_j + \int_j \sigma_y \, dV_j + \int_j \sigma_z \, dV_j \right) = \sum_{i=1}^{m} \bar{F}_i . \bar{r}_i$$

Imagine now the generalized structure to be divided into k uniaxially stressed members and n-k sheets under biaxial stresses. Equation 2.11 can then be written as

$$\sum_{j=1}^{k} \int \sigma_1 \, dV_j + \sum_{j=k+1}^{n} \left(\int_j \sigma_x \, dV_j + \int_j \sigma_y \, dV_j \right) = \sum_{i=1}^{m} \bar{F}_i . \bar{r}_i \quad (2.14)$$

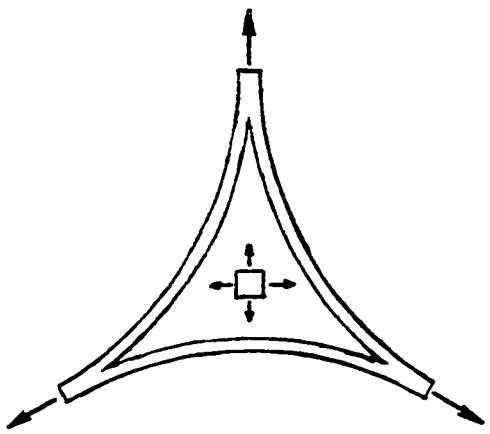

Fig. 2.4. Typical Templeman structure.

where it is implied, by the appearance of the first term that coordinates will be chosen for its integration so that

$$\sigma_x = \sigma_1 , \quad \sigma_y = \sigma_z = 0 .$$

Such a coordinate system could be curvilinear, and for the typical structure shown in Fig. 2.4 the origin would be at the centers of the circular arcs. It is emphasized that this is done strictly for convenience and is not a prerequisite to the validity of the equation. A Cartesian coordinate system could also be employed in which case σ_x and σ_y would be the x and y components of σ_1 while $\sigma_z = 0$. In such a case, dV_j would also have to be expressed in terms of the same Cartesian coordinate system. Thus, it is the convenience of expression of dV_j that is being considered in the selection of the coordinate system, and not necessarily colinearity with the stresses.

For least volume, Templeman assumed that, if maximum shear strength is the criterion of failure, and if the stresses in the sheet are of like sign, then the least volume of the structure is obtained when all the stresses are constant and equal to the maximum allowable stress f_t or f_c. Note that, if the sheet is in tension, so must be the arched members and vice-versa. Therefore, in equation 2.14 replacing σ_x, σ_y and σ_1 by f, and, dividing throughout by f, the result is

$$\sum_{j=1}^{k} \int_j dV_j + \sum_{j=k+1}^{n} \left(\int_j dV_j + \int_j dV_j \right) = \frac{1}{f} \sum_{i=1}^{m} \bar{F}_i . \bar{r}_i \quad . \quad (2.15)$$

But noting that $\int_j dV_j = V_j$, and that the elements 1 to k are the uniaxially stressed and the k+1 to n are the biaxially stressed, equation 2.15 can be written in the equivalent form

$$V^u + 2V^b = \frac{1}{f} \sum_i \bar{F}_i . \bar{r}_i \qquad (2.16)$$

where V^u denotes the volume of the uniaxially stressed members of the structure and V^b, as before, the volume of the biaxially stressed sheets. Or,

$$V_T = \frac{1}{f} \sum_i \bar{F}_i . \bar{r}_i - V^b \qquad (2.17)$$

for which use is made of the identity

$$V_T = V^u + V^b$$

where V_T is the total volume of the structure.

Equation 2.17 is Templeman's assertation here proven in a more rigorous manner. His other assertions with respect to fully biaxially or fully triaxially loaded structures (see equations 1.9 and 1.10) could be derived just as rigorously.

Applications and Significance of Theorem

The theorem is so general that the full range of problems where it will be useful can be neither predicted nor foreseen at this time. Conceptually, equation 2.10 could be used to develop the general conditions to be fulfilled for minimum volume structures, to develop the optimum form for a particular structure, to test statical equilibrium, and so on. In this dissertation the theorem will be used to develop the least volume conditions leading up to a hierarchy of structures according to structural efficiency, and it will also be used in several sample structural optimization problems.

Interestingly, in some of the examples dealing with open-top shell domes, equation 2.10 was found not to apply in the first try. A re-

examination of the statical equilibrium of those problems disclosed that those particular shells would not be in equilibrium under the assumed stress distribution and that either localized bending would have to be included in the computation of equation 2.10, or that a stiffening ring would have to be applied. To preclude bending the stiffening rings were applied and in every case equation 2.10 could then be shown to apply identically, thus illustrating a possible use of the equation in checking the correctness of assumed stress patterns as suggested in the previous paragraph.

Significance as pertains to least volume

Equation 2.11 is rewritten for convenience,

$$\sum \left(\int \sigma_1 dV + \int \sigma_2 dV + \int \sigma_3 dV \right) = \sum \bar{F}_i . \bar{r}_i \qquad (2.18)$$

where σ_x, σ_y and σ_z have been replaced by σ_1, σ_2 and σ_3 to indicate that the coordinate system used for each element may be local instead of global.

It is obvious, observing equation 2.18, that for any single value of $\sum \bar{F}_i . \bar{r}_i$ not zero (and of course for a given system of loads), the absolute minimum volume will be obtained when σ_1, σ_2 and σ_3 are all of the same sign and numerically as large as allowable everywhere throughout the structure, if such is possible. In that case, if f is the allowable stress for the material when stressed triaxially,

$$V^t_{T_{min}} = \frac{1}{3f} \sum \bar{F}_i . \bar{r}_i . \qquad (2.19)$$

Equation 2.19 was, as mentioned before, first proposed by Templeman (36). Since equation 2.19 was derived from equation 2.18 which applies

to hyperstatic as well as to static structures, this is considered to be a mathematical proof, heretofore considered so elusive as discussed in the Strength designs section of chapter one (see also Barnett (2)), of the concept that the fully stressed structure, static or hyperstatic, is the least volume structure for a single system of loads. Equations similar to equation 2.19 can be written for the two and one dimensional stress states by letting $\sigma_1 = 0$ or $\sigma_2 = \sigma_3 \equiv 0$ respectively. Then,

$$V^b_{T_{min}} = \frac{1}{2f} \sum \bar{F}_i . \bar{r}_i , \tag{2.20}$$

and,

$$V^u_{T_{min}} = \frac{1}{f} \sum \bar{F}_i . \bar{r}_i \tag{2.21}$$

where f, in each case, is the maximum allowable stress for the stress state existing in the structure. Comparing these last three equations it can be seen that, for generally comparable systems of loads, a triaxially, fully and homogeneously stressed structure would have a lesser volume than a uniaxially stressed structure, assuming of course that such structures are possible for the given loads. Here the term "homogeneously stressed" is used to denote that all stresses in the structure are tensile, or that all are compressive.

Continuing to assume that $\sum \bar{F}_i . \bar{r}_i$ is not zero, it can be shown that structures which are not homogeneously stressed will have lesser efficiency than the corresponding homogeneously stressed structures. That this is so for uniaxially loaded structures was shown by Owen (25) as discussed in chapter one. For biaxially loaded structures, when $\sum \bar{F}_i . \bar{r}_i$ is not zero it is not possible for the structure to be fully stressed everywhere with stresses of different signs since if this were so the left side of equation 2.18 would vanish. Thus, assume that σ_1 is everywhere equal to the

maximum allowable stress. Assume further that σ_2 has some value, variable if desired, but less than the allowable and everywhere of different sign than σ_1 . For biaxially stressed cases,

$$\int \sigma_1 \, dV + \int \sigma_2 \, dV = \sum \bar{F}_i . \bar{r}_i .$$

Now replace σ_1 by its known value, f, and σ_2 by $-\zeta_2$ where ζ_2 is the absolute numerical value of σ_2. This yields,

$$f V - \int \zeta_2 \, dV = \sum \bar{F}_i . \bar{r}_i$$

and

$$V = \frac{1}{f} \sum \bar{F}_i . \bar{r}_i + \int \zeta_2 \, dV. \qquad (2.22)$$

Comparing equation 2.22 with equation 2.20, it can be seen that the homogenously stressed structure again results in a lesser volume. For a triaxially stressed structure, it could be shown, by a similar procedure, that the homogeneously stressed structure has lesser volume. Furthermore, in the case of a triaxially loaded structure, if it is possible to have the structure fully stressed everywhere but with one stress component of different signs than the others, then

$$- \int \zeta_1 dV + \int \zeta_2 dV + \int \zeta_3 dV = \sum \bar{F}_i . \bar{r}_i$$

But, since the structure is fully stressed, $\zeta_1 = \zeta_2 = \zeta_3 = f$, and the first two terms cancel out, leaving

$$\int \zeta_3 dV = \sum \bar{F}_i . \bar{r}_i$$

or

$$V = \frac{1}{f} \sum \bar{F}_i . \bar{r}_i .$$

Therefore such structure would not be any better than a uniaxially stressed structure (assuming that the allowable stresses, f, and the systems of loads are comparable).

The above comments are predicated on $\sum \bar{F}_i . \bar{r}_i$ not being zero. Should $\sum \bar{F}_i . \bar{r}_i$ be zero, barring the trivial case when the forces are concurrent on a point or on a line (in which case no structure is necessary to preserve equilibrium and $V_T \equiv 0$), then homogeneously stressed structures are not possible. As discussed earlier in the observations with regard to shear stresses, when $\sum \bar{F}_i . \bar{r}_i$ is zero, the forces are either parallel or couples. In that case shear must be present in a biaxially or a triaxially stressed structure, and at least some portion of the structure must have one stress of different sign than the others for the left hand side of equation 2.18 to be zero. These structures will be referred to as of a "mixed state of stress." Uniaxially, biaxially and triaxially stressed structures in a mixed state of stress will be separately considered.

Uniaxially stressed structures in a mixed stress state can be fully stressed. In that case, if f_t and f_c are the same, the total volume of the tension members will be the same as the total volume of the compressive members. For minimum volume such structures would be Michell structures. It will be shown in a later section that if the geometric restrictions (that make the use of a Michell structure mandatory if least volume is to be achieved) are relaxed, then it is sometimes possible to decrease the volume. Thus, Michell structures are not considered as efficient as those in which it is possible to have a homogeneously stressed structure.

Biaxially stressed structures in a mixed state of stress may also be fully stressed. This corresponds to a structure in which the entire structure has stresses of different signs in two orthogonal directions at

each point. An example of this would be a hyperbolic-paraboloidal shell. For this case equation 2.18 is insufficient to assess the structure's relative merits with respect to homogeneously stressed structures. However, since uniaxially stressed Michell structures (in a mixed state of stress) can sometimes be shown to be less efficient than homogeneous structures if the geometry constraints are relaxed, it is presumed, intuitively that, if geometry is relaxed, it may also be possible to reduce the volume of a biaxial, mixed, and fully stressed structure by replacing it with a fully and homogeneously stressed structure.

Triaxially stressed structures may not be fully stressed if $\sum \bar{F}_i.\bar{r}_i$ is zero. When $\sum \bar{F}_i.\bar{r}_i$ is zero, the requirement that the left hand side of equation 2.18 vanish makes it imperative that if one of the stresses, say σ_1, is everywhere equal to its maximum allowable value, then the other two must be of a different sign and less than their maximum allowable value. (This again seems to confirm, as discussed earlier, that no Michell strain fields exist in three-dimensions.) Structures of this type do not utilize the material to its full capabilities and must be considered less efficient than triaxially stressed structures in a mixed state of stress when $\sum \bar{F}_i.\bar{r}_i$ is not zero since in this latter case it is conceptually possible to fully stress the material in all directions.

Beams, and other flexural members in a biaxial state of stress are special cases of mixed stressed structures, generally with $\sum \bar{F}_i.\bar{r}_i = 0$, in which it is not possible, in practical cases, to achieve the allowable stress everywhere for either σ_1 or σ_2. These structures must be considered the least efficient of all mixed stress state structures with

$$\sum \bar{F}_i . \bar{r}_i = 0.$$

Hierarchy of structures

The discussion of the preceding section can be summarized in an ordered hierarchy of class levels of increasing efficiency (or decreasing volume) according to the state of stress existing throughout the structure.

The possibility of devising some such classification was suggested by Otto (23) who published a chart in which the structural forms were classed with respect to the type of action (bending, tension, compression) used to support the loads. In the same chart he indicated, empirically, whether more or less material is required in their execution.

A hierarchy of structures based on the previous section appears in Fig. 2.5 where only the most efficient member of each stress state condition is shown. The symbol + (or -) is used therein to signify that the particular stress is everywhere equal to the maximum allowable stress in tension (or compression). It is certainly not implied that it is possible to design a structure to fit a specific stress condition for any given system of loads. Indeed, it is expected that in general the system of loads must be somewhat changed to substitute a design of a generally more efficient level for one of another level, if such substitution is possible.

Two additional points to be kept in mind when looking at the hierarchical levels of Fig. 2.5 are:

1. All structures are actually three-dimensional and consequently the lines that separate one structural level from another cannot be

	$\sum \bar{F}_i \cdot \bar{r}_i \neq 0$			$\sum \bar{F}_i \cdot \bar{r}_i = 0$			
	Stress State[a]			Stress State			
	σ_1	σ_2	σ_3	σ_1	σ_2	σ_3	Structural Examples
				$(\pm)$[b,c]	0	0	Beams, rigid frames
				(+)	(−)	0	Plates
I[d]	(±)	0	0				Trusses (plane & spatial), lattices
I[d]	+	(−)	0				Shells
I[d]	+	+	−	(+)	(+)	−	Solids massive enough to warrant 3-dimensional elasticity
				↑[e]			
				↑ ±	0	0	Michell structures
II	+	0	0				Trusses, lattices, arches, cables and nets
				+	−	0	Shells (hyperbolic paraboloid)
				↑			
III	+	+	0				Shells, membranes
IV	+	+	+				Solids (trivial), fluids

↑ Increasing material efficiency

[a] At each level a second stress state has all signs reversed.

[b] ( ) means that the particular stress is not everywhere equal to the maximum allowable for the stress condition of the level.

[c] ± implies that some parts of the structure, or some members, are in tension and some are in compression, but all are uniaxially stressed.

[d] The ordering of level I stress states is not assured.

[e] The horizontal line indicates that the stress state of $\sum \bar{F}_i \cdot \bar{r}_i = 0$ above the line, cannot be more efficient than the corresponding stress state of $\sum \bar{F}_i \cdot \bar{r}_i \neq 0$ below the line.

Fig. 2.5. Hierarchical structural class levels.

clearly drawn. Thus, a structure can be more clearly ascribed to one level rather than another the more exactly it fulfills the requirement of that level.

2. In moving towards the more efficient levels, often more of the loads are passed to the supports (or are passed to them more efficiently). Thus, it cannot be generally said that any one level is superior to a preceding level in a true economic sense. It can only be said that structures of the higher levels (exclusive of supports) are lighter than those of preceding levels when supporting comparable load systems.

The hierarchy of structures shown may not include every possible case. However, it can be used to state three general guidelines:

1. Fully stressed structures are more efficient (provide lesser volume) than comparable not fully stressed structures.

2. Structures in homogeneous states of stress are more efficient than comparable structures in mixed states of stress.

3. Triaxially and homogeneously stressed structures are more efficient than comparable biaxially stressed structures which in turn are more efficient than comparable uniaxially stressed structures.

Significance as pertains to hyperstatic structures

The applicability of the theorem is not restricted with respect to the degree of redundancy of a structure. It applies to hyperstatic as well as to static structures. Consequently, the theorem indicates that, if all parts of the structure are fully stressed, then the volume required to support a given system of loads is the same for a hyperstatic or a static structure. (This was noted (in chapter one) to be the case

for the Maxwell structures of Fig. 1.1). The theorem further indicates quite generally that the least volume structure, optimized for a single load system, is a fully stressed structure (static or hyperstatic). The actual volume required depends on the intensity and geometry of the loads ($\sum \bar{F}_i . \bar{r}_i$), and on the allowable stress in the material.

Since equation 2.10 applies to the loaded structure, the geometry used should also be that of the structure under load. Consequently, upon removal of the loads, there will generally be residual stresses in hyperstatic structures due to lack of fit of the unstressed elements of the structure. However, when subjected to the design loads, such structures will be compatible and fully stressed. Such geometrical prestressing, using the geometry of the loaded structure in the design process, is similar to the reverse deformation method advanced by Rozvani (29), and to the load balancing method of T. Y. Lin (17).

Concept of optimization by variation of $\sum \bar{F}_i . \bar{r}_i$

As discussed in chapter one, the loads and the structural form are interrelated, a change in one implying a change in the other. Thus, it is most logical to assume that the locations of the loads may be varied in some permissible fashion (say along their lines of action), and the reactions may be allowed to vary in magnitude as well as orientation so as to preserve equilibrium, in order to optimize or reduce the volume of the structure. It must be pointed out that in general this makes it necessary for the supports to be resistant to horizontal thrust as well as vertical loads. This is not considered a major drawback of the con-

cept. If a tension ring is used, and it is desired to consider its volume as well, the method can be modified to do so. How this can be done is discussed in chapter three.

The minimization process can be conceived as being composed of two generalized steps. First, a topological optimization is made transforming the structure from one class to a more efficient class, and second, a geometrical optimization is made within the second class.

For illustration, consider a Michell structure as shown in Fig. 2.6 (radial members are omitted from the sketch for clarity). Then, assume that it is now permissible to raise the load and force it to act on the structure at a higher point as shown in Fig. 2.7. According to Cox (10), the volumes of the two structures are identically the same, a curious feature of such Michell structures. Note however, that for the structure with the raised load, $\sum \bar{F}_i.\bar{r}_i$ is no longer equal to zero. Thus, except for the parallelism of the forces (according to equation 2.10, or from Maxwell's theorem) the least volume structure, since $\sum \bar{F}_i.\bar{r}_i$ is negative, would be one devoid of tension members, i.e. an all compression structure. It is only necessary to relax the geometrical conditions on the loads (supports) at A and B in Fig. 2.7 and allow them to rotate. Then the minimum volume structure would be a two strut structure as shown in Fig. 2.8. By expressing $\sum \bar{F}_i.\bar{r}_i$ in terms of this new load system the structural form transformation is effected. The volume of this new structure will be less than that of the original Michell structure provided that the rotation of the support reactions does not unduly numerically increase $\sum \bar{F}_i.\bar{r}_i$. The numerical value of $\sum \bar{F}_i.\bar{r}_i$ should be

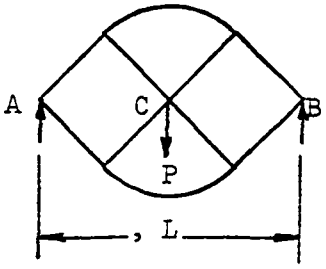

Fig. 2.6. Michell structure with $\sum \bar{F}_i . \bar{r}_i = 0$.

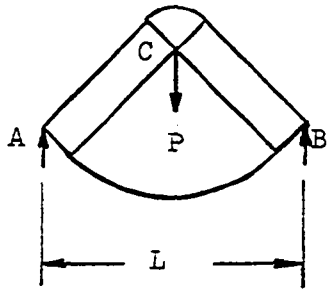

Fig. 2.7. Michell structure with $\sum \bar{F}_i . \bar{r}_i \neq 0$.

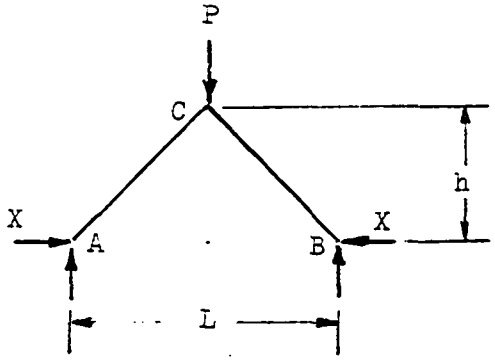

Fig. 2.8. Modified structure .

minimized by suitably selecting h. Such a minimization of $\sum \bar{F}_i.\bar{r}_i$ will not result in a return to $\sum \bar{F}_i.\bar{r}_i = 0$ if $\sum \bar{F}_i.\bar{r}_i$ has been properly expressed. That this is so will be presently shown mathematically.

The volume of the Michell structures of Fig. 2.6 and of Fig. 2.7 can be computed to be (as shown for example by Cox (10)), if $f_t = -f_c = f$;

$$V = \frac{1}{f}(1 + \frac{\pi}{2}) \frac{PL}{2} \tag{2.23}$$

Solving for X in terms of P and h, the value of $\sum \bar{F}_i.\bar{r}_i$ can be computed, for the structure of Fig. 2.8, as

$$- \sum \bar{F}_i.\bar{r}_i = P[\frac{L^2}{4h} + h] \tag{2.24}$$

Setting the first partial derivative of $\sum \bar{F}_i.\bar{r}_i$ with respect to h equal to zero, the minimum numerical value of $\sum \bar{F}_i.\bar{r}_i$ can be shown to occur when h is equal to L/2.

Substituting this value in equation 2.24, and making use of equation 2.11, or of Maxwell's theorem, the volume of the new all compression structure of Fig. 2.8 can be computed as

$$V = \frac{1}{f} PL \tag{2.25}$$

Comparison of equation 2.25 with 2.23 shows that the volume of this structure is about 4/5 that of the Michell structure. If the absolute value of the maximum allowable tensile stress is greater than that of the compressive stress, then a lowering of the load would still yield a lesser volume for the modified structure than for the Michell structure.

A plot of equation 2.24 is shown in Fig. 2.9. It is easy to see that it is not possible to return to $\sum \bar{F}_i.\bar{r}_i = 0$ since no homogeneosly stressed structure is possible then. As h approaches zero, $\sum \bar{F}_i.\bar{r}_i$

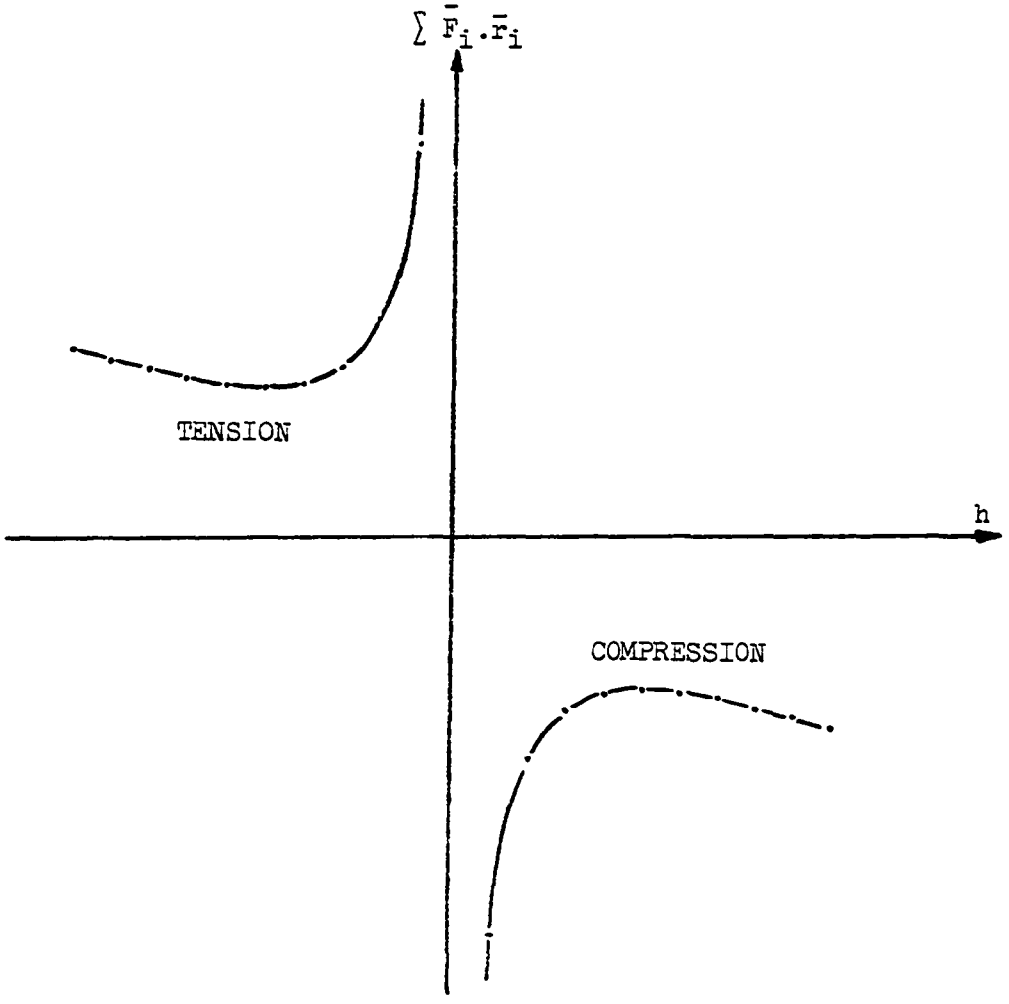

Fig. 2.9. Plot of $\sum \bar{F}_i . \bar{r}_i$.

aproaches $\pm\infty$.

Several investigators such as Cox (10), Owen (25), and Templeman (36) have similarly noted that the volume of structures can sometimes be reduced by adding loads (hence changing $\sum \bar{F}_i.\bar{r}_i$). Owen, who also considered the two strut structure of Fig. 2.8 and noted its greater efficiency than the corresponding Michell structure, also used this method of variating $\sum \bar{F}_i.\bar{r}_i$ to investigate the most efficient sag-to-span ratio of suspension bridges.

It is not entirely clear under what general conditions (if such exist) this result is attainable. Conceptually and physically, the raising of the load in going from the structure of Fig. 2.6 to that of Fig. 2.7 is equivalent to allowing an increase in the volume of the compression members and an exactly equal decrease in the tension members (so that the total volume is not changed), while at the same time allowing $\sum \bar{F}_i.\bar{r}_i$ to vary in such a way as to maintain the equality of equation 2.11. Conceptually, and, less clearly physically, the rotation of the reactions corresponds to a continuing decrease of the tension volume, accompanied by a lesser increase in the compression volume, until the tension volume vanishes.

Although attempted, it was not possible to prove conclusively in this dissertation that this second variation is always possible, or under what geometrical conditions it is possible. If such a modification is physically possible within the same general class of structure so that the systems of loads remain comparable, then, obviously the volume of the final, homogeneously and fully stressed structure (all tension or all

compression) will be less than that of the original mixed-stressed (tension and compression) structure.

If the modification is possible only by a transformation of the structure to a different class, then the system of loads on the new class may not be comparable to that of the first. Consequently the volume of the new class structure will be less only if $\sum \bar{F}_i . \bar{r}_i$ has not been unduly increased to force the new class of structures to apply. This will be illustrated in the third alternative design of the sequence of examples in chapter five, and will be discussed in the section on Comparison of volumes of that chapter.

CHAPTER THREE - METHODOLOGY FOR SOME OPTIMAL STRUCTURAL DESIGN PROBLEMS

General

Loads

This chapter will outline a general methodology which can be used (with the theorem developed in chapter two) in optimal synthesis of three-dimensional structures. The specific methodology to be developed will be applicable to structures which must support vertical loads, but in which the vertical loads may be raised to any point above the level of the supports. This type of load system arises in many practical cases such as roofs. In those cases, the primary loads usually are vertical (concentrated or distributed live load and distributed dead load); while the secondary live loads may or may not be vertical (a man walking on the roof, wind loads). For some structures, of course, wind loads may be just as severe or more severe compared to other loads. But since they are variable, they do not constitute a single system of loads and the method to be developed will not then be applicable. Furthermore, since the wind loads are more or less infrequently applied, it does not seem justifiable, except in rare cases, to optimize a structure with respect to a single specific wind load. For roofs of dome shape, Benjamin (3) considered the self load and the snow loads to be the primary loads in the preliminary design. Having considered the snow loads as primary loads, the other live loads were ignored. Finally, the preliminary design was modified by accommodating the additional wind load effects.

General forms of structures

As discussed in chapter two, least volume structures are homogenously and fully stressed.

The only frameworks that can be homogeneously stressed under the loads to be considered are lattices or tension nets of cables, if the supports are allowed to absorb the thrusts of the structure. As will be seen in the illustrative examples of chapter four, the minimization process results in structural shapes of high rise (or sag) -to-span ratios. It is difficult to provide sufficient rigidity to high sag tension structures. Because of this, and because of the desirability to have some rigidity in the structure against loads other than the ones for which it was optimized, only compression structures will be given further consideration.

Parenthetically, it should be noted that shallow and very rigid all tension structures are possible (not considering the supporting compression ring) by draping cables into nets describing an anticlastic surface; or into two surfaces of opposite curvature and joined by short vertical cables. Such nets, however, are kept in tension under load by high prestressing forces. Under load, the tensile stress in one of the two sets of cables is decreased, thus this set can really be considered to act as a set of compression members (Zetlin (41)). If the large prestressing forces are included as part of the load system, then $\sum \bar{F}_i.\bar{r}_i$ becomes positive as it should be for an all tension structure. Whether or not such a net of cables, excluding the compression ring, is of lesser volume than the structures obtained by the methods advanced in this dissertation depends on the relative magnitudes of the respective $\sum \bar{F}_i.\bar{r}_i$. For

the cable supported roofs being considered, the prestressing forces must be high and consequently $\sum \bar{F}_i \cdot \bar{r}_i$ will probably be higher than for a comparable compression structure. Thus, tension nets will not be considered any further.

Application of the Theorem and the Concept of Variable $\sum \bar{F}_i \cdot \bar{r}_i$

Generalized formulation

The generalized loading system used in this dissertation is shown in Fig. 3.1. The optimization problem to be solved can be defined as follows. Find the vertical coordinates, z_i, for a specific lattice or shell, which, when loaded with the system of loads, P_i, results in the least volume lattice or shell. Mathematically, this is a programming problem where the objective function is

$$V|_{min} = g(\alpha_i)|_{min} \tag{3.1}$$

to be minimized subject to three sets of constraints;

statical equilibrium, $$h(F_i, r_i, Q_i, \ell_i, \phi_i) = 0 \; ; \tag{3.2}$$

geometry and stresses, $$k(Q_i, \sigma_i, \alpha_i, f) = 0 \; ; \tag{3.3}$$

and, compatibility of deformations, $$p(Q_i, \alpha_i, \delta_i) = 0 \; . \tag{3.4}$$

The objective function, equation 3.1, is normally one of geometry with variables in it, α_i, such as the areas and lengths of the members in the case of lattices, or with thicknesses and differential elements of length or area in the case of shells.

The constraints similar to equation 3.2 include all the equations of equilibrium of all parts of the structure, and, generally, include such

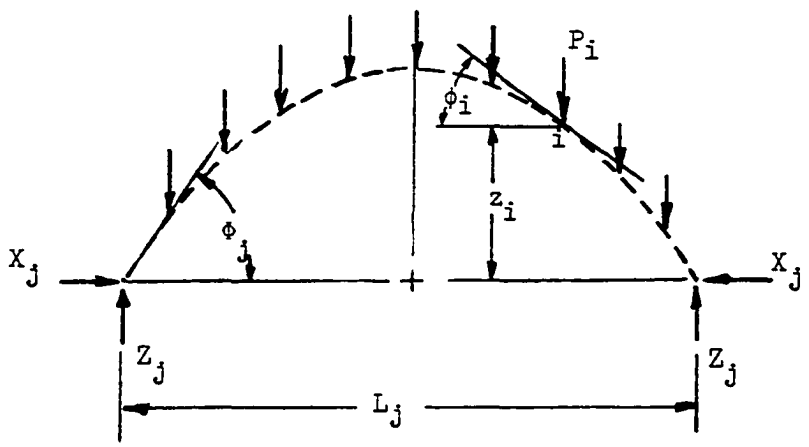

Fig. 3.1. Loading system used.

variables as all the forces in the system (internal, Q_i, and external, F_i) and the necessary geometric variables such as lengths, ℓ_i, r_i, and angles, ϕ_i.

The constraints similar to equation 3.3 are needed to relate the geometric variables of the objective function to those of the constraints of equilibrium. Therefore, these constraints will generally include those of the objective function and those of the equilibrium conditions, as well as other variables such as stresses, σ_i, and the allowable stresses, f, (usually constant) in the structure.

For statically determinate structures, only the objective function and the first two sets of constraints are sufficient to arrive at a solution. In such structures (determinate) the compatibility constraints are automatically satisfied. However, in the case of indeterminate structures, the compatibility constraints (similar to equation 3.4 and which introduce additional variables, i.e. structural deformations and displacements, δ_i) must be used in conjunction with the others to arrive at a unique solution.

Other side constraints, such as buckling, may be part of a specific problem. Such side constraints are not included in the set of constraints since the method to be developed is a strength design method, and, as discussed in chapter one, optimization in such a case is normally obtained with respect to only strength constraints.

Use of theorem of zero absolute potential energy

By the use of the theorem, when the structure is fully and homogeneously stressed, it is possible to replace the objective function by a new equivalent objective function,

$$V|_{min} = \sum F_i \cdot r_i|_{min} \tag{3.5}$$

It is noted that this new objective function is expressed only in terms of forces and the necessary geometric variables. These are the same variables appearing in constraints 3.2.

With this substitute objective function the programming problem is often considerably simplified.

Simplifications due to the use of the theorem

As discussed in chapter two, the minimum volume structure will be a fully and homogeneously stressed structure (i.e. all members everywhere stressed to the maximum allowable stress in compression, or all in tension). Assuming such a stress pattern to apply will in some cases reduce a statically determinate structure to a mechanism (for purposes of design computations), or a statically indeterminate structure to a determinate one. However, since the geometry is undefined during the optimization process, this simplification is not always assured and depends on the specific problem being considered.

As shown in Fig. 3.1, the system of loads, F_i, include the applied loads, P_i, and the reactions, X_j and Z_j. The reactions are dependent on the applied loads and on the geometry of the structure. In the case of structures which can be made statically determinate for design purposes,

as well as in the case of statically determinate ones, it is possible to relate these loads with only the statical equilibrium set of constraints (equations 3.2). When the structure is indeterminate, however, they cannot be related without making use of the compatibility constraints (equations 3.4) which, in turn, require the consideration of the geometry constraints similar to equations 3.3.

In the optimization of the substitute objective function, it is sufficient to consider only those constraints which are necessary to relate X_j, Z_j and P_i. Thus, in many cases the optimization process is considerably reduced since only the constraints of statical equilibrium (equations 3.2) need be considered. The number of variables involved is also greatly reduced.

For a final design the constraints of geometry similar to equation 3.3 will eventually have to be used, but only after the optimum general geometry has been determined in the optimization process. Thus, the use of the theorem, coupled with the concept of variation of $\sum \bar{F}_i.\bar{r}_i$ (see the last section of chapter two), results in two distinct advantages when the structure is reducible to a statically determinate one. These advantages are that,

1. the programming problem is considerably simplified by a reduction of the constraints that must be satisfied, and
2. a detailed design of all parts of the structure need not be considered until after the programming problem is solved.

The method is limited to the consideration of a single system of loads. Conceptually it appears, however, that it may be possible to

modify the objective function so that multiple systems of loads can be considered. It also seems that it may be possible, from a mathematical point of view, to specify additional side constraints (such as buckling). Neither of these was done. It is not clear whether or not any advantages would still ensue from the use of the theorem in either or both of these latter cases.

Methods of Solution

Two methods of solution are generally available for the optimization process of a statically determinate structure.

1. Classical Method. This method consists of two steps:

   a. all the constraint equations of the statical equilibrium set are used to reduce the number of variables in the objective function to a minimum, and

   b. the reduced objective function is minimized with respect to the remaining variables by classical mathematical methods.

2. Numerical Method. Any suitable programming method may be used to optimize the objective function subject to the given constraints.

When the structure is not reducible to a determinate structure by the assumption that it is fully and homogeneously stressed, a solution may still be possible by using an analogous structure to relate X_j, Z_j and P_i, after which $\sum \bar{F}_i . \bar{r}_i$ is optimized by the classical method. Such solutions however, are a minimum only for the specific class of structures considered in the analogy, and there is no assurance that a different class would not yield a lesser minimum.

These methods will be discussed in more detail in the context of lattice and shell optimization techniques below, and will be illustrated by application to specific problems in chapter four.

Lattices of One Layer

To understand the reasons for choosing lattices of one layer to illustrate the application of the procedures outlined above, consider the cross section of a generalized lattice of two layers shown in Fig. 3.2. If such a structure is to be all under compression as is required if the volume is to be a minimum, then the inclined members have the function of distributing the loads between the two layers. The minimum volume would be obtained when the upper layer merges into the lower layer, the distance between the two layers is zero, and the inclined members vanish. Thus, minimum volume is obtained with a lattice of one layer. There are, however, some marked benefits to be obtained with a two-layered lattice. Among these are greater rigidity, greater assurance of safety against overall buckling, and the capability to offer some bending resistance as a safeguard against overloads. The volume of the inclined members is the material price paid for such benefits. Borrego (4) has catalogued many different lattice grid geometries and their combinations into multi-layered lattice systems.

In accordance with the generalized loading system of Fig. 3.1, the objective function can be expressed as,

$$\sum \bar{F}_i \cdot \bar{r}_i \Big|_{min} = \left(\sum \{-X_j L_j\} + \sum \{-P_i z_i\} \right) \Big|_{min} \qquad (3.6)$$

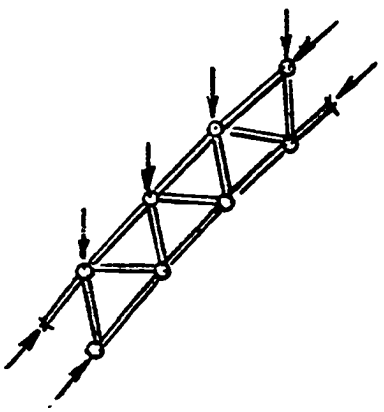

Fig. 3.2. Cross-section of generalized lattice of two layers.

The negative signs indicate that a compressive structure is required. In that case, the stress of all parts of the structure, is $\sigma = -f_c$, and the volume can be expressed as

$$V = -\frac{1}{f_c} \sum \bar{F}_i . \bar{r}_i$$

Since the absolute value of $\sum \bar{F}_i . \bar{r}_i$ is to be minimized, it is convenient at this point to reverse the sign convention and treat inward loads as resulting in positive $\bar{F}_i . \bar{r}_i$ terms, it being understood that a positive $\sum \bar{F}_i . \bar{r}_i$ will require a compressive structure, and a negative one a tension structure. Consequently,

$$\sum \bar{F}_i . \bar{r}_i = \sum X_j L_j + \sum P_i z_i \tag{3.7}$$

To minimize equation 3.7 it is necessary to relate X_j to P_i, z_i and L_j since X_j in fact depends on the others.

To this effect, it is often convenient to note (Fig. 3.1) that,

$$\sum Z_j = \sum P_i \tag{3.8}$$

and, since no bending is to be permitted to arise,

$$X_j = \frac{Z_j}{\tan \Phi_j} \tag{3.9}$$

while

$$\tan \Phi_j = f(z_i) \tag{3.10}$$

Classical method

As discussed earlier in this chapter, it is necessary when using the classical method, to utilize all the equations of equilibrium to reduce the variables in $\sum \bar{F}_i . \bar{r}_i$ to the minimum number of independent variables.

Let s be the total number of variables appearing in $\sum \bar{F}_i . \bar{r}_i$ and in the equilibrium constraint equations, and let r be the number of constraint equations. Then the minimum number of independent variables, n, in which $\sum \bar{F}_i . \bar{r}_i$ can be expressed is $n = s-r$.

After $\sum \bar{F}_i . \bar{r}_i$ is expressed in terms of these n number of variables, n additional equations are made available for obtaining the solution by letting

$$\frac{\partial(\sum \bar{F}_i . \bar{r}_i)}{\partial x_j} = 0 \ , \quad j = 1, 2, 3 \ldots \ n \qquad (3.11)$$

where x_j are the remaining n independent variables. Which variables are retained as independent is immaterial to the process, while the use of the equilibrium equations to drive out the s-n dependent variables insures that the solution vector will satisfy the equilibrium constraints.

However, there is no assurance that equations 3.11 will have a simultaneous solution within the feasible region, or even a solution at all. If the jth of equations 3.11 does not have a solution within the acceptable limits for the given variable, x_j, then the minimum $\sum \bar{F}_i . \bar{r}_i$ will be found at one of the limits for x_j (Burington (7)). When a simultaneous solution of equations 3.11 is not possible, or does not yield a solution in the feasible space, then the number of combinations to be investigated by separately testing the limits of each variable increases rapidly with the increase in the number of variables involved. Therefore, this method becomes very laborious if the statical equilibrium constraints are many, or if the number of independent variables (number of degrees of freedom) in $\sum \bar{F}_i . \bar{r}_i$ is greater than two.

For simple illustrative purposes consider the two-dimensional frames for Fig. 3.3 and Fig. 3.4. In both, it is assumed that the loads P_i and the dimensions L and x_i are given, but that the ordinates, z_i, are variable. The optimum z_i are to be found for minimum volume.

The $\sum \bar{F}_i . \bar{r}_i$ of the first frame (Fig. 3.3) can be expressed as

$$\sum \bar{F}_i . \bar{r}_i = X_0 L + P_1 z_1 + P_2 z_2 \qquad (3.12)$$

Equation 3.12 includes three variables (X_0, z_1 and z_2). The equations of statics will introduce three more variables (Z_0, Z_3 and X_3). Therefore, the total number of variables is six. There are three equations of statics. However, note that when all the members are assumed to be fully and homogeneously stressed, there will be no bending at points 1 and 2. The frame becomes a mechanism and consequently z_1 and z_2 must always be in proper proportion for the equivalent pin-connected frame to be in unstable equilibrium. Thus, the conditions that the moment at points 1 and 2 be zero provide two additional equations of statics for a total of five equations. Therefore, the optimization of this structure is a problem with only one degree of freedom (six variables minus five equations). Consequently, prior to the optimization of equation 3.12, all the equations of statics must be used to express equation 3.12 in terms of only one unknown.

For the second frame (Fig. 3.4), using node 0 as the origin, $\sum \bar{F}_i . \bar{r}_i$ can be expressed as

$$\sum \bar{F}_i . \bar{r}_i = X_2 L + P_1 z_1 - Z_2 z_2 \qquad (3.13)$$

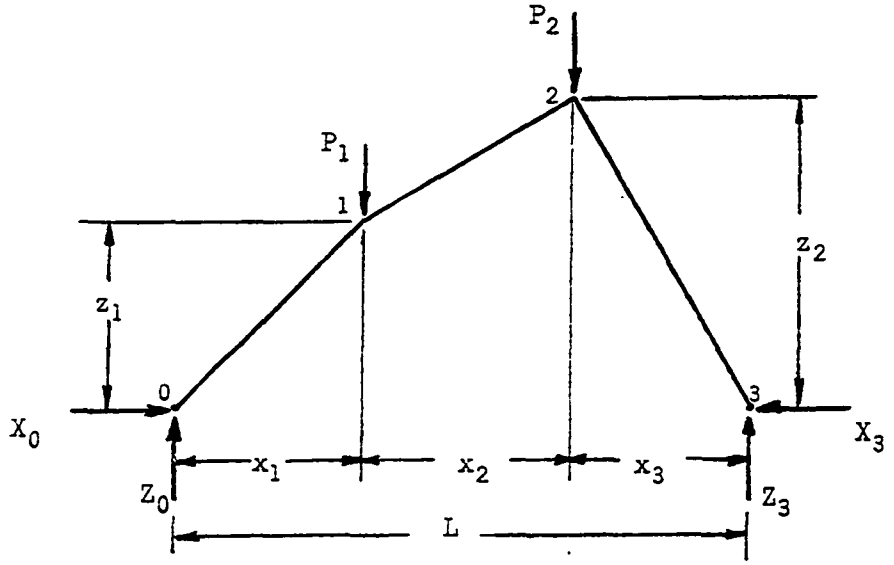

Fig. 3.3. Frame of one degree of freedom.

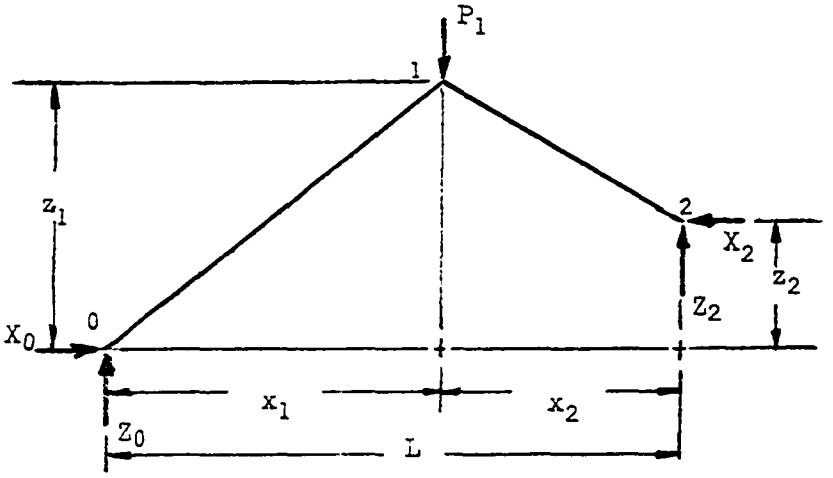

Fig. 3.4. Frame of two degrees of freedom.

Equation 3.13 includes four variables (X_2, Z_2, z_1, and z_2), and two more (X_0, Z_0) will be introduced by the equations of statics for a total of six variables. There are again three equations of statics, plus, this time the condition that the moment at point 1 be zero, for a total of four equations. The optimization of this frame has two degrees of freedom. The equations of statics must be used to express equation 3.13 in terms of only two variables prior to the optimization process.

It may be shown, performing the optimization of the second frame, that its optimal solution occurs when the two supports are at the same level (i.e. $z_2 = 0$), regardless of the horizontal position of point 1. This result may be used to illustrate an additional feature of the method. That is, if the class (within which the optimal solution is sought) is too broadly defined, the solution may converge on a structural form of greater efficiency (lesser volume), not itself a member of the desired class. (This result was noted by Prager (27) in connection with other optimization problems). Thus, if the structural form desired is one with z_2 equal to some finite value other than zero, then z_2 should have been so specified. Allowing z_2 to vary enlarges the class to a more general class (where all values of z_2 are permissible) and the solution will obviously be optimal for this larger class and not necessarily for the one desired. The restrictions necessary to sufficiently limit the class of structures to be considered are not so obvious in more complicated structures.

Nonlinear programming solutions

When the number of independent variables (and the equations of statics linking X_j, P_i and z_i as well) are too many, then a nonlinear programming solution becomes useful.

In applying such a solution, equation 3.7 expressing $\sum \bar{F}_i . \bar{r}_i$ in terms of X_j, P_i and z_i (or suitable alternatives) becomes the objective function to be minimized. There is no requirement to eliminate the dependent variables from the objective function. The equations of statics linking X_j, P_i and z_i become the constraints to be satisfied by the nonlinear programming technique while optimizing the objective function. Nonliner programming techniques are required because the constraints will, in general be nonlinear, involving products of variables.

Nonlinear programming solutions are interesting because conceptually, some side constraints such as buckling or other limiting factors could be added, if desired, to the constraints of statics. This, however, was not done on any of the examples of this dissertation.

Shell analogy solutions

When the grid system desired in the lattice makes the structure indeterminate, it is not possible, by means of only the equilibrium constraints (equation 3.2), to relate X_j, L_i, P_i and z_i as is necessary to ultimately express the objective function (equation 3.7) in terms of the required number of independent variables. It will then be necessary to include considerations of compatibility of deformations (equations 3.4) which in turn require an a priori definition of geometry and relative bar sizes.

Since all that is required is a method for linking X_j, L_j, P_i and z_i, an alternate approach is to use an analogous shell in place of the lattice structure. In so doing, the constraint conditions of the lattice programming problem are replaced by the equations of equilibrium applied to the shell, provided that the conditions required for the shell to be analogous to the lattice are satisfied.

Because of the specific use to be made of the analogy, the only conditions that must be satisfied are: 1) geometrical similarity and 2) force resultant correspondence. It is not necessary that strains in lattice and shell be analogous unless the same analogous shell is also to be used to investigate deformations or residual stresses in the unloaded lattice.

Geometric similarity is easily satisfied by assuming that the nodes of the lattice lie on the middle surface of the shell.

Force resultant correspondence is satisfied by 1) replacing the discontinuous loads (on the nodes of the lattice) by either line loads or distributed loads on the shell but with the same force resultants, and 2) by insisting that the resultants of the bar forces and of the shell tractions on the appropriate portion or element of the shell be the same.

The procedure to insure correspondence of the bar forces - shell traction resultants is very straight forward. It is primarily a geometrical procedure of assigning the bar fields, or portions of the shell whose traction resultant must equal the particular bar force or forces. For detailed discussions see Benjamin (3) or Parikh and Norris (26) who

also discuss strain correspondence.

The establishment of the analogy requirements, when coupled with the further requirements that equilibrium of the shell be satisfied, yields relationships between the stresses at each point throughout the shell. These relationships must be integrated to obtain a geometrical equation describing the shape of the shell. Finally, the equation of the shape of the shell is used in the objective function to reduce it to an expression in only one variable permitting the minimization of the objective function with respect to this one variable by classical mathematical methods.

Step by step the procedure is as follows:

1. Replace the load system on the lattice by the equivalent load system on the shell and rewrite $\sum \bar{F}_i . \bar{r}_i$.

2. Establish member force-shell traction requirements to be satisfied.

3. Assume all lattice members to be fully and homogeneously stressed, and check to see if this imposes any specific requirements on the shell tractions (i.e., if $N_1 = f(N_2)$).

4. If no requirements ensue from step 3, then it is believed that, when the loads are distributed over the surface of the shell, the assumption that $\sigma_1 = \sigma_2 = f_c$ will result in minimum lattice volume. This assumption is suggested since then the shape of the shell would be a "funicular" surface for the loads.

5. Either step 3 or step 4 will result in a mathematical equation linking N_1 and N_2, the shell tractions. Using this relationship, and using the three equations of equilibrium for each element of the shell

based on membrane theory, it is then possible and necessary to obtain a general expression for the shape of the shell (z = function of position on the shell). It is not necessary to consider compatibility constraints.

6. Rewrite $\sum \bar{F}_i.\bar{r}_i$ (equation 3.7) for the shell using the expression for z of step 5. After completion of this step $\sum \bar{F}_i.\bar{r}_i$ should now be expressed in terms of only one unknown, say the maximum ordinate (rise) in the shell.

7. Minimize $\sum \bar{F}_i.\bar{r}_i$ with respect to the remaining variable.

The completion of step 7 yields the optimum geometry for the lattice. For a final design, the shell stresses should be computed making use of the final geometry of the structure, and the relations of step 2 are then used to compute the bar forces in the lattice. Ultimately, of course, as in the other two methods, the equations of compatibility must be used to specify the unloaded configuration of the structure and its residual stresses in that state to be able to construct it.

In practical applications, step 5 usually will involve the use of numerical integration procedures.

To avoid the difficulties of numerical integration, it may be acceptable to assume that the optimum will be of a specific integrable shape (say paraboloidal, hyperboloidal, spherical). To do so, of course, limits the class of structures within which the optimum is to be found to the class selected (all members of the class of the same shape). Furthermore, such an assumption may be incompatible, in some cases, with the requirements of step 3, or with the requirement that all members of the lattice be homogeneously stressed. Such possibilities should be checked before proceeding with the assumed general shape.

It is noted that minimization of $\sum \bar{F}_i . \bar{r}_i$ of the analogous shell while yielding a least volume lattice (of that class) does not necessarily also minimize the volume of the shell itself. The least volume shell shape will be the same as the lattice (and obtainable by minimization of $\sum \bar{F}_i . \bar{r}_i$ alone) only if the shell is itself homogeneously and fully stressed. Shell volume minimization is discussed in a separate section in this chapter.

For comparison, in the examples of chapter five, the optimum geometry for lattices is found by consideration of both the lattice and the analogous shell. The corresponding lattice and shell volumes are compared therein.

Advantages and disadvantages of the methods

1. Classical method. This method is limited to consideration of a single system of loads and, from a practical point of view, to statically determinate structures. It becomes laborious when the equations of statical equilibrium are many or when the independent variables of the problem are more than two. Within the practical limitations on the number of variables, it is better than the other methods in that it yield a global optimum for the system of loads considered, and provides a "feel" for the increase in volume that may result from deviation from the optimal solution. This method would probably not be useful from a practical point of view if side constraints (buckling, etc.) are part of the problem.

2. Nonlinear programming method. This method, as presented here, is also limited to statically determinate structures and a single system of loads. It is particularly suited for the solution of problems with a

large number of variables and constraints. The solution formed through its use is also a global optimum, but there is no "feel" for the changes in the volume due to deviation from the optimal solution. It may be possible to modify and extend this method to adapt it to the consideration of additional side constraints and multiple systems of loads, but it is not clear whether expressing the objective function in terms of $\sum \bar{F}_i . \bar{r}_i$ will be advantageous in those cases.

3. Shell analogy method. This method is the only one of the three that is suitable for statically indeterminate structures. It is limited to a single system of loads. Since a specific class of shell (conoidal, paraboloidal, etc.) must be assumed to avoid numerical integration difficulties, the solution is optimal for only that class of lattice. The lattice therefore, is only optimal for all lattices with nodes similarly related and it is thus not a global optimum solution for the original problem. Nevertheless, information with respect to such restricted optimal solutions is useful when lacking a means to obtain a global optimum.

Considerations of the tension ring

The optimization process described herein assumes that the supports are able to resist the thrust of the dome or dome-like structures. It is only with this assumption that it is possible to design an all compression structure. Often, however, because of the nature of the media in which the supports are to be built, or because the structure is to be supported by columns or walls, no such requirements can be made

of the supports. Then, it is expedient to use a tension ring around the perimeter of the lattice or dome to take the horizontal components of the thrusts of the structure by pure tension. If the ring is considered as part of the structure, then the structure is really a composite of compression and tension members. Thus, it is pertinent to ask if this method of obtaining the optimal structural form for least all compressive volume does not do so at the expense of uneconomically large tension rings. This question will be pursued in this section.

Consider a generalized compression lattice with a tension ring. Such a structure is shown in Fig. 3.5 where the lattice and the ring are shown as two free body diagrams.

If the subscripts L, R and T denote the lattice, the ring and the total structure respectively, then, for the lattice

$$-f_c V_L = \left(\sum \bar{F}_i . \bar{r}_i \right)_L, \tag{3.14}$$

and for the ring,

$$f_t V_R = \left(\sum \bar{F}_i . \bar{r}_i \right)_R, \tag{3.15}$$

while, for the entire structure,

$$f_t V_R - f_c V_L = \left(\sum \bar{F}_i . \bar{r}_i \right)_T \tag{3.16}$$

In the above and throughout the rest of this section, since tension and compression members are involved, the sign convention for $\sum \bar{F}_i . \bar{r}_i$ will be as originally assumed (outward loads result in positive $\sum \bar{F}_i . \bar{r}_i$) and tension stresses are positive.

Comparing these three equations, it is obvious that

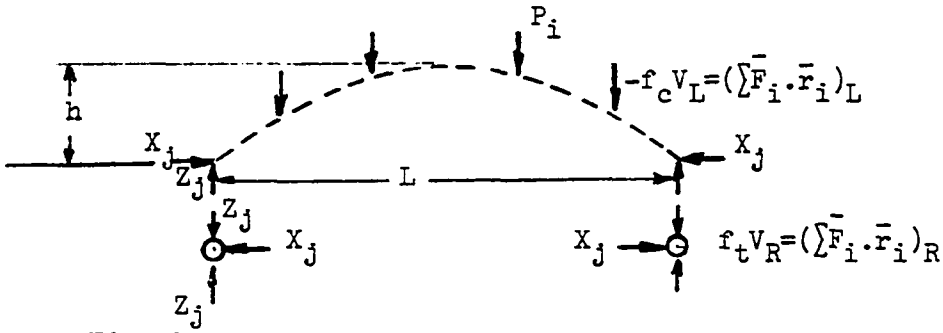

Fig. 3.5. Generalized compression lattice with tension ring.

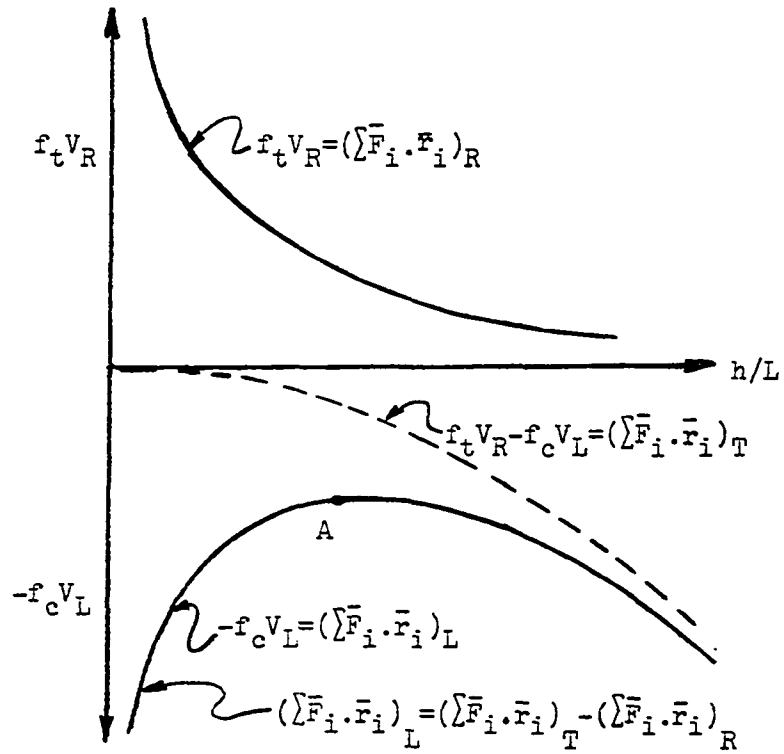

Fig. 3.6. Graphical representation of equations 3.14 through 3.18.

$$\left(\sum \bar{F}_i . \bar{r}_i \right)_T = \left(\sum \bar{F}_i . \bar{r}_i \right)_L + \left(\sum \bar{F}_i . \bar{r}_i \right)_R, \tag{3.17}$$

or

$$\left(\sum F_i . r_i \right)_L = \left(\sum F_i . r_i \right)_T - \left(\sum F_i . r_i \right)_R \tag{3.18}$$

The result of equation 3.18 can be verified by superposition of the force systems if it is noted that $\left(\sum \bar{F}_i . \bar{r}_i \right)_T$ results from consideration of the vertical forces alone, and $\left(\sum \bar{F}_i . \bar{r}_i \right)_L$ from both the vertical forces and the horizontal force system of the ring on the lattice. Equations 3.14 through 3.18 are graphically represented in Fig. 3.6 against varying rise-to-span ($^h/_L$) ratios of the generalized structure. Point A in that graph corresponds to the minimum volume lattice.

Fig. 3.7 shows a plot of the volumes of the lattice, the tension ring and the total structure. In Fig. 3.7, point A denotes the minimum volume lattice and point B the ring-lattice structure of minimum total volume. It is apparent that if the volume of the total structure is to be minimized, then the rise-to-span ratio must be increased beyond that of the minimum volume lattice. For lesser rise-to-span ratios, the thrusts are higher and thus both the volume of the lattice and the volume of the ring increase. Since the tangent to the V_L curve at A is zero, and V_R decreases with increasing rise-to-span ratios, it is always possible to decrease the total volume by small increases of the rise-to-span ratio. For larger increases of the rise-to-span ratios, however, the increase of the volume of the lattice quickly overtakes the reductions due to the lesser tension ring volume and the total volume begins to increase once more. Thus, if a tension ring is used, the possibility of decreasing the total volume of the structure by a small increase in the rise-to-span ratio should be investigated, even though the reduction of

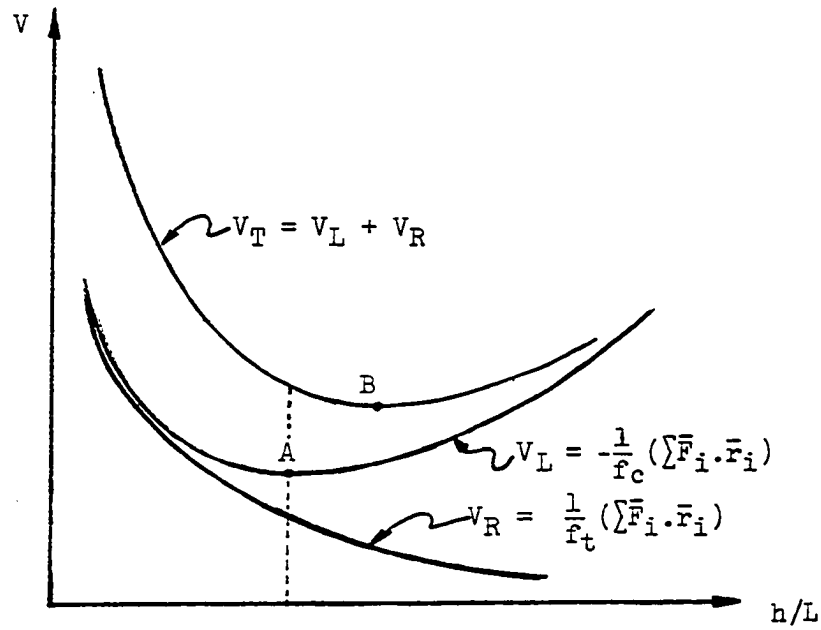

Fig. 3.7. Plot of the volumes of the lattice, the tension ring and the total structure versus rise-to-span ratio.

total volume thus achieved may not be too great. To find the point B at which the total volume is a minimum, the function to be minimized is $V_T = V_L + V_R$, and

$$V_T = \frac{1}{f_c}\left|\left(\sum \bar{F}_i \cdot \bar{r}_i\right)_L\right| + \frac{1}{f_t}\left|\left(\sum \bar{F}_i \cdot \bar{r}_i\right)_R\right|, \tag{3.19}$$

or,

$$V_T = \frac{1}{f_c}\left|\sum P_i z_i\right| + \left[\frac{f_t + f_c}{f_t f_c}\right]\left|\sum X_j L_j\right| \quad . \tag{3.20}$$

If the allowable tensile and compressive stresses of the material are numerically equal, then equation 3.20 reduces to

$$V_T = \frac{1}{f}\left\{\left|\sum P_i z_i\right| + 2\left|\sum X_j L_j\right|\right\} \quad . \tag{3.21}$$

Some of the examples of chapter four were optimized with and also without tension rings in order to illustrate the method and compare the results.

Shells Under a Membrane State of Stress

Shell examples presented

The illustrative examples of chapter four and five were selected primarily to illustrate the application of the methods developed in this chapter to the optimization of lattices. Therefore, the shell geometries considered therein are contingent upon the geometry of the lattice to which each serves as an analogy. Those examples, although not constituting an illustration of the methods to be suggested in this section for shell optimization, do illustrate most of the points discussed below.

The shell example of chapter four (a paraboloidal shell) is an

optimum within its class and serves to illustrate the procedures used when numerical integration is to be avoided. In that case the selection of an integrable shape (paraboloid) makes it impossible to have $\sigma_\theta = f_c$ everywhere. The resulting optimal solution (presented with and without tension ring) is optimal only with respect to all other paraboloidal shells supporting the same loads. It may be added that generally the easiest shapes to construct are those whose geometry can be expressed in closed form mathematical expressions.

Shells of absolute minimum volume

The expression, derived from the theorem of zero absolute potential energy, that will be used in the search for a minimum volume shell is

$$\int \sigma_1 \, dV + \int \sigma_2 \, dV = \sum \bar{F}_i . \bar{r}_i \tag{3.22}$$

When the shell is to support loads similar to those considered for lattices, equation 3.22 becomes

$$\int \sigma_1 \, dV + \int \sigma_2 \, dV = \sum X_j L_j + \sum P_i z_i, \tag{3.23}$$

where the summations of the right side are actually obtained by integration of the horizontal component of the shell force per unit length around the perimeter of the shell multiplied by the corresponding position vector, and by integration of the distributed load (assumed here to be distributed on the horizontal projection of the area) multiplied by the differential area of the shell over which it acts and by the corresponding position vector.

To obtain the global minimum shell to support a given system of loads, it follows from equation 3.23, and from the hierarchy of structures of

chapter two, that $\sigma_1 = \sigma_2 = f$ everywhere. In that case,

$$V_{min} = \frac{1}{2f} \left\{ \sum X_j L_j + \sum P_i z_i \right\}_{min} \qquad (3.24)$$

This volume, however, will be a global minimum only for the given $\sum X_j L_j$ and $\sum P_i z_i$. It may be that in order to force $\sigma_1 = \sigma_2 = f_c$ everywhere the horizontal reactions, and hence $\sum X_j L_j$, must be so increased that a lesser volume would result with a structure in which only σ_1 (or σ_2) is equal to f_c. The two structures cannot be considered comparable. In many practical cases the use of the equations of equilibrium (coupled with the requirement that $\sigma_1 = \sigma_2 = f_c$ (or f_t)) when substituted in equation 3.24, give rise to complicated differential equations which must be integrated prior to the optimization process. It is suspected that many of the resulting equations could only be integrated by numerical procedures. The integration is equivalent to finding the equation for the middle surface of the shell that would resist the given system of loads by constant stress, while the subsequent optimization is equivalent to finding the optimum rise-to-span ratio.

That shell or membrane structures under uniform biaxial compression or tension are inherently more efficient than other shell shapes is certainly not new. Thus, often use is made of spherical shapes for containers which must resist very high internal or external pressures, for example, gas containers, nuclear reactor containment vessels and deep depth submersibles. Otto (23) discussed the great efficiency of membranes, and as pointed out in chapter two, considers them as the lightest of all structural systems.

Many different investigators have obtained the geometries required for a shell or membrane to resist a given system of loads under constant membrane stress in all directions. Some achieve this by variability of the shape alone, the thickness being constant. Others have varied both the shape and thickness. For an example of the latter (attributed to W. Flugge), which was obtained by numerical integration, see Timoshenko and Woinowsky-Krieger (38).

To obtain the shape required for a uniform thickness and uniform stress shell, in 1959 Harrenstien (15) advanced the use of a soap film analogy when complex boundary shapes are involved. The shape of the soap film and of the shell are analogous, but the load on the soap film must be the reverse of that on the shell. Since the soap film supports the loads under constant tension, the shell similarly shaped and loaded with the reverse loads will support such loads by constant compression. A problem with such a method resides in the difficulty of applying suitable loads to the soap film (such as, for example, distributed loads acting in a vertical direction and not perpendicular to the surface of the soap film). Otto and Stromeyer (24) also used soap bubbles to determine suitable shapes for constant stress (tension) membranes. Brotchie (5) developed mathematical solutions for several direct design problems, some of which involve constant thickness and constant stress shells.

The most promising of all, however, is a finite element method of creating a mathematical membrane. The method was recently developed by Smith and Wilson (32) and is conceptually the same as Harrenstien's method mentioned above, but mathematically liberated from the physical

limitations of the soap film analogy. Smith and Wilson advocated the use of the method to obtain shapes of shells or of dams that are more efficient and hence of lesser volume. They were not assured, however, that they had in fact attained the least volume shape by their method alone. To choose the best among several shapes of the same class they actually computed and compared the volumes. It is felt that the theorem of zero absolute potential energy could enhance their method by providng the assurance required that the minimum shape has been obtained, while the concept of the minimization of $\sum \bar{F}_i.\bar{r}_i$ could be incorporated into their finite element formulation of the problem to yield, in one step, the least volume shape for the loads considered.

Least volume shells of integrable shapes

An optimum shell within a particular class of integrable shell shapes can be found by using a slightly different objective function. This function is obtained by rewriting equation 3.22 in the equivalent form,

$$V = \frac{1}{f_c} \sum \bar{F}_i.\bar{r}_i - \frac{1}{f_c} \int \sigma_2 \, dV \qquad (3.25)$$

where it is assumed that the thickness of the shell is so selected that $\sigma_1 \geq \sigma_2$ and $\sigma_1 = f_c$ everywhere. The minimum volume within such a class of shells would be one where the entire right hand side is minimized.

To minimize the right hand side, the only difficulty is the necessity to first integrate the second term. The expression of $\sum \bar{F}_i.\bar{r}_i$ in terms of the ordinates, z, is no problem since the equation for the shape of the shell is known.

The optimization should present no insurmountable difficulty if the

following procedure is followed.

1. Using the equations of equilibrium, determine which of the two tractions is larger for each region of the shell. Assume that $N_1 \geq N_2$ everywhere.

2. Proportion the shell so that $\sigma_1 = f_c$ everywhere. Then,

$$t_r = \frac{N_1}{f_c},$$

and, consequently

$$\sigma_2 = \frac{N_2}{t_r}$$

or,
$$\sigma_2 = \left(\frac{N_2}{N_1}\right) f_c \ . \tag{3.26}$$

3. Using the latter result in equation 3.25,

$$V = \frac{1}{f_c} \sum \bar{F}_i \cdot \bar{r}_i - \int \frac{N_2}{N_1} dV \tag{3.27}$$

4. The ratio N_2/N_1 will generally be a function which when multiplied by a suitabily selected expression for dV can be integrated to yield another function.

5. After the integration of step 4, it may be necessary to change the variable in either the resulting function or in $\sum \bar{F}_i \cdot \bar{r}_i$ so that the entire right hand side of equation 3.27 is expressed in terms of the same variable.

6. Minimize the entire right hand side with respect to the remaining variable.

Completion of step 6 results in the shape of the minimum shell of the class selected.

The paraboloidal shell example of chapter four illustrates this method.

Occasionally, the minimization of step 6 may be complicated as the resulting equation may be a transcendental equation. However, since the equation is of only one degree of freedom, a solution is readily obtained in that case by graphical methods. This was done in the last example of chapter five (although that example is one in which $\sigma_1 = \sigma_2 = f_c$).

CHAPTER FOUR - ILLUSTRATIVE EXAMPLES

General

The examples presented in this chapter are designed to illustrate the applicability of the methods developed in chapter three (classical method, numerical solution and shell analogy) to optimize latticed roof structures. Also presented is an example in which the optimization of a paraboloidal shell roof with and without tension ring is illustrated.

Since the aim of this chapter is to illustrate the methods, the structures considered are not necessarily practical structures. For simplicity of computations, the structures are optimized with respect to a downward load of total magnitude W which is assumed to be evenly distributed over the horizontal projection of each structure. Thus, extensive use is made of symmetry as appropriate to simplify the solutions.

The solution of each example is carried out to the point where the optimum geometry of the structure is determined. Thereafter, the process of design is considered a straight forward procedure which would include: 1) determination of specific geometry (bar areas, shell thickness, etc.), 2) determination of unloaded geometry and residual stresses (by the reverse deformation method of Rozvani (29)), and 3) modification of the design as appropriate to accommodate secondary loads.

Rectangular Grid Lattices

In this example, the general formulation of the classical and numerical solution to the optimization of a rectangular, fixed-jointed grid lattice covering a rectangular area will be considered first. These

methods will then be applied to a square grid lattice.

Typical formulation

Fig. 4.1 shows a typical rectangular grid in horizontal projection with the coordinate and numbering systems to be used.

Note that the assumption that the structure is fully and homogeneously stressed immediately simplifies the optimization problem. By this assumption, which is necessary if least volume is to be obtained (see chapter two), the indeterminate fixed-jointed grid is rendered to be in unstable equilibrium with the design load.

It is pertinent to investigate the degrees of freedom of such a structure since, as discussed in chapter three, $\sum \bar{F}_i . \bar{r}_i$ must be expressed in terms of only the correct number of independent variables (by using all available equations of statics or geometry) prior to the minimization process, to insure that the solution will satisfy geometry and statics. The number of unknowns include:

1) two reaction components per reaction point (X and Z, or Y and Z), or 4 (m + n) reaction components;

2) one z coordinate for each interior node, ij, or m(n) z coordinates; and

3) two force components (T_z and T_x, or T_z and T_y) for each member, or a total of $2[(m + 1) n + (n + 1) m]$ force components;

or a grand-total of $5 (m) n + 6 m + 6 n$ unknowns.

The number of equations available include:

1) two equations of equilibrium at each reaction point, or 4 (m + n) equations;

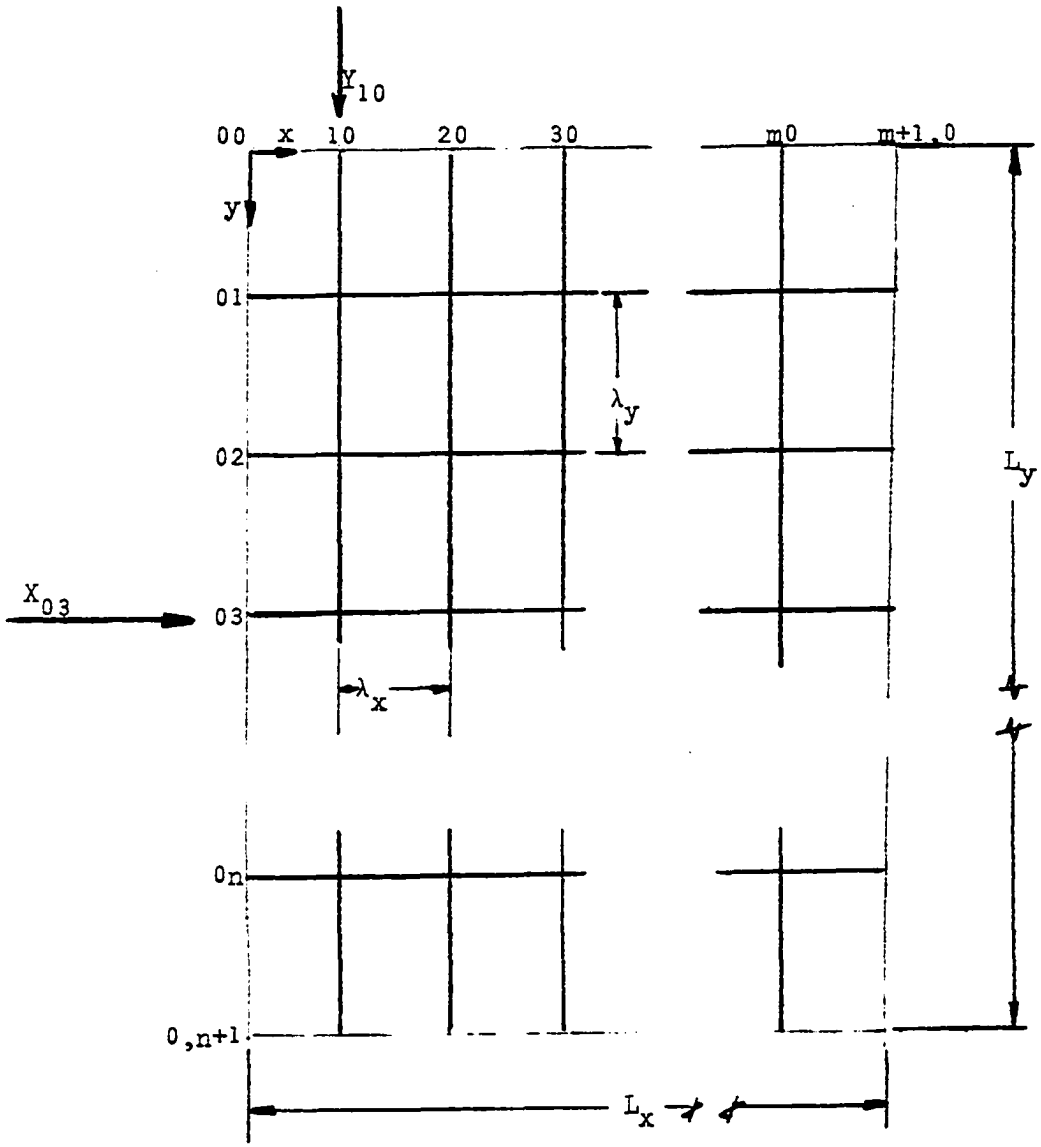

Fig. 4.1. Typical rectangular grid.

2) three equations of equilibrium at each interior point, or 3 m (n) equations; and

3) one equation per member relating its force components, T_z and T_x (or T_z and T_y) with the horizontal (λ_x or λ_y) and vertical projections of the member, or (m + 1) n + (n + 1) m equations; or a total of 5 (m) n + 5 m + 5n equations.

Thus, in the general case, subtracting the equations from the unknowns, such a rectangular grid lattice has m + n degrees of freedom.

When using the classical method it is necessary to write the usual objective function (volume) in terms of $\sum \bar{F}_i.\bar{r}_i$ and to use all the available equations to reduce the unknowns in $\sum \bar{F}_i.\bar{r}_i$ to only a number of unknowns equal to the number of degrees of freedom. The expression can then be minimized by classical methods. Alternately the original expression for $\sum \bar{F}_i.\bar{r}_i$ can be minimized by programming procedures. Both these methods will be illustrated.

The general forms of the equations are:

1) For the objective function,

$$V = \frac{1}{f_c} \sum \bar{F}_i.\bar{r}_i = \frac{1}{f_c} \{ L_x \sum X_{ij} + L_y \sum Y_{ij} + \sum P_{ij} z_{ij} \} \qquad (4.1)$$

2) For the equations of equilibrium at the reaction points,

$$Z_{ij} - T_{z_{ij,(i+1,j)}} = 0 \qquad (4.2)$$

$$X_{ij} - T_{x_{ij,(i+1,j)}} = 0 \qquad (4.3)$$

and similar equations for the y grid lines.

3) For the equations of equilibrium of interior points,

$$\left.\begin{aligned} T_{x_{(i-1,j),ij}} - T_{x_{ij,(i+1,j)}} &= 0 \\ T_{y_{(i,j-1),ij}} - T_{y_{ij,(i,j+1)}} &= 0 \end{aligned}\right\} \qquad (4.4)$$

$$T_{z_{(i-1,j),ij}} + T_{z_{(i,j-1),ij}} - T_{z_{ij,(i+1,j)}} - T_{z_{ij,(i,j+1)}} - P_{ij} = 0 \qquad (4.5)$$

where all bar forces, T, are assumed positive if compressive.

4) For the equations of geometry for each member in the x-grid lines,

$$[T_{x_{ij,(i+1,j)}}][z_{i+1,j} - z_{ij}] - \lambda_x [T_{z_{ij,(i+1,j)}}] = 0, \qquad (4.6)$$

and a similar equation for each member in the y grid lines.

In the above equations the sign convention adopted, to simplify computer applications is that the loads act vertically down and the reactions are up and inwardly directed, while all the members are assumed to be in compression. Then all the variables in the equations are positive.

Note that the volume could also be minimized by expressing the objective function as

$$V = \sum a_i \ell_i,$$

where a_i and ℓ_i are respectively the area and the length of each member. Such formulation was used for example by Schmit and Kicher (31) and by Crockett (11) for three bar trusses. However, the use of such straight forward formulation introduces two additional unknowns per member, and consequently, increases the number of constraint equations by twice the number of members in the structure.

Classical solution

For simplicity the lattice to be optimized will be a square lattice consisting of 4 x 4 grid lines subjected to a total load, W, horizontally distributed and allocated equally to each node. Thus, each interior node carries an equal load, P = W/25, while a load of W/100 passes directly to each corner support point, and W/50 to other support points. These loads on the supports will be ignored. Such a lattice is shown in Fig. 4.2. Because of symmetry only one-eighth of the lattice as shown in Fig. 4.3 need be considered. Such a structure, after the use of all the conditions of symmetry, can be shown to have two degrees of freedom.

It is convenient to introduce two more unknowns P_1 and z_{4_1} where P_1 is the portion of the load P taken by grid line 1 and z_{4_1} is the ordinate of point 4 in grid line 1. This frees the two grid lines for independent application of the equations of statics. Two other equations must be added also and they are:

$$P_1 + P_2 = P, \text{ and } z_{4_1} = z_{4_2} = z_4$$

where the subscripts 1 and 2 refer to grid lines 1 and 2.

Using these and all the equations generated by equations 4.2 through 4.6, equation 4.1 can be reduced to

$$V = \frac{P}{f_c}\left(14z_4 + \frac{2Pz_4}{P + 4P_1} + \frac{4Pz_4}{3P - 2P_1} + \frac{8L^2}{5z_4} + \frac{4P_1L^2}{5Pz_4} \right) \qquad (4.7)$$

where the two remaining independent variables are P_1 and z_4.

Using the classical method, V_{min} occurs when,

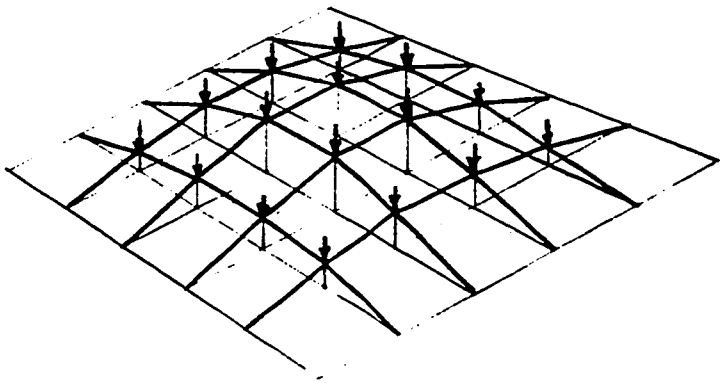

Fig. 4.2. Lattice to be considered.

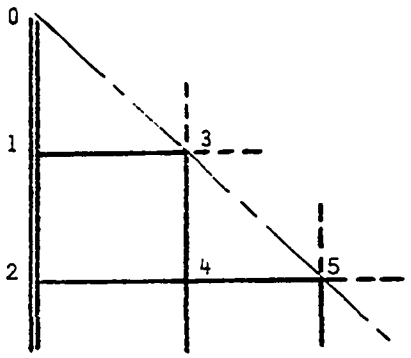

Fig. 4.3. One-eighth of the lattice remaining after the use of symmetry.

$$\frac{\partial V}{\partial P_1} = \frac{P}{f_c}\left[- \frac{8Pz_4}{(P+4P_1)} + \frac{8Pz_4}{(3P-2P_1)} + \frac{4L^2}{5Pz_4} \right] \geq 0, \qquad (4.8)$$

$$\frac{\partial V}{\partial z_4} = \frac{P}{f_c}\left[14 + \frac{2P}{P+4P_1} + \frac{4P}{3P-2P_1} - \frac{8L^2}{5(z_4)^2} - \frac{4PL^2}{5P(z_4)^2}\right] = 0. \qquad (4.9)$$

The two equations 4.8 and 4.9 may have no solution within the permissible range of values for z_4 and P_1 ($z_4 \geq 0$ and $0 \leq P_1 \leq P$). Then, the minimum volume within the acceptable or feasible region will be found at one of the limits (i.e. $z_4 = 0$ or $z_4 = \infty$ and $P_1 = 0$ or $P_1 = P$).

The least volume structure, if it exists, must satisfy equation 4.9 since it is obvious, from equation 4.7, that $z_4 = 0$ or $z_4 = \infty$ yield infinite solutions. Thus, either equation 4.8 must also be satisfied or the minimum will be found at $P_1 = 0$ or $P_1 = P$.

Evaluation of equation 4.8 at $P_1 = P$ shows that it is positive for all values of z_4. Therefore the volume decreases with decreasing P_1 in the vicinity of that limit and the least volume solution is not to be found there but with lesser values of P_1.

Evaluation of equation 4.8 at $P_1 = 0$ and consideration of its derivative with respect to z_4 shows that it does not change sign between $P_1 = 0$ and $P_1 = P$ for all values of z_4 such that

$$z_4 < L\sqrt{\frac{9}{80}} = L\ (0.335410197).$$

Consequently, only two possibilities remain, either 1) the two equations have a common solution at a z_4 value equal to or greater than the one just given, or 2) $P_1 = 0$ and equation 4.9 is satisfied with $P_1 = 0$ and z_4 less than the given value. It can be verified that the

second possibility applies, and consequently, the minimum volume is obtained when,

$$P_1 = 0, \text{ and } z_4 = L\sqrt{\frac{6}{65}} = L\ (0.30382181) \tag{4.10}$$

Using these values, equations 4.2 through 4.6 can be used to obtain the value of all the other variables. Among them,

$$\left.\begin{aligned} z_3 &= L\sqrt{\frac{6}{65}} \\ \text{and,} \\ z_5 &= 4L\sqrt{\frac{2}{195}}, \end{aligned}\right\} \tag{4.11}$$

and, from equation 4.7

$$V_{min} = \frac{PL}{f_c}\left(16\sqrt{\frac{13}{30}}\right) \tag{4.12}$$

A three-dimensional plot of the surface defining the volume, V, in terms of P_1 and z_4 is shown in Fig. 4.4. The volume, V, is plotted versus z_4 for several values of P_1 between $P_1 = 0$ and $P_1 = P$ in Fig. 4.5. A similar plot of V versus P_1 for several values of z_4 appears in Fig. 4.6. (These three plots were obtained using a program for an IBM 360 computer which computed the value of the volume for discrete values of z_4 and P_1 within the range desired for them and then produced three-dimensional views of the surface as it would appear when viewed from any specified combination of viewing angles.) In all three plots point A is the value of z_4 at or above which $(\partial V/\partial P_1) = 0$ has a solution within the limits of P_1. Point B corresponds to the global minimum (within the feasible space) represented by the values given by equation 4.10.

Fig. 4.7 shows the shape of the minimum volume lattice.

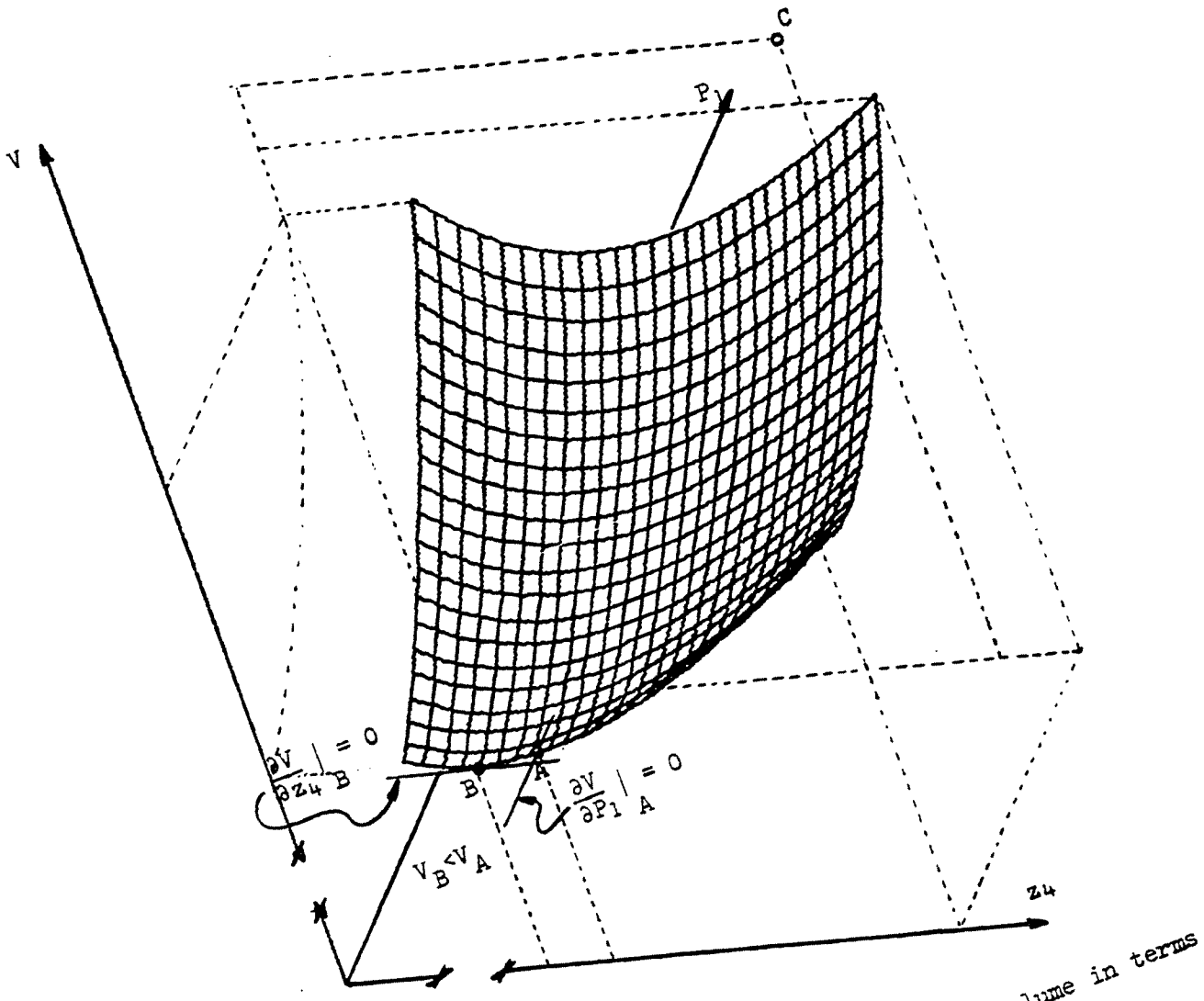

Fig. 4.4. Three-dimensional plot of the volume in terms of z_4 and P_1.

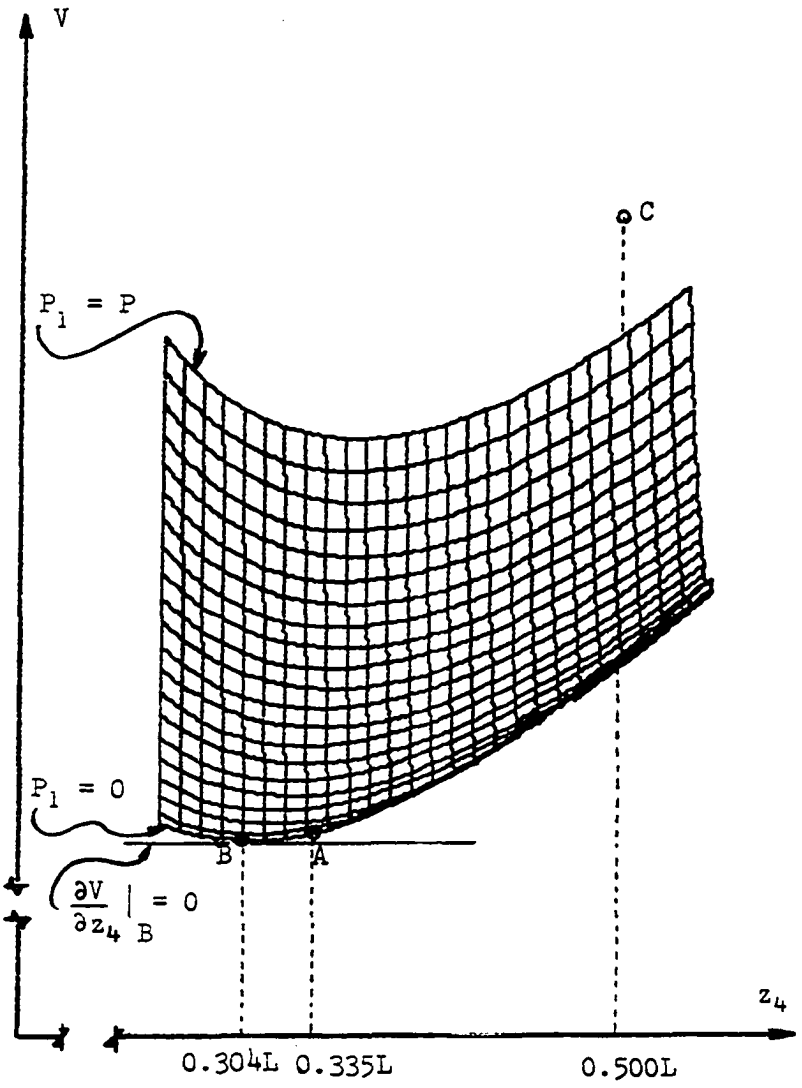

Fig. 4.5. Plot of the volume versus z_4 for several P_1.

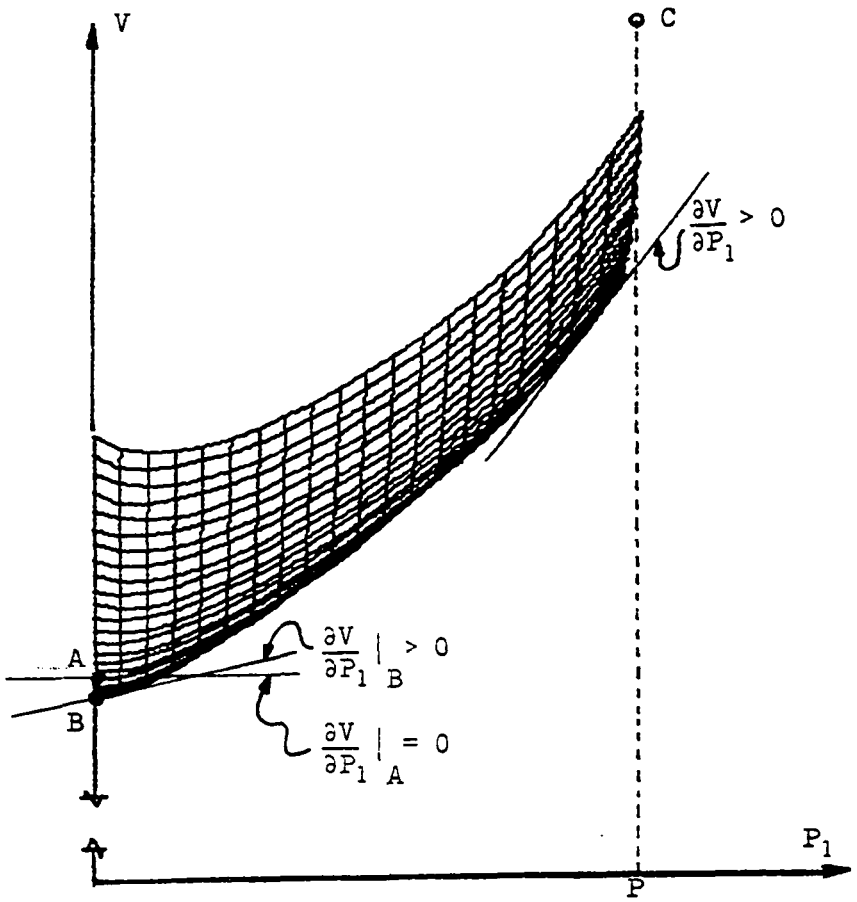

Fig. 4.6. Plot of the volume versus P_1 for several z_4.

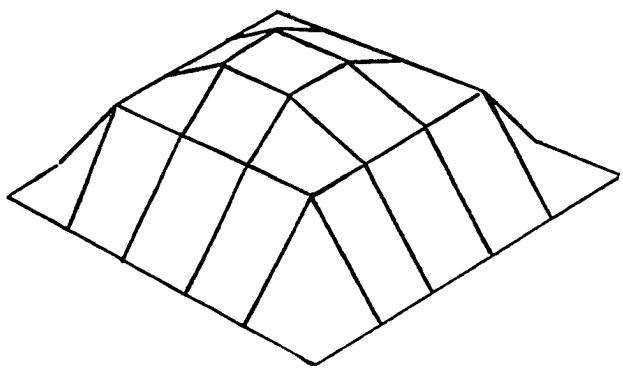

Fig. 4.7. Minimum volume lattice.

Nonlinear programming solution

The use of a numerical procedure permits the optimization of equation 4.1 (the objective function) subject to the satisfaction of all the equations of statics and geometry, equations 4.2 through 4.6 (the constraints), without having to manipulate all the equations to express the objective function in terms of only the proper number of independent variables.

The program selected for use was AUKLET, written by Sposito and Soults (35), which, is based on the sequential unconstrained minimization technique developed by Fiacco and McCormick (13).

The program requires as input all of the equations defining the problem (objective and constraint equations) as well as their first and second partial derivatives. To avoid overflowing the computer data bank assigned by the program, and to reduce the laboriousness of preparing the input data, it was decided to use symmetry for the computer solution as well. Furthermore, a separate subroutine was used to develop and feed the computer the partial derivatives. In addition, 1) equations 4.2 were eliminated by eliminating Z_{ij} from the set of variables since it does not appear in any other equations nor in the objective function; 2) equations 4.3 and 4.4 were eliminated (since it is obvious that they generate the requirement that all T_x and all T_y be equal to the X or Y value of that particular grid line) by replacing T_x and T_y in equation 4.6 with the corresponding X and Y values.

Thus, the set of constraint equations consisted of the three equations 4.5 of vertical equilibrium (one at each of the three nodes), and a

geometric equation 4.6 for each of the four remaining members with vertical force components (numbers 13, 24, 34 and 45). The number of equations (seven) is seen to be the correct number needed since nine unknowns remain, namely X_1, X_2, z_3, z_4, z_5, $T_{Z_{13}}$, $T_{Z_{24}}$, $T_{Z_{34}}$ and $T_{Z_{45}}$, of which only the first five appear in the objective function.

For the computer solution the unknowns were non-dimensionalized by dividing all the variables (and equations) by L or P as appropriate, and numbered X (i) where i varies from 1 through 9 in the same order as they appear in the previous paragraph (ie X (4) = z_4 and X (7) = $T_{Z_{24}}$).

Two problems were encountered with the computer use of the program due to the unusual character of the feasible region defined by the constraint equations. The character of the feasible space, presently to be discussed, made it necessary to provide the computer an initial feasible solution (one satisfying all the constraint equations), and eventually to modify the constraint equations.

The program is designed for a convex feasible space. A convex space is one in which if a line connects two points belonging to the space, then all points on the line must also belong to the same space. Each constraint which is expressed in terms of an equality violates the convexity requirement since it describes a curve in two-dimensional space (if it contains two variables), a surface in three-dimensional space (if it contains three variables), and so on. The standard practice in the case of such a constraint is to expand the space corresponding to that particular constraint by replacing it by two constraints, a negative and a positive one each with some slack. For example, the constraint,

$$g(x_i) = 0 \qquad (4.13)$$

would be replaced by

$$g(x_i) + \varepsilon_1 \geq 0 \quad \text{and,} \quad -g(x_i) + \varepsilon_2 \geq 0 \tag{4.14}$$

where ε_1 and ε_2 are small quantities. In effect the surface is given a thickness of $\varepsilon_1 + \varepsilon_2$.

In this problem, however, all the constraints are equalities. Consequently, the space is so restricted that the expansion made by replacing all constraints by two equations similar to equations 4.14 still rendered the computer unable to generate its own ititial feasible solution from which to begin the iterative search, and unable to generate a second feasible solution once given an initial feasible solution (except in one instance).

To surmount this difficulty, the feasible space was expanded by simply replacing all equality constraints (all of them) similar to equation 4.13 by

$$g(x_i) \geq 0. \tag{4.15}$$

Since the optimum is expected to lie on the boundary of the feasible space, and since the equalities condition of equations 4.15 will then hold, it was expected that the optimum for the expanded feasible space would be the same as for the original more restricted space. That all equalities be satisfied in the final solution could be verified by making sure that the values of all the constraint equations (which are part of the standard output of the program) be suitably close to zero.

The expansion of the feasible space could also have been used to advantage in computing the initial feasible solution since the modified constraint equations 4.14 could be readily satisfied. In fact, it may be

better to do so in other cases since a solution satisfying the equalities within normal accuracies may be slightly outside of the feasible space due to round-off errors, thus hanging-up the computer. In this case, however, since a feasible solution could be readily obtained, and it was desired to start the computer far from the optimum, it was decided to first generate an initial point satisfying the equalities. This was easily done by choosing an arbitrary value for P_1, directly evaluating all the vertical shears, $T_{Z_{13}}$, $T_{Z_{24}}$, $T_{Z_{34}}$ and $T_{Z_{45}}$), and using geometry and the equations of equilibrium to compute X_1, X_2, z_3, z_4 and z_5.

From the classical solution it was known that at the optimum $P_1 = 0$. Thus to be far from the origin an initial value of $P_1 = P$ was assumed. Then, to insure that the point was well within the feasible region, z_4 was arbitrarily increased by adding 0.2 to it alone to make it 1.2. The initial feasible point could thus be depicted as point C in Figs. 4.4, 4.5 and 4.6. The initial feasible solution, the computer obtained solution and the exact solution from the classical method are shown in Table 4.1.

The accuracy of the numerical optimization solution (to six significant figures in most cases) can be seen to be more than adequate for most practical purposes. Greater accuracy could be obtained if required by modifying the convergence criteria used by the program to end the iterations.

The values of the constraints for this final solution are all less than 1×10^{-7} verifying that all the equalities are satisfied. That the solution found is a global minimum can thus be assured, and further

Table 4.1. Least volume square lattice

Variable	Initial Feasible Point, ($P_1 = P$)	Computer Found Optimum[a]	Exact Analytical Optimum[b]
$X(1) = (X_1/P)$	1.0	0.32914088	0.32914029
$X(2) = (X_2/P)$	0.2	0.98742059	0.98742088
$X(3) = (z_3/L)$	0.3	0.30382146	0.30382181
$X(4) = (z_4/L)$	0.5	0.30382195	0.30382181
$X(5) = (z_5/L)$	1.2[c]	0.40509601	0.40509575
$X(6) = (T_{Z_{13}}/P)$	1.5	0.50000015	0.50000000
$X(7) = (T_{Z_{24}}/P)$	0.5	1.50000001	1.50000000
$X(8) = (T_{Z_{34}}/P)$	1.0	4.94×10^{-8}	0.00000000
$X(9) = (T_{Z_{45}}/P)$	0.5	0.50000009	0.50000000
$F(X) = (V_{min} \times \frac{8PL}{f_c})$	1.85[d]	1.3165614	1.31656118

[a] Iterations = 39. CPU Time = 6.6 sec. I/O Time = 13.8 sec. Region Used = 152K.

[b] Computed from analytical solution (equations 4.10, 4.11 and 4.12) by taking square roots of ratios of whole numbers.

[c] Increased by 0.2 from value of 1.0 which satisfies the equalities to insure that point is well into the feasible region.

[d] Increased by 0.10 to correspond with increase of X(5).

verified by noting that the value of the dual objective function at this last point was 1.3165617 (in agreement with the primal objective function to seven significant figures).

Network Domes

General

The optimization techniques developed in this thesis are particularly useful in the optimization of dome like lattices. Some domes, for example a Schwedler dome with two diagonals in every bay, are indeterminate even after all joints are assumed to be pin-connected and thus require the use of the shell analogy method. The network dome, however, is a type of dome which is determinate, and stable if it has an odd number of sides (Benjamin (3)). A typical network dome of five sides is shown in Fig. 4.8. The dome illustrated has two levels above the supports and an open top.

This section will synthesize a least volume network dome optimized for a vertical load of total magnitude W assumed to be evenly distributed over the horizontal projection of the dome. The dome selected will have nine sides and five levels above the supports including the peak center point, as the dome will have a closed top. The dome will be optimized using the nonlinear programming method.

Typical formulation

A partial plan view of the network dome to be optimized is shown in Fig. 4.9 where the node numbering system to be used is indicated. The nodes are evenly spaced from the center to the supports, so that the in-

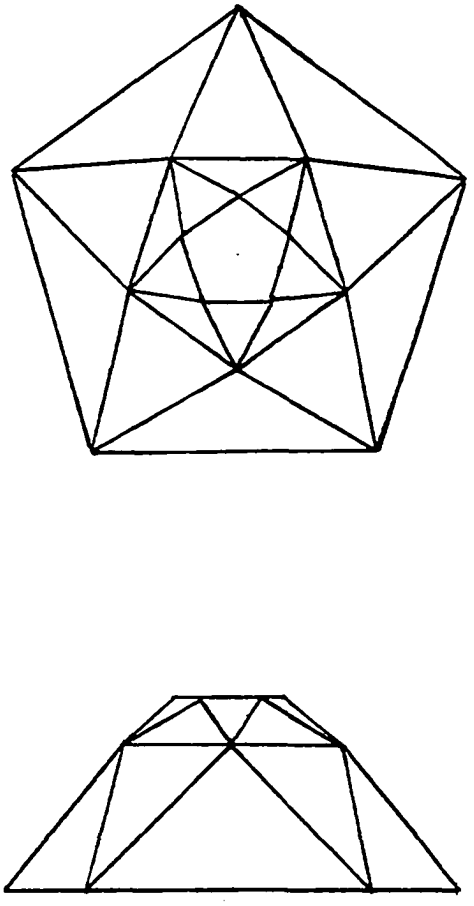

Fig. 4.8. Typical network dome.

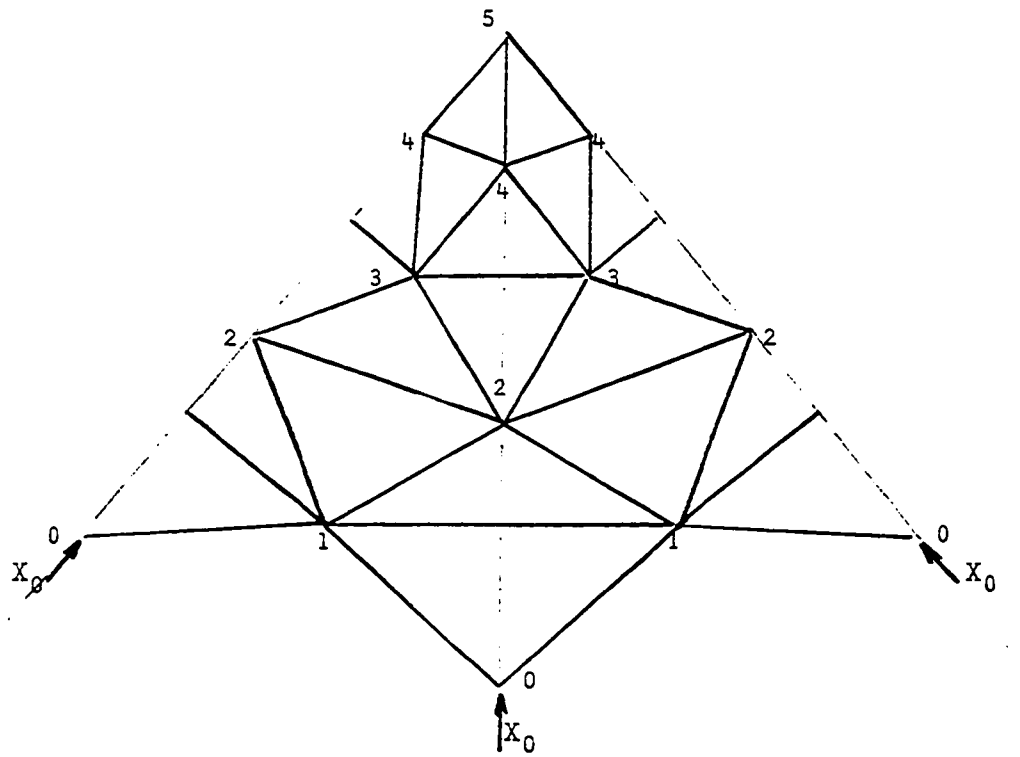

Fig. 4.9. Partial plan view of dome to be optimized.

cremental radial distance from a node in one level to the next is $r_0/5$ where r_0 is the radius to the support points, 0.

Because of symmetry, only one-ninth of the structure including one node of each type need be considered.

The load applied at each node corresponds to the load on the horizontal area bounded by two meridians drawn through the midpoints between that node and the adjacent nodes on the same level, and by two arcs drawn at the midpoints between that node and nodes of adjacent levels. Thus,

$$P_5 = \left\{ \frac{W}{2\pi r_0^2} \right\} \frac{2\pi (r_0/10)^2}{9} = \frac{W}{900} \tag{4.16}$$

where P_5 is the portion of the load at node 5 on the one-ninth portion of the structure to be considered. It can be similarly shown that

$$\left.\begin{aligned} P_4 &= 8\, P_5, \\ P_3 &= 16\, P_5, \\ P_2 &= 24\, P_5, \\ P_1 &= 32\, P_5. \end{aligned}\right\} \tag{4.17}$$

The objective function to be optimized, using the theorem of zero absolute potential energy is

$$\begin{aligned} V_{min} &= \left\{ \frac{1}{f_c} \sum \bar{F}_i \cdot \bar{r}_i \right\}_{min} \\ V_{min} &= \frac{9}{f_c} \left(X_0\, r_0 + \sum P_i\, z_i \right)_{min}, \quad i = 1,2,\ldots 5 \end{aligned} \tag{4.18}$$

where X_0 is the horizontal component of the reactions at nodes 0, and z_i is the vertical height of node i measured from the level of the supports.

It is convenient, for computer applications to convert equation 4.18 to a nondimensional expression. This can be done by dividing throughout

by factoring out the term $P_5 r_0$. Doing so, and making use of expressions 4.16 and 4.17, the objective function, equation 4.18, becomes,

$$V_{min} = \frac{Wr_0}{100 f_c} \left\{ \left(\frac{X_0}{P_5}\right) + 32\left(\frac{z_1}{r_0}\right) + 24\left(\frac{z_2}{r_0}\right) + 16\left(\frac{z_3}{r_0}\right) + 8\left(\frac{z_4}{r_0}\right) + \left(\frac{z_5}{r_0}\right) \right\}_{min} \tag{4.19}$$

where it is only necessary to minimize the nondimensional expression inside the brackets.

Since the structure, when assumed to be pin-connected, is stable (and determinate) it is expected that the problem will be of five degrees of freedom. This is surmised since each z_i can be independently varied and the equilibrium constraints can still be satisfied. This will be verified by consideration of the total number of variables and the total number of equations available.

Prior to a consideration of the equations of equilibrium, it is useful to write some general geometric expressions for the tangential, radial and vertical components of lengths of the members, which may later on be combined to yield direction cosines as needed. For this purpose, let L represent length, subscripted by T, R and Z when the tangential, radial and vertical components are meant. Each member will be labeled by the numbers of the two nodes it joins, and superscripts will be used to denote the node at which the component is computed. Then, the total lengths L_{ii} and L_{ij} are,

$$\left.\begin{aligned} L_{ii} &= r_i \sin 20^\circ \\ \text{or,} \quad L_{ii} &= \sqrt{(L_{R_{ii}})^2 + (L_{T_{ii}})^2} \quad , \end{aligned}\right\} \tag{4.20}$$

$$\left.\begin{aligned} \text{and,}\quad L_{ij} &= \sqrt{\left[\left(L^{i}_{R_{ij}}\right)^2 + \left(L^{i}_{T_{ij}}\right)^2\right] + \left(L_{Z_{ij}}\right)^2}\,, \\ \text{or}\quad L_{ij} &= \sqrt{\left[\left(L^{j}_{R_{ij}}\right)^2 + \left(L^{j}_{T_{ij}}\right)^2\right] + \left(L_{Z_{ij}}\right)^2}\,, \end{aligned}\right\} \qquad (4.21)$$

where the quantities in brackets are constant even though

$$L^{i}_{R_{ij}} \neq L^{j}_{R_{ij}} \quad \text{and} \quad L^{i}_{T_{ij}} \neq L^{j}_{T_{ij}}.$$

Furthermore, for i = 0, 1,2...4 and j = 1,2...4,

$$\left.\begin{aligned} L_{T_{jj}} &= L_{jj} \cos 20^{\circ}, \\ L^{i}_{T_{ij}} &= r_i \sin 20^{\circ}, \\ L^{j}_{T_{ij}} &= r_j \sin 20^{\circ}; \end{aligned}\right\} \qquad (4.22)$$

$$\left.\begin{aligned} \text{while}\quad L_{R_{jj}} &= L_{jj} \sin 20^{\circ}, \\ L^{i}_{R_{ij}} &= r_i - r_j \cos 20^{\circ}, \\ L^{j}_{R_{ij}} &= r_i \cos 20^{\circ} - r_j; \end{aligned}\right\} \qquad (4.23)$$

$$\left.\begin{aligned} L_{Z_{jj}} &= 0, \\ \text{and}\quad L_{Z_{ij}} &= z_j - z_i. \end{aligned}\right\} \qquad (4.24)$$

Member 45 is a special case for which

$$\left.\begin{aligned} L_{T_{45}} &= 0, \\ L_{R_{45}} &= (r_0/5), \\ \text{and,}\quad L_{Z_{45}} &= z_5 - z_4. \end{aligned}\right\} \qquad (4.25)$$

In all these only $L_{Z_{ij}}$ involve variables (z_i).

There are in general three equations of equilibrium to be satisfied at each node. However, the equilibrium of forces in a tangential direction will be automatically satisfied by symmetry at every node, as will the equilibrium of forces in a radial direction at node 5. In addition, the equilibrium of forces in a vertical direction at node 0 is not needed since the vertical reaction needs not be computed and it does not appear in any other equations.

Using T to denote the force in each bar (positive if compressive), and letting the subscripts and superscripts have the same meanings as above, the equations of equilibrium are then, 1) considering equilibrium of vertical forces

$$\left.\begin{aligned} &\text{at node 5, } T_{Z_{45}} - P_5 = 0, \\ &\text{at node 4, } 2T_{Z_{34}} - T_{Z_{45}} - P_4 = 0, \\ &\text{at node j, } 2T_{Z_{j-1,j}} - 2T_{Z_{j,j+1}} - P_j = 0, \; j=1,2,3; \end{aligned}\right\} \qquad (4.26)$$

and, 2) considering equilibrium of forces in the radial direction.

$$\left.\begin{aligned} &\text{at node 4, } 2\,T^4_{R_{34}} - 2\,T_{R_{44}} - T_{R_{45}} = 0, \\ &\text{at node j, } T^j_{R_{j-1,j}} - T_{R_{jj}} - T^j_{R_{j,j+1}} = 0, \; j=1,2,3 \\ &\text{and, at node 0, } 2T^0_{R_{01}} - X_0 = 0. \end{aligned}\right\} \qquad (4.27)$$

In addition, it is necessary to insist that there be no bending in any bar (or joint). Thus, the force components in the bars must be related as follows:

$$\frac{T_{R_{ij}}^{i}}{L_{R_{ij}}^{i}} = \frac{T_{Z_{ij}}}{L_{Z_{ij}}} = \frac{T_{R_{ij}}^{i}}{L_{R_{ij}}^{j}} \tag{4.28}$$

Member 45 has only one radial component whether computed at node 4 or 5. Consequently equation 4.28 gives only one equation for member 45. For each of the other inclined members, equation 4.28 gives rise to two equations one pairing the first two terms and the other one pairing the last two terms. Using equations 4.23, 4.24 and 4.25 in equations 4.28, and expanding, one obtains

$$\left.\begin{aligned}
&\text{for member 45, } (T_{R_{45}})\, z_5 - (T_{R_{45}})\, z_4 - (T_{Z_{45}})\,(r_0/5) = 0,\\
&\text{for member ij } (T_{R_{ij}}^{j})\, z_j - (T_{R_{ij}}^{j})\, z_i - (T_{Z_{ij}})\,(r_i \cos 20^\circ - r_j) = 0,\\
&\text{and, } (T_{R_{ij}}^{i})\, z_j - (T_{R_{ij}}^{i})\, z_i - (T_{Z_{ij}})\,(r_i - r_j \cos 20^\circ) = 0,
\end{aligned}\right\}$$

where $i = 0,1,\ldots 3$ and $j = 1,2,\ldots 4$. (4.29)

Equations 4.26 (five equations), 4.27 (five equations), and 4.29 (nine equations) comprise the needed equations of equilibrium, a total of nineteen equations. For computer applications, it is convenient to non-dimensionalize them by dividing equations 4.26 and 4.27 by P_5, and dividing equations 4.29 by $P_5\, r_0$.

A total number of 24 variables appear in the objective and constraint equations. The number of degrees of freedom is then five (24-19), as expected. For the numerical optimization process the variables will be labeled as follows:

$X(1)$ through $X(5)$ = (z_i/r_0) through (z_5/r_0)

$X(6)$ = (X_0/P_5)

$X(7)$ through $X(10)$ = $(T_{R_{11}}/P_5)$ through $(T_{R_{44}}/P_5)$

$X(11)$through $X(14)$ = $(T^0_{R_{01}}/P_5)$ through $(T^3_{R_{34}}/P_5)$

$X(15)$ = $(T_{R_{45}}/P_5)$

$X(16)$through $X(20)$ = $(T_{Z_{01}}/P_5)$ through $(T_{Z_{45}}/P_5)$

and $X(21)$through $X(24)$ = $(T^1_{R_{01}}/P_5)$ through $(T^4_{R_{34}}/P_5)$

Least volume without considering tension ring

It is assumed that the supports can provide the necessary thrusts and thus no tension ring is needed. When this is the case, equation 4.19 is the correct expression for the entire volume of the structure (all in compression), and it is the objective function to be optimized subject to the nineteen constraints of equilibrium, equations 4.26, 4.27 and 4.29 (after nondimensionalization).

The program AUKLET, modified as already discussed, was again used. The comments with respect to the difficulties due to the non-convexity of the feasible region made in connection with the square lattice apply here as well since all the constraints in this case are also equalities, i.e.

$$g(x_i) = 0. \tag{4.30}$$

In this case, the feasible region was expanded by using the substitute constraint equations

$$g(x_i) + \varepsilon \geq 0, \tag{4.31}$$

where ε , a small quantity, was added to insure that round-off errors would not lead the computer to reject as non-feasible the initial point fed in.

The initial feasible solution was readily obtained by the following steps:

1. Obtain all vertical force components by consideration of the vertical shears (equations 4.26).
2. Arbitrarily select the heights between adjacent nodes $(z_j - z_i)$ and substitute these values, together with the shears of step 1, in equations 4.29 to find the radial force components of all inclined members working from the top down.
3. Use the radial force components of step 2 in equations 4.27 to find the radial force components of the ring members.
4. If all variables are positive, then obtain z_i from the condition that $z_0 = 0$ working up from the supports.

The first guess resulted in some negative variables which could be made positive by modifying only the pertinent $z_j - z_i$ terms. A solution thus obtained satisfies all the equalities. If all variables are positive, then the solution is an acceptable initial feasible solution.

After the first run, it was found that for some constraints the equalities were not being satisfied as evidenced by finite remaining slack. This first solution was then an optimum for the modified constraints of equations 4.31 and not for the true constraints of equations 4.30. Several trials were then made successively forcing the computer to satisfy the equalities by either adding a second constraint equation

of the type

$$-g\,(x_i) + \varepsilon \geq 0$$

or by adding this second equation and discarding the original constraint of the type similar to equation 4.31.

Since the computer seemed to have difficulty in converging rapidly (probably because the small differences between large numbers in constraints equations 4.29), it became necessary to use a better initial feasible solution. Intuitively, it was expected, as noted before in chapter three, that the optimum solution might be found when the dome would become a member of a more efficient class. In this case that would occur when the ordinates z_i are so related that the forces in the ring members are zero. The ring members vanish, and the remaining lamella-like dome would be in unstable equilibrium with the applied loads.

The proportions which the ordinates, z_i, must maintain for zero ring force are obtainable from the equations of equilibrium (equations 4.26, 4.27 and 4.29). Using them in $\sum \bar{F}_i . r_i$ (equation 4.19) reduces the latter to an expression in only one unknown and amenable to direct mathematical optimization. Thus, the assumption that the ring members would vanish reduces this problem to one degree of freedom and allows the classical method to be used.

Nevertheless, since such a solution depends on the validity of the assumption, it was decided to use the assumption only to provide a better starting point for the computer, but to allow the computer to solve the five-degree-of-freedom optimization problem and verify the assumption.

With the new starting point the computer converged upon a solution

in which all constraints had slacks of less than 6.81×10^{-3} and in which all the ring members had essentially zero forces. A partial list of the initial and final values of the variables appears in Table 4.2. The close agreement of the computer solution with the expected solution supports the assumption that the ring members would vanish at the optimum. The computer solution appears to have lesser volume than the expected optimum. However, it is felt that the difference is due to the small ε that were added to the constraint equations, and which expanded the feasible region to include a surface slightly below the surface describing the real feasible space.

A schematic drawing of the dome is shown in Fig. 4.10, and a half cross-section of the surface on which the nodes lie is shown in Fig. 4.11.

In an actual dome, to resist secondary loads, either the joints must be fixed, or ring members must be provided.

The nonlinear programming method of optimization would be useful if it is desired to insist upon the existence of the ring members. In that case, a solution could be obtained by adding constraints of the type

$$T_{ii} - K_i \geq 0$$

where K_i is any desired constant, with the dimensions of force, specified for the given ring member. The K_i values should be selected giving consideration to the known lengths of these members thus keeping their respective slenderness ratios above the value of incipient buckling.

Least volume considering tension ring

If the supports are not able to provide the necessary horizontal components of the thrusts, a tension ring would probably be required.

Table 4.2. Least volume network dome without tension ring

Variable	Initial Feasible Point[a]	Computer Found Optimum[b]	Expected Optimum[c]
$X(1) = (z_1/r_0)$	0.4	0.36181012	0.36174314
$X(2) = (z_2/r_0)$	0.8091	0.73173258	0.73173243
$X(3) = (z_3/r_0)$	1.117	1.0103416	1.0105236
$X(4) = (z_4/r_0)$	1.261	1.1401758	1.1404472
$X(5) = (z_5/r_0)$	1.279	1.1566119	1.1568632
$X(6) = (X_0/P_5)$	50.27	55.572985	55.586177
$F(X) = (V_{min} \times \frac{Wr_0}{100f_c})$	111.74	111.15597	111.17235
$G(X)$[d]		111.15913	
$X(7) = (T_{R_{11}}/P_5)$	0.0	0.0001290	0.0
$X(8) = (T_{R_{22}}/P_5)$	0.0	0.0001858	0.0
$X(9) = (T_{R_{33}}/P_5)$	0.0	0.0004165	0.0
$X(10) = (T_{R_{44}}/P_5)$	0.002	0.0032194	0.0

[a] Based on expected solution .

[b] Iterations = 72. CPU Time = 46.9 sec. I/O Time = 93.8 sec. Region Used = 162K.

[c] Computed by the classical method together with the expectation that the ring members will vanish at the optimum.

[d] Value of the dual objective function.

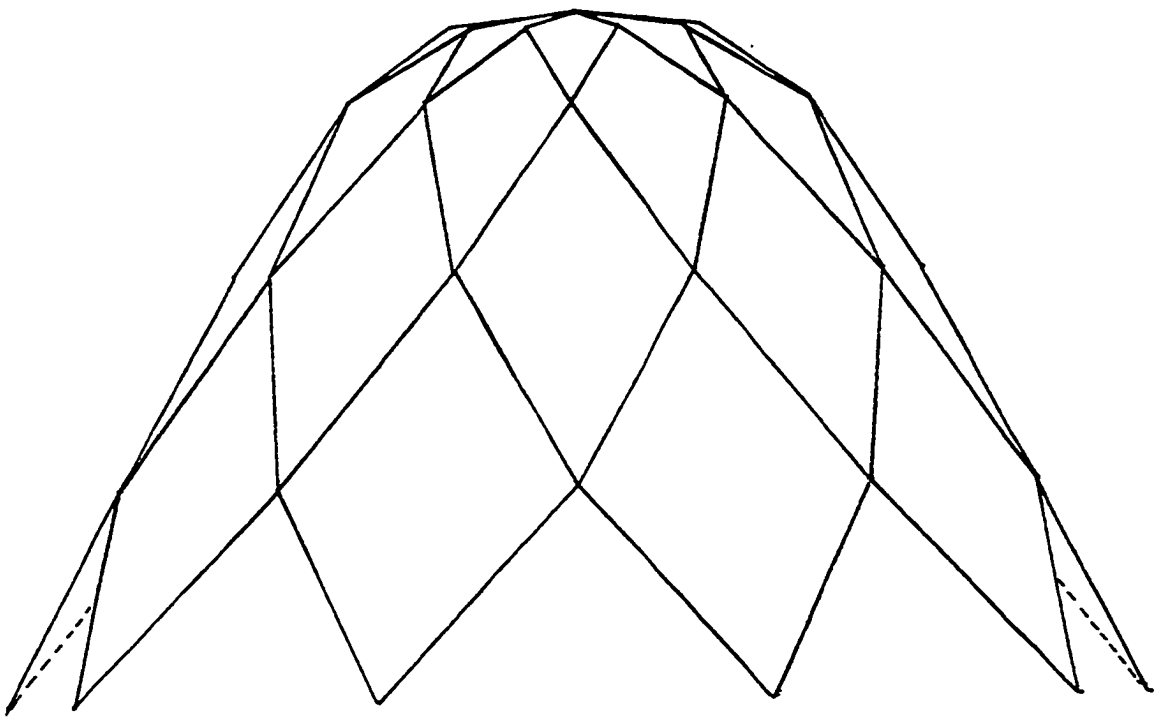

Fig. 4.10. Schematic drawing of optimum network dome.

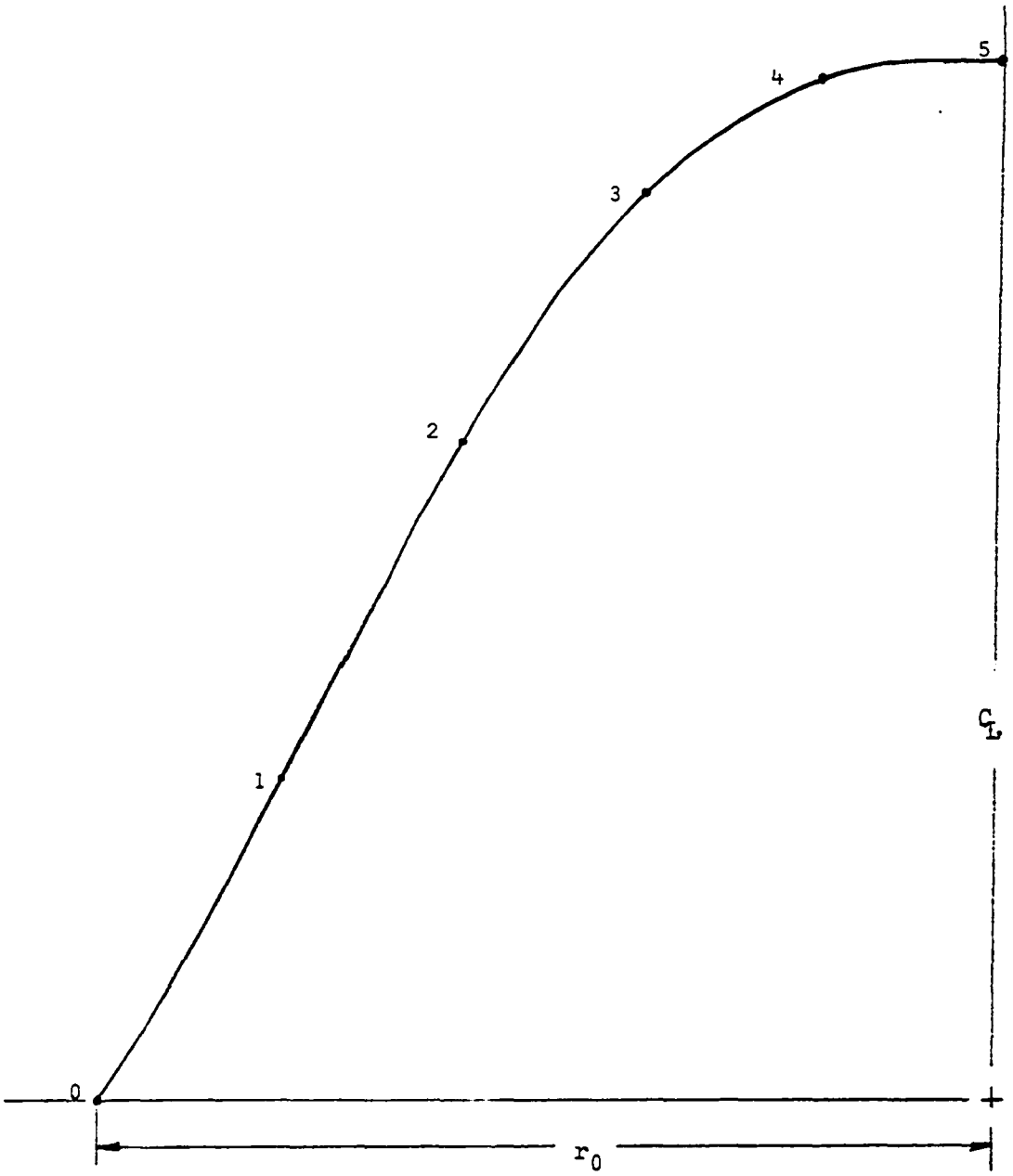

Fig. 4.11. Half cross-section of surface on which the nodes lie.

The volume of the ring may be taken into consideration, as suggested in chapter three, if it is desired to minimize the total volume of the structure including the volume of the dome (totally in compression) and of the ring (in tension).

The loads on the ring are the thrusts (X_0) at each node 0. Consequently, applying the theorem of zero absolute potential energy to the ring alone, its volume V_R may be written as,

$$V_R = \frac{1}{f_t} \left| \sum \bar{F}_i . \bar{r}_i \right|$$

or

$$V_R = \frac{2}{f_t} \left| X_0 r_0 \right| \qquad (4.32)$$

where the use of f_t implies that the ring will be designed to be uniformly stressed to f_t, the allowable tensile stress for the material of the ring.

The total volume of the structure, V_T, is

$$V_T = V_D + V_R$$

where V_D is the volume of the dome exclusive of the ring and is given by equation 4.18. Thus, using equations 4.18 and 4.32, the total volume of the structure is

$$V_T = \frac{2}{f_c} \left| X_0 r_0 + \sum P_i z_i \right| + \frac{2}{f_t} \left| X_0 r_0 \right|$$

Assuming that $f_c = f_t$, this last equation can be written as

$$V_T = \frac{2}{f} \left(2 X_0 r_0 + \sum P_i z_i \right) \qquad (4.33)$$

Equation 4.33 is the objective function to be minimized for minimum volume of the entire structure. It differs from the objective function used earlier (not considering the ring) only in that the $X_0 r_0$ term is now

counted twice.

The dome with the tension ring will be different from the one just optimized only in that the ordinates will be increased to reduce the horizontal components of the thrusts due to the double weighing of such horizontal forces in the optimization function. Consequently, the dome with the tension ring is also expected to be of least volume when the compression ring members in the lattice disappear.

Table 4.3 shows the results obtained when using the classical method and the computer assisted nonlinear programming method.

Lamella domes

The framing geometry of a network dome is similar to that of a lamella dome with horizontal rings. Such a lamella dome is in reality a many sided network dome. Thus, the same formulation used above would be applicable to a lamella dome.

Lamella domes are reported by Makowski (18) to be very efficient structures for spans of up to 1,200 feet, or possibly even more, and which can easily support, mainly by axial forces, any large concentrated loads that they may be subjected to. Loads imposed on the domes are rapidly dispersed throughout their framework and this, according to Makowski, "leads to considerable saving of material."

Paraboloidal Lattice

General

In this example, a paraboloidal dome, with a statically indeterminate lattice geometry, will be optimized by the shell analogy method.

Table 4.3. Least volume network dome with tension ring

Variable	Initial Feasible Point[a]	Computer Found Optimum[b]	Expected Optimum[c]
$X(1) = (z_1/r_0)$	0.4	0.51170981	0.51158205
$X(2) = (z_2/r_0)$	0.8091	1.0348285	1.0348259
$X(3) = (z_3/r_0)$	1.117	1.4288139	1.4290962
$X(4) = (z_4/r_0)$	1.261	1.6124373	1.6128359
$X(5) = (z_5/r_0)$	1.279	1.6357160	1.6360516
$X(6) = (X_0/P_5)$	50.27	39.293727	39.305363
$F(X) = (V_{min} \times \frac{Wr_0}{100f_c})$	111.74	157.19429	157.22145[d]
$G(X)$[e]		157.20244	
$X(7) = (T_{R_{11}}/P_5)$	0.0	0.0001699	0.0
$X(8) = (T_{R_{22}}/P_5)$	0.0	0.0002445	0.0
$X(9) = (T_{R_{33}}/P_5)$	0.0	0.0005482	0.0
$X(10) = (T_{R_{44}}/P_5)$	0.002	0.0042325	0.0

[a]Based on expected solution.

[b]Iterations = 137. CPU Time = 88.5 sec. I/O Time = 177.0 sec. Region Used = 162K. Largest slack in the constraints = 6.76×10^{-3} .

[c]Computed by the classical method together with the expectation that the ring members will vanish at the optimum.

[d]If the tension ring is present but not considered, the corresponding value for the total volume of ring and lattice would be 166.75853.

[e]Value of the dual objective function.

The dome chosen for the example is shown in Fig. 4.12. It has the geometry of a Schwedler dome with two sets of diagonals. However, in a Schwedler dome the diagonals are tension diagonals designed to buckle and be inactive under compressive stresses (Benjamin (3)). Here both diagonals will be designed to carry compressive stresses to achieve a homogeneous state of stress in the dome. This may not be practical in a real life design but is done here only to demonstrate the shell analogy method, and to further show that a hyperstatic and a static structure have the same least volume when optimized for the same system of loads.

The dome will be optimized with respect to a total load, W, distributed on the horizontal projection. Since it is to be optimized by the shell analogy, the load allocated to each node will not be computed but instead the same distributed load will be assumed to act on the analogous shell thus satisfying correspondence of loads.

It is to be noted that, under symmetrical loads the diagonals of the structure to be optimized carry no stress (Benjamin (3)). Thus, as the dome is to be optimized for symmetrical loads (uniformly distributed on the horizontal projection), the proper procedure for an absolute minimum would be to remove the diagonals and optimize the resulting fixed-jointed Schwedler dome. Intuitively, it may be expected, as was the case with the network dome, that the global optimum would then occur when the ring members all vanish leaving only the free-standing ribs joined at the crown of the dome. For the purposes of this example, however, the diagonal and ring members will not be allowed to vanish, and the nodes of the structure will be assumed to lie on a paraboloidal surface. The optimum to be

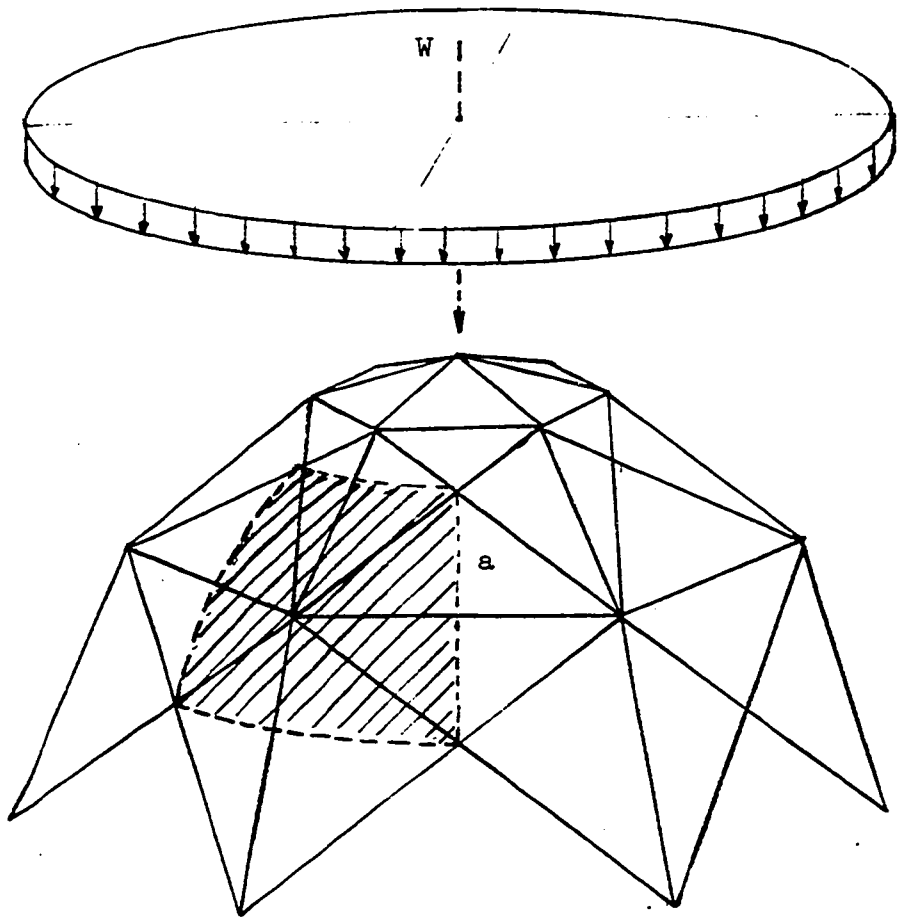

[a]Shaded area is isolated in Fig. 4.13.

Fig. 4.12. Dome to be optimized.

found will then be optimum among all similar domes.

Formulation and solution by shell analogy

Since the shape of the dome is assumed to be paraboloidal, the analogous shell will have to be a paraboloidal shell, thus satisfying the geometrical requirements for analogy.

The relationships between the dome bar forces and the shell tractions are not needed initially since the shape of the lattice and of the shell have been already selected to be paraboloidal. These relationships will be eventually needed to verify that it is possible for the lattice to be homogeneously stressed while satisfying the required bar force-shell traction relationships. The relationships will nevertheless be developed now using the analogous portions of the lattice and shell shown in Fig. 4.13. The portion of the lattice corresponds to the shaded portion in Fig. 4.12. In Fig. 4.13 the loads on shell and lattice are omitted for clarity. The shell must be analogous to the lattice in a geometrical sense and with respect to all force resultants. Geometrical analogy is satisfied by the assumption of paraboloidal shape for both, and by insisting that a, b_1 and b_2 are the same lengths in both portions which are similarly situated on the respective structure. Force analogy must be achieved for the loads on both portions and for the resultants of the bar forces and of the shell tractions.

For load analogy the load on the node of the lattice must equal the total load which is assumed evenly distributed (on the horizontal projection) and acting over the surface of the shell.

For lattice force and shell traction analogy the resultants in the

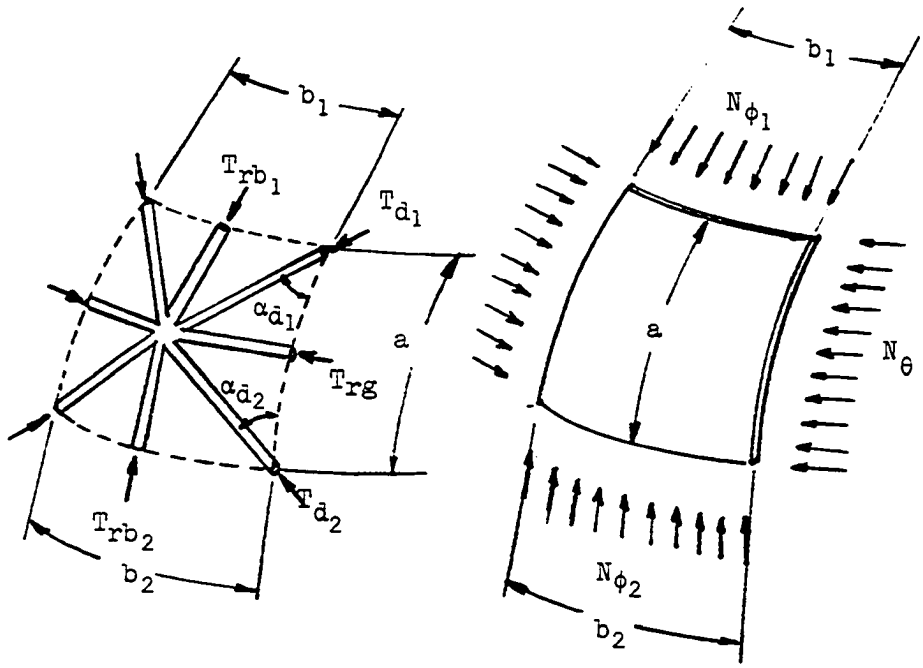

Fig. 4.13. Analogous portions of lattice and shell.

meridian (ϕ) and ring (θ) directions of both must be equal. Mathematically,

$$\left.\begin{aligned} T_{rb_1} + 2\,T_{d_1}\cos\alpha_{d_1} &= N_{\phi_1}\,b_1, \\ T_{rb_2} + 2\,T_{d_2}\cos\alpha_{d_2} &= N_{\phi_2}\,b_2, \\ \text{and}\qquad T_{rg} + T_{d_1}\sin\alpha_{d_1} + T_{d_2}\sin\alpha_{d_2} &= N_\theta\,a, \end{aligned}\right\} \tag{4.34}$$

where the subscripts rb, d and rg refer to the meridional ribs, the diagonal and the ring members, and the subscripts 1 and 2 are used to denote the members or forces above and below the center of the portions respectively.

Satisfaction of equations 4.34 with a homogeneously stressed lattice implies that both N_ϕ and N_θ must be compressive in the final shell. No other requirements arise and the N_ϕ/N_θ ratio may vary in any fashion throughout the shell.

Consider now the analogous paraboloidal shell. The shell is shown in Fig. 4.14. Since the load is axially symmetric, for convenience, a circular cylindrical coordinate system will be used with the origin at the zenith of the shell as shown in the same figure.

The equation of the shell is

$$z = z_b\,(r^2/r_b^{\,2}) \quad \text{and} \quad dz/dr = 2\,z_b(r/r_b^{\,2}) \tag{4.35}$$

where r_b is the radius of the shell at the supports (a given constant), and z_b is the height of the shell, constant for any one shell, but in reality the variable with respect to which $\sum \bar{F}_i.\bar{r}_i$ will be minimized.

The load intensity (p) on the shell, per horizontal unit area, is

$$p = \frac{W}{\pi r_b^{\,2}}, \tag{4.36}$$

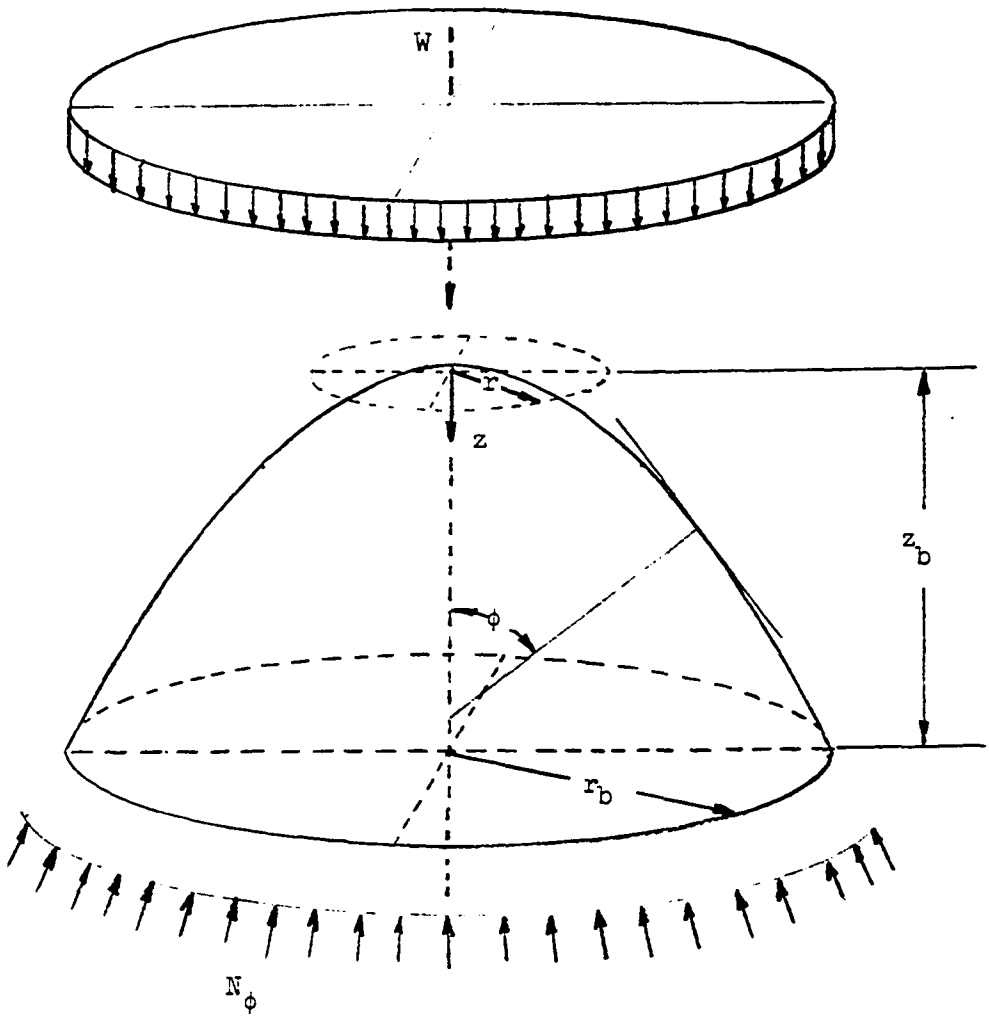

Fig. 4.14. Analogous paraboloidal shell.

where W is the total load. Consideration of the vertical equilibrium of a free body diagram of the portion of the shell above a cutting plane at an arbitrary radius, r, yields

$$N_\phi = \frac{Wr}{2\, r_b^2 \sin\phi} \,. \tag{4.37}$$

The radii of curvature, R_ϕ and R_θ for the shell are

$$\left.\begin{aligned} R_\theta &= \frac{r}{\sin\phi}\,, \\ \text{and} \quad R_\phi &= \frac{\{1 + (dz/dr)^2\}^{3/2}}{\frac{d^2z}{dr^2}} \\ \text{or} \quad R_\phi &= \frac{r_b^2}{2z_b \cos^3\phi} \,. \end{aligned}\right\} \tag{4.38}$$

Considering the equilibrium of a small section of the shell,

$$\frac{N_\phi}{R_\phi} + \frac{N_\theta}{R_\theta} = Z \tag{4.39}$$

where Z is the intensity of the load orthogonal to the middle plane of the shell, considered positive when inwardly directed (since here N_ϕ and N_θ are positive when compressive). In this case,

$$Z = p\cos^2\phi. \tag{4.40}$$

Using equations 4.38 and 4.40 in equation 4.39, N_θ can be expressed as

$$N_\theta = \frac{W\cos\phi}{4\pi z_b} \tag{4.41}$$

Note that N_ϕ and N_θ are both compressive and neither changes sign for any paraboloidal shell (since $\phi \leq \pi/2$ always). Were N_θ to become tensile at some point, then, after $\sum \bar{F}_i \cdot \bar{r}_i$ is minimized, it would be necessary to insist that ϕ_b at the supports be limited to be no larger than the which causes $N_\theta = 0$ or else a homogeneously stressed structure would

not be possible.

For the shell, $\sum \bar{F}_i.\bar{r}_i$ may be expressed as

$$\sum \bar{F}_i.\bar{r}_i = \sum X_b r_b + \sum P_i(z_b - z_i)$$

$$\sum \bar{F}_i.\bar{r}_i = N_{\phi_b}(\cos \phi_b)\, 2\pi\, r_b^2 + \int_0^{r_b} \frac{W}{\pi r_b^2}(z_b - z)\, 2\pi\, r\, dr$$

where the subscript b refers to the variables evaluated at the support. Using equations 4.35 and 4.37 this reduces to

$$\sum \bar{F}_i.\bar{r}_i = \frac{W r_b}{\tan \phi_b} + \frac{2W z_b}{r_b^2} \int_0^{r_b} \left(r - \frac{r^3}{r_b^2}\right) dr.$$

Noting that $\tan \phi = dz/dr$, evaluating the latter (equation 4.35) at $r = r_b$, and evaluating the definite integral,

$$\sum \bar{F}_i.\bar{r}_i = \frac{W}{2}\left\{\frac{r_b^2}{z_b} + z_b\right\}. \qquad (4.42)$$

Letting the derivative of $\sum \bar{F}_i.\bar{r}_i$ with respect to z_b equal to zero, it can be shown that for minimum $\sum \bar{F}_i.\bar{r}_i$,

$$z_b = r_b. \qquad (4.43)$$

The shape of the resulting shell is as shown in Fig. 4.14 which was purposely drawn with $z_b = r_b$.

At the supports, from equation 4.35

$$\tan \phi_b = 2$$

and consequently,

$$\cos \phi_b = \frac{1}{\sqrt{5}},$$

$$\sin \phi_b = \frac{2}{\sqrt{5}}.$$

Therefore, from equations 4.37 and 4.41,

$$\left.\begin{aligned} N_\phi\Big|_b &= \frac{\sqrt{5}\,W}{4\pi r_b}\,, \\ \text{and} \qquad N_\theta\Big|_b &= \frac{W}{4\sqrt{5}\,\pi r_b}\,. \end{aligned}\right\} \tag{4.44}$$

Applying equations 4.34 at the supports,

$$\left.\begin{aligned} T_{rb_1} + 2\,T_{d_1}\cos\alpha_{d_1} &= \frac{\sqrt{5}\,W}{4\pi r_b}\cdot b_1 \\ \text{and,} \qquad T_{d_1}\sin\alpha_{d_1} &= \frac{W}{4\sqrt{5}\,\pi r_b}\cdot\frac{a}{2}, \end{aligned}\right\} \tag{4.45}$$

where the notation is as used in equation 4.34. The last of equations 4.45 results from the last of equations 4.34 where $T_{rg} = T_{d_2} = 0$, and a has been adjusted to be consistent. Equations 4.45 imply that the nodes are very close to each other and thus $N_{\phi_1} \simeq N_{\phi_b}$. Assuming further that $\alpha_{d_1} = 45^\circ$ and thus

$$\sin\alpha_{d_1} = \cos\alpha_{d_1} = 1/\sqrt{2},$$

while

$$a/2 \simeq b_1/2\,,$$

results in the following values

$$\left.\begin{aligned} T_{d_1} &= \frac{W\,a}{4\sqrt{10}\,\pi r_b}\,, \\ \text{and} \qquad T_{rb_1} &= \frac{W\,b_1}{\sqrt{5}\,\pi r_b}\,. \end{aligned}\right\} \tag{4.46}$$

Equations 4.46 show that it is possible to have correspondence of forces and shell tractions without violating the requirement that all members of the lattice be homogeneously stressed (all in compression). Equations

4.46 or their equivalents could be written for all members. If all the members are then proportioned (by selection of their areas) to be stressed to f_c, then the resulting design would be a least volume design for the class chosen (nodes lying on a paraboloidal surface). Furthermore, this would be a statically indeterminate structure of least weight in its class.

This is, however, only a solution and not a unique solution. Other solutions are possible of equal (but no lesser) volume. This will now be demonstrated.

Equations 4.45 were written assuming that there would be no compressive ring at the support level. There is no mathematical reason to preclude the use of such a ring (even though it may not be practical). Rewriting equations 4.45 with such a ring provided,

$$\left.\begin{aligned} T_{rb_1} + 2T_{d_1} \cos \alpha_{d_1} &= \frac{\sqrt{5}\, W}{4\pi\, r_b} \cdot b_1 \\ \text{and,} \qquad T_{rg} + T_{d_1} \sin \alpha_{d_1} &= \frac{W}{4\sqrt{5}\, \pi r_b} \cdot \frac{a}{2} \end{aligned}\right\} \qquad (4.47)$$

Equations 4.47 can be satisfied (thus insuring that the analogy holds) with any arbitrarily selected value for T_{d_1} provided it is less than the value given by equation 4.46 (if it is greater then T_{rg} would have to be negative and thus a tensile force). Assuming, for example, that $T_{d_1} \equiv 0$ yields the solution

$$\left.\begin{aligned} T_{rb_1} &= \frac{\sqrt{5}\, Wb_1}{4\pi\, r_b} \\ \text{and} \qquad T_{rg} &= \frac{W\, a}{8\sqrt{5}\, \pi r_b} \end{aligned}\right\} \qquad (4.48)$$

Similar equations can be written at every node always assuming that the diagonals vanish.

The solution indicated by the typical equation 4.48 would have the form of a Schwedler dome without diagonals and would be a statically determinate solution. Since it satisfies the correspondence of forces with the shell, the shell analogy solution applies. The removal of the diagonals with the corresponding increases in the volumes of the ribs and ring members does not alter $\sum \bar{F}_i . \bar{r}_i$ nor disturb equilibrium. Thus, if the ribs and rings of this second solution are also designed to be fully stressed, the volume of this second structure is also a minimum (of the same magnitude of that of the first structure).

Consequently, this is a demonstration that statically determinate and statically indeterminate structures, when optimized are fully stressed, and that when supporting the same loads, their least volumes are identical.

Paraboloidal Shell

In this example the geometry (height-to-span ratio) of a paraboloidal shell will be optimized for least volume of the shell, with and without the consideration of a tension ring.

Least volume without tension ring

From the previous example the following equations, applicable to the shell, are repeated for convenience,

$$z = z_b \ (r^2/r_b^2), \quad dz/dr = 2 z_b \ (r/r_b^2), \tag{4.49}$$

$$\left.\begin{aligned} N_\phi &= \frac{Wr}{2\pi r_b^{\,2} \sin\phi}, \\ N_\theta &= \frac{W \cos\phi}{4\pi z_b}, \end{aligned}\right\} \qquad (4.50)$$

and, $$\sum \bar{F}_i.\bar{r}_i = \frac{W}{2}\left\{\frac{r_b^{\,2}}{z_b} + z_b\right\}. \qquad (4.51)$$

It can be shown that $N_\phi \geq N_\theta$ for all ϕ, the equality holding when $\phi = 0$ (zenith of the shell). Consequently, this shell belongs to level I in the hierarchy of structures (i.e. N_ϕ can be such that $\sigma_\phi = f_c$ but $\sigma_\theta \leq f_c$ and is compressive everywhere). Thus, to obtain a global minimum for the given load (of total value W, distributed over the horizontal projection) it would be necessary to first change the shape of the shell to make $\sigma_\theta = f_c$ everywhere, then minimize $\sum \bar{F}_i.\bar{r}_i$, and finally check that $\sum \bar{F}_i.\bar{r}_i$ has not been unduly increased in forcing $\sigma_\theta = f_c$ (moving from level I to level III in the hierarchy of structures).

Interjection of the requirement that $\sigma_\phi = \sigma_\theta = f_c$ would require a change in shape and lead to differential equations that can only be integrated (to obtain the equation for z) numerically. The optimization would not yield a closed form solution.

Therefore, to avoid that complication, the example, as its title implies, will only seek to obtain a paraboloidal shell of minimum volume (among all paraboloidal shells).

The volume of the shell, using the theorem of zero absolute potential energy, can be expressed as

$$V = \frac{1}{f_c}\sum \bar{F}_i.\bar{r}_i - \frac{1}{f_c}\int \frac{N_\theta}{t_r}\, dV \qquad (4.52)$$

where the use of f_c implies that the thickness of the shell, t_r, will be so selected that $\sigma_\phi = f_c$, that is

$$t_r = \frac{N_\phi}{f_c} . \tag{4.53}$$

Using the first of equations 4.50,

$$t_r = \frac{W\, r}{2\, f_c \pi r_b^{\,2} \sin\, \phi} \tag{4.54}$$

To obtain the least volume it is necessary to minimize the entire right hand side of equation 4.52.

Equation 4.52 can be rewritten, by making use of equations 4.50, 4.51 and 4.54 as

$$V = \frac{W}{2f_c}\left\{ \frac{r_b^{\,2}}{z_b} + z_b \right\} - \frac{1}{f_c}\int \frac{W \cos\, \phi}{4\pi\, z_b} \left\{ \frac{2\, f_c \pi\, r_b^{\,2} \sin\, \phi}{W\, r} \right\} dV.$$

Simplifying,

$$V = \frac{W}{2f_c}\left\{ \frac{r_b^{\,2}}{z_b} + z_b \right\} - \int \frac{r_b^{\,2} (\cos\phi) \sin\, \phi}{2\, z_b\, r} dV \tag{4.55}$$

Since the shell is axially symmetrical, dV may be replaced by its equivalent expression, $2\pi r t_r\, d\ell$ where $d\ell$ is the differential element of length along the meridian, and noting that

$$d\ell = \frac{dr}{\cos\, \phi},$$

equation 4.55 becomes

$$V = \frac{W}{2f_c}\left\{ \frac{r_b^{\,2}}{z_b} + z_b \right\} - \int_0^{r_b} \frac{2\, \pi r_b^{\,2} \sin\, \phi}{2\, z_b} (t_r)\, dr, \tag{4.56}$$

where the appropriate limits of integration have been added.

Using equation 4.54 to replace t_r in equation 4.56, and simplifying,

$$V = \frac{W}{2f_c}\left\{\frac{r_b^2}{z_b} + z_b\right\} - \frac{W}{2f_c}\int_0^{r_b}\frac{r}{z_b}\,dr. \tag{4.57}$$

Evaluating the integral and collecting terms,

$$V = \frac{W}{2f_c}\left\{\frac{r_b^2}{2z_b} + z_b\right\} \tag{4.58}$$

Letting $\partial V/\partial z_b = 0$ for minimum volume,

$$z_b = \frac{r_b}{\sqrt{2}}. \tag{4.59}$$

Expression 4.59 is the solution desired. The shape of the resulting shell is shown in Fig. 4.15. Its volume is

$$V = \frac{Wr_b}{2f_c}\sqrt{2} \tag{4.60}$$

Consideration of tension ring

To optimize the total volume of the shell with a tension ring, it suffices, as discussed in chapter three, to double the term in $\sum \bar{F}_i.\bar{r}_i$ that reflects the contribution to it of the horizontal forces along the periphery of the shell.

Doing so, equation 4.57 yields

$$V = \frac{W}{2f_c}\left\{\frac{2r_b^2}{z_b} + z_b\right\} - \frac{W}{2f}\left\{\frac{r_b^2}{2z_b}\right\},$$

or,

$$V = \frac{W}{2f_c}\left\{\frac{3r_b^2}{2z_b} + z_b\right\}. \tag{4.61}$$

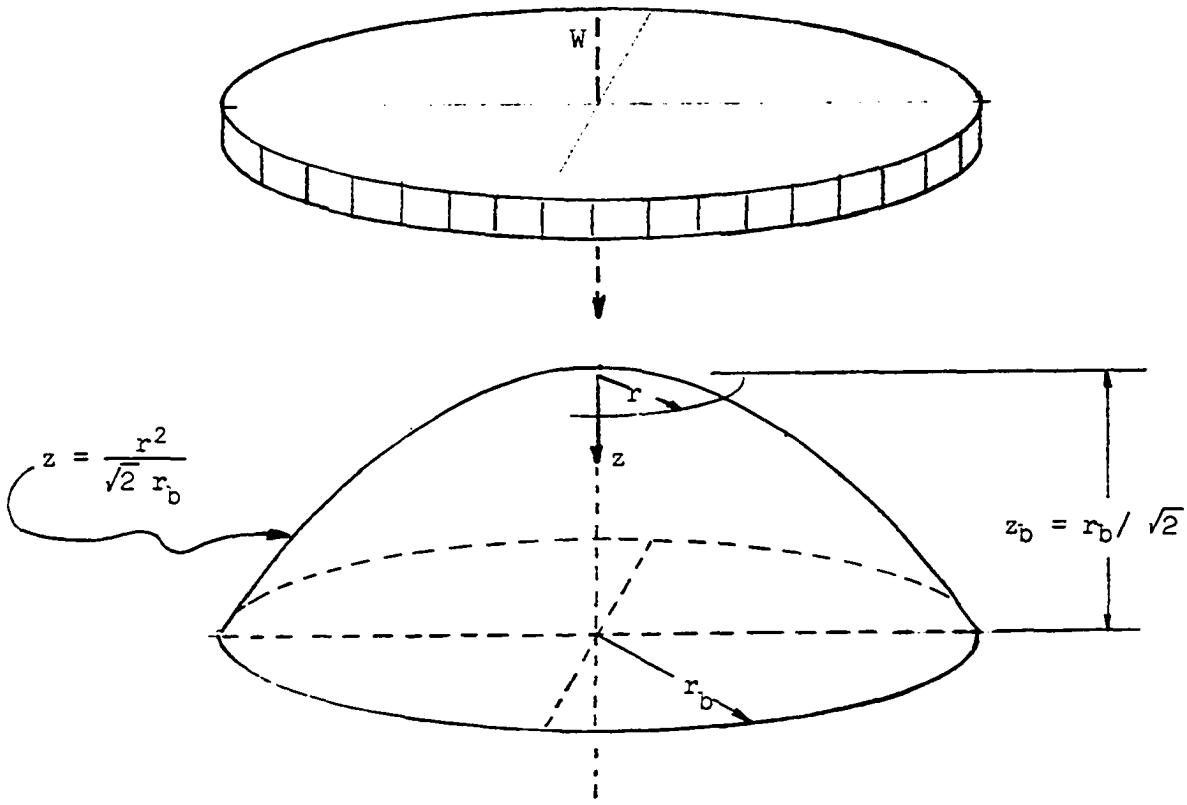

Fig. 4.15. Optimum paraboloidal shell without tension ring.

Again letting $\partial V / \partial z_b = 0$ for minimum volume,

$$z_b = r_b \sqrt{\frac{3}{2}} \quad \text{or,} \quad z_b = 1.225\, r_b .$$

The resulting shell is shown in Fig. 4.16.

The volume of the shell-ring structure is

$$V^*_{S+R} = \frac{W r_b \sqrt{6}}{2 f_c} \quad , \tag{4.62}$$

where the * indicates a minimum volume and the subscript S+R implies minimization of the entire shell-ring structure. If only the shell had been minimized (either ignoring the ring or making the assumption that the supports could absorb the horizontal thrusts) the volume, with similar notation can be expressed as (equation 4.60)

$$V^*_S = \frac{W r_b}{2 f_c} \sqrt{2} \quad . \tag{4.63}$$

If a ring was present but ignored, the volume of the ring alone can be computed from its own $\sum \bar{F}_i . \bar{r}_i$ as

$$V_R = \frac{W}{2 f_c} \left\{ \frac{r_b^2}{z_b} \right\},$$

which, since $z_b = r_b / \sqrt{2}$ (equation 4.59), becomes

$$V_R = \frac{W r_b}{2 f_c} \sqrt{2} \tag{4.64}$$

The total volume of the structure with a ring but where only the shell was optimized is,

$$V_{S+R} = V^*_S + V_R$$

or, adding equations 4.63 and 4.64

$$V_{S+R} = \frac{W r_b}{2 f_c} \sqrt{8} \quad . \tag{4.65}$$

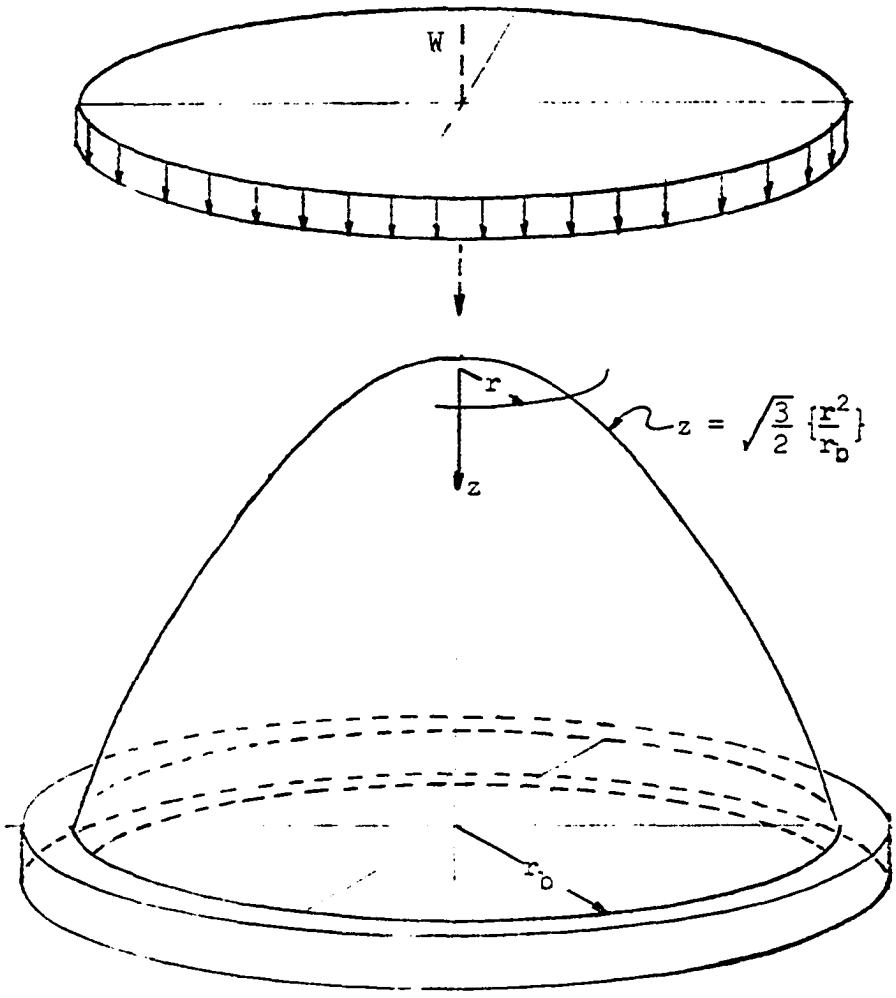

Fig. 4.16. Optimum paraboloidal shell with tension ring.

Comparing equations 4.65 and 4.62 shows that by considering the ring in the optimization process the volume was reduced by 13.4% from the volume of the shell which was optimized while ignoring the tension ring. At the same time, the rise was increased from

$$z_b = r_b/\sqrt{2} \quad \text{(optimization on shell only)}$$

to

$$z_b = r_b\sqrt{3/2} \quad \text{(optimization on shell-ring)}$$

representing a 22.5% increase.

CHAPTER FIVE - SEQUENCE OF ALTERNATIVE DESIGNS FOR SINGLE SYSTEM OF LOADS

General

The purpose of this chapter is to explore the changes in least volume which occur, when supporting the same loads, as a transition is made from a structure of one hierarchical level to one of another level (see chapter two).

To do so, three different latticed structures and their corresponding analogous shells are optimized. Their volumes are then compared.

Load System

Assume that it is required to synthesize a structure to support a ring of vertical loads. The supports are also to be disposed in a circular plan and can absorb the thrusts required. It is permissible to raise the ring load at any desired height above the supports. Such a load system is shown in Fig. 5.1.

First Lattice Alternative - Conoidal

For the first alternative structural system, consider the structure whose cross-section is shown, schematically, in Fig. 5.2. It will be optimized by the classical method first.

In Fig. 5.2, the total load, W, is divided into 2n loads of magnitude P acting at the top nodes. There are n "frames", similar to the one shown, and arranged at an angle of $360°/2n$ from each other. Lines 1-1 and 2-2 indicate a radial force applied at points 1 and 2 and do not necessarily

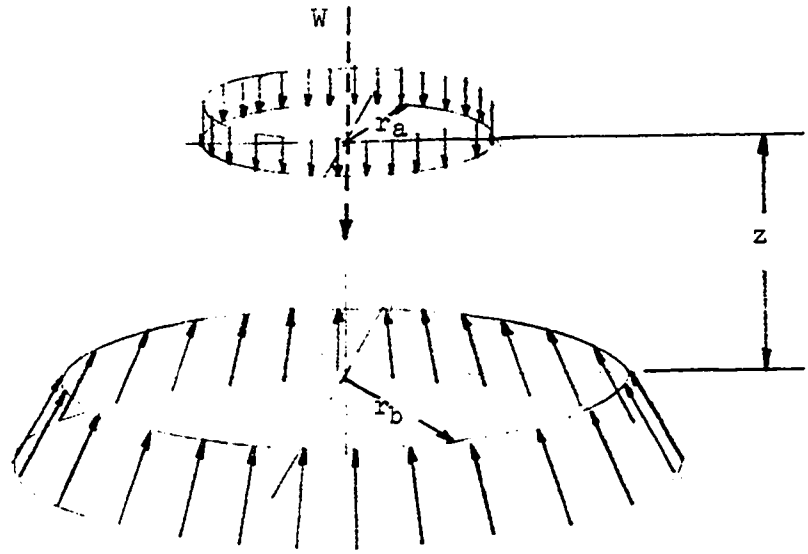

Fig. 5.1. Load system.

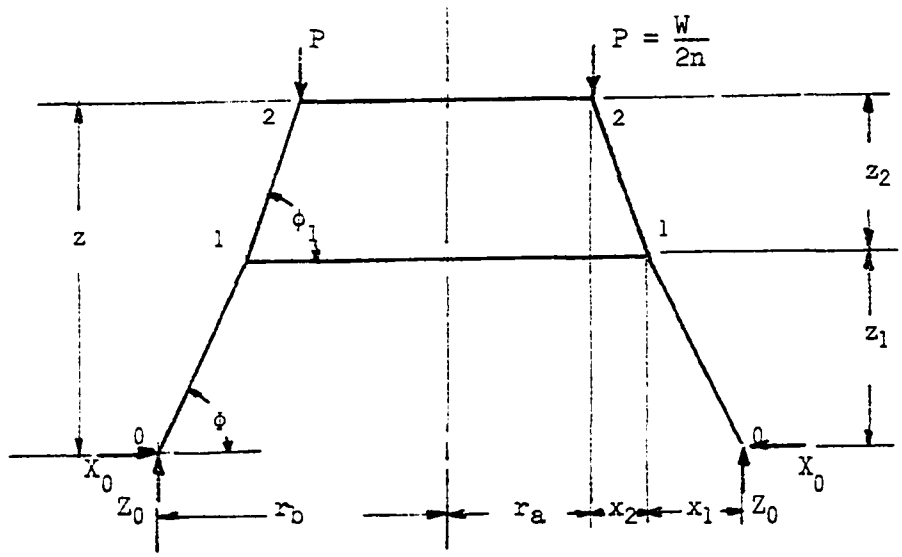

Fig. 5.2. Schematic drawing of first alternative.

imply a member directly joining opposite points 1 and 2. In the actual structure, these radial forces could be provided by either compression rings or by members directly joining opposite nodes.

The position of point 1 could be restricted if desired. Such restriction, however, would lead to the synthesis of a structure of least volume within that class (i.e. with restricted position of point 1). To allow as much latitude as possible, the position of point 1 will be considered as free to vary.

It can be shown (from a consideration of the number of variables and of the equations of equilibrium, as discussed in chapter three) that the optimization of the structure of Fig. 5.2 is a problem with three degrees of freedom. Consequently, all the constraints of equilibrium must be used to express $\sum \bar{F}_i . \bar{r}_i$ in terms of only three variables prior to optimization.

For convenience, the following relationships are written,

$$\left.\begin{aligned} \tan \Phi &= z_1/x_1 \ , \\ \tan \Phi_1 &= z_2/x_2 \ , \\ x_1 + x_2 &= r_b - r_a \ , \\ z_1 + z_2 &= z \ , \end{aligned}\right\} \qquad (5.1)$$

and,

$$X_0 = \frac{P}{\tan \Phi} \ , \qquad (5.2)$$

where all the variables are defined in Fig. 5.2.

Using the theorem of zero absolute potential energy, and the concept of variation of $\sum \bar{F}_i . \bar{r}_i$, the objective function for the problem at hand can be written as,

$$V|_{min} = \frac{1}{f_c} \{ \sum \bar{F}_i . \bar{r}_i \}|_{min} \qquad (5.3)$$

Classical method

Using the equations of equilibrium, as indicated above, and selecting x_1, Φ and ϕ_1 as the variables to be retained, the objective function can be written as,

$$V|_{min} = \frac{2nP}{f_c} [\frac{r_b}{\tan \Phi} + x_1 \tan \Phi + (r_b - r_a - x_1) \tan \phi_1]|_{min} \qquad (5.4)$$

It is not necessary to consider any other constraints because the assumption that the structure is homogeneously stressed renders the structure statically determinate (in unstable equilibrium with the given loads, for computation purposes).

The three additional equations needed to obtain a unique and optimum solution are:

$$\left.\begin{aligned} \frac{\partial V_{min}}{\partial \Phi} &= \frac{2nP}{f_c} [-r_b \csc^2\Phi + x_1 \sec^2\Phi] = 0 , \\ \frac{\partial V_{min}}{\partial \phi_1} &= \frac{2nP}{f_c} [(r_b - r_a - x_1) \sec^2\phi_1] = 0 , \\ \text{and } \frac{\partial V_{min}}{\partial x_1} &= \frac{2nP}{f_c} [\tan \Phi - \tan \phi_1] = 0 . \end{aligned}\right\} \qquad (5.5)$$

The third of these equations can be satisfied only if

$$\Phi = \phi_1 ,$$

and the second implies, since $\sec^2\phi_1 \neq 0$, that

$$x_1 = r_b - r_a .$$

Consequently, from equation 5.1, $x_2 \equiv 0$.

These results are consistent with each other and hence can be satisfied simultaneously. They imply that for least volume, member 0-1-2 is straight and the force represented by line 1-1 vanishes. Furthermore, the significance of the location of point 1 vanishes and point 1 can be considered to coincide with point 2.

After thus satisfying the last two of equations 5.5, it is necessary, for a global minimum, to satisfy the first.

It can be verified that the first of equations 5.5 can be satisfied if

$$\tan \Phi = \sqrt{r_b/x_1}$$

or

$$\tan \Phi = \sqrt{r_b/(r_b-r_a)} \tag{5.6}$$

which can also be expressed as

$$\tan \Phi = \frac{1}{\sqrt{1 - (r_a/r_b)}} \tag{5.7}$$

Then, using the first of equations 5.1, since $z = z_1$,

$$z = \sqrt{(r_b - r_a)r_b} \quad , \tag{5.8}$$

or,

$$z = r_a\sqrt{(r_b/r_a)^2 - (r_b/r_a)} \quad , \tag{5.9}$$

and, using equation 5.4,

$$V_{min} = \frac{W}{f_c}\left[r_b\sqrt{(r_b - r_a)/r_b} + \sqrt{(r_b - r_a)r_b} \right] ,$$

where 2nP has been replaced by its equivalent, W. The latter expression reduces to

$$V_{min} = \frac{2W}{f_c}\sqrt{(r_b - r_a)r_b} \quad , \tag{5.10}$$

or,

$$V_{min} = \frac{2Wr_a}{f_c}\sqrt{(r_b/r_a)^2 - (r_b/r_a)} \quad , \tag{5.11}$$

Equation 5.11 can also be expressed as

$$V_{min} = \frac{Wr_a}{f_c} \left\{ \frac{r_b/r_a}{\tan \Phi} + z/r_a \right\} \quad , \qquad (5.12)$$

with the appropriate values used for Φ and z. All these equivalent expressions for V_{min} represent the total volume of all the inclined legs and the top compression ring, and can be verified by actual computation of the volumes of individual members when stressed to f_c. The resulting structure is shown in Fig. 5.3.

Thus, expressing $\sum \bar{F}_i . \bar{r}_i$ in a sufficiently general form resulted in a transformation from the class of structures schematically shown in Fig. 5.2 to the more efficient class and global optimum of Fig. 5.3, wherein the legs of the tower lie on the surface of a frustrum of a circular cone with bases of radius r_b and r_a, and height z.

Shell analogy

The shell analogous to the structure of Fig. 5.2 would be one composed of two frustrums of cones with stiffening compressive rings at levels z_1, where the two frustrums meet, and at z_2, the top of the top frustrum. For simplicity, only the shell analogous to the resulting structure of Fig. 5.3 will be considered. Shown in Fig. 5.4, such a shell consists of one frustrum of a cone, geometrically similar to the lattice, and with a stiffening compressive ring at the top level.

Note that for load correspondence between the lattice and the shell, the shell load, as shown in Fig. 5.4, is a circular line load of magnitude P_S which is

$$P_S = \frac{W}{2\pi r_a} \quad .$$

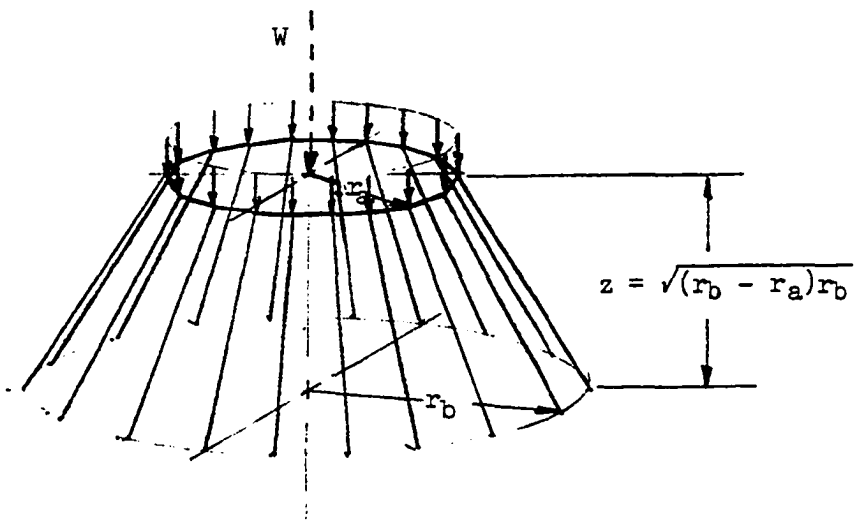

Fig. 5.3. Resulting structure, a global minimum.

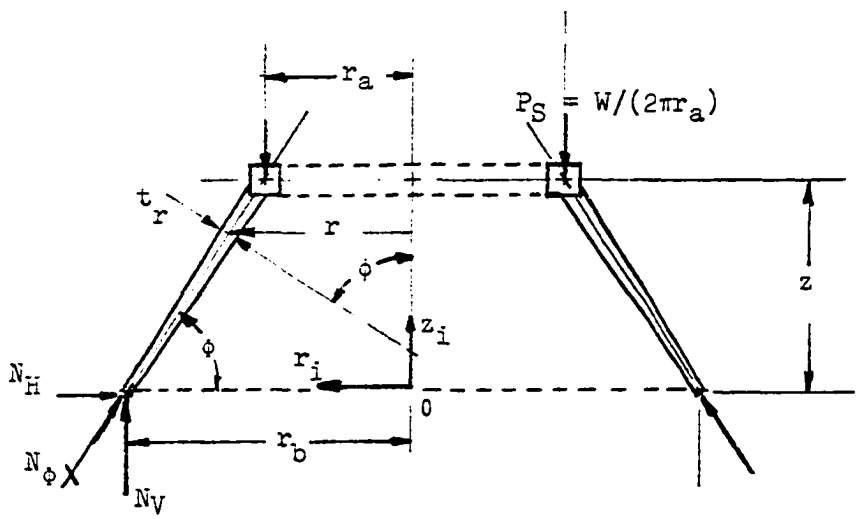

Fig. 5.4. Analogous shell in form of truncated cone.

Referring to Fig. 5.5, correspondence between the shell tractions and the bar forces of the lattice dictates that, if T_L is the force in one of the inclined legs, then

$$T_L = N_\phi \, r(\pi/n) \quad ,$$

where N_ϕ is the shell traction in the meridian direction, a function of r so that T_L remains constant. Since the lattice has no ring members (except at the top),

$$N_\theta = 0 \tag{5.13}$$

on the shell, and $T_R = F_R$

where T_R is the force in the ring members of the lattice, and F_R is the force in the compressive ring of the shell.

Referring to Fig. 5.4,

$$\sum \bar{F}_i . \bar{r}_i = N_H(2\pi r_b) r_b + Wz \tag{5.14}$$

where N_H is the horizontal component of N_ϕ, the shell tractions in the meridian direction at the supports.

It is now necessary to use the equations of equilibrium of the shell to reduce the independent variables in equation 5.14 to one. In this case, z will be retained.

From geometry, $N_H = \dfrac{N_V}{\tan \phi}$

where N_V is the vertical component of N_ϕ, and

$$\tan \phi = z/(r_b - r_a) \quad ,$$

while, from equilibrium of vertical forces,

$$N_V = \frac{W}{2\pi r_b} \quad .$$

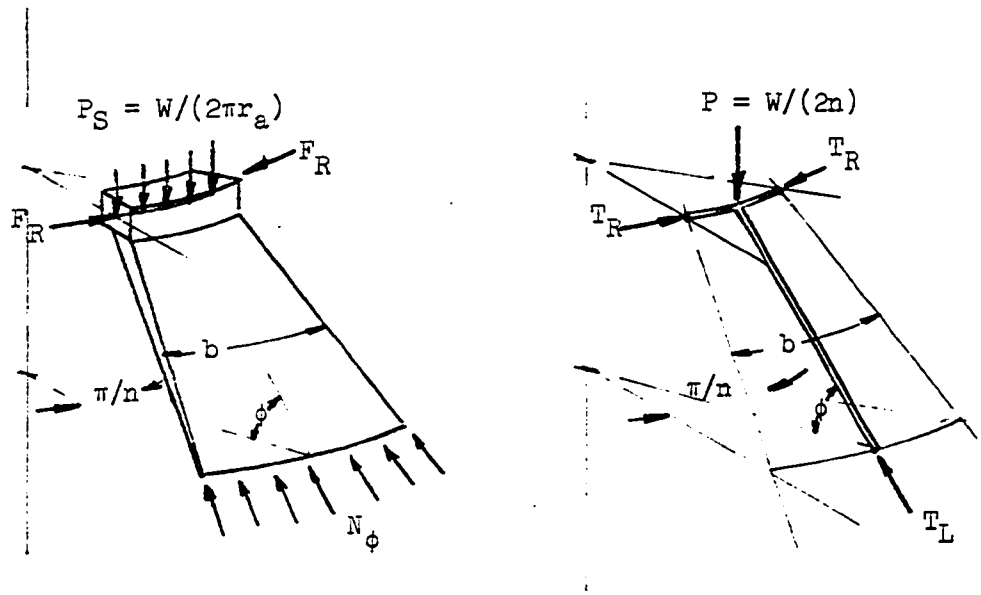

a. Shell element. b. Lattice element.

Fig. 5.5. Analogous elements of shell and lattice.

Using these last three equations in equation 5.14,

$$\sum \bar{F}_i . \bar{r}_i = W \left\{ \frac{(r_b - r_a) r_b}{z} + z \right\} \quad . \tag{5.15}$$

Letting $$\frac{\partial \{ \sum \bar{F}_i . \bar{r}_i \}}{\partial z} = 0 \quad ,$$

for minimum $\sum \bar{F}_i . \bar{r}_i$, $$z = \sqrt{(r_b - r_a) r_b} \quad , \tag{5.16}$$

which, by comparison, is seen to be identical with equation 5.8 for the lattice.

Continuing with the analogous shell, the volume of the lattice, V_L, is

$$V_{L_{min}} = \frac{1}{f_c} \left\{ \sum \bar{F}_i . \bar{r}_i \right\}_{min} \quad , \tag{5.17}$$

and, using equation 5.16 into 5.15, equation 5.17 becomes

$$V_{L_{min}} = \frac{2W}{f_c} \sqrt{(r_b - r_a)\, r_b} \quad , \tag{5.18}$$

which is seen to be identical to equation 5.10.

Thus, using an analogous shell, the form of the lattice structure for minimum lattice volume was found by minimization of $\sum \bar{F}_i . \bar{r}_i$ for the shell.

Correspondence of bar forces and shell traction resultants

In this case, since a solution for the lattice was already available to compare with the shell analogy solution, it is obvious at this point that the analogous shell yields the correct solution. In the more general case, it would be necessary to confirm that the conditions for the bar forces and shell traction correspondence are satisfied. The conditions in this case are that N_ϕ be an inverse function of r so that T_L be con-

stant, and that $N_\theta = 0$. To demonstrate that these conditions are satisfied, the state of stress in the shell will be investigated.

Summing forces in the vertical direction when considering a portion of the structure above any arbitrary r, yields

$$2\pi r(N_\phi \sin \phi) = W \quad , \tag{5.19}$$

or

$$N_\phi = \frac{W}{2\pi r \sin \phi} \quad . \tag{5.20}$$

Note that, as expected, N_ϕ is inversely proportional to r. Since ϕ is constant ($\varphi = \Phi$), T_L will be constant.

Letting t_r be the thickness of the shell (a function of r),

$$\sigma_\phi = \frac{W}{2\pi r\, t_r \sin \phi} \quad , \tag{5.21}$$

Considering a small element of the shell as in Fig. 5.6, and summing forces in a direction perpendicular to the shell, yields

$$N_\theta = 0$$

as expected, and consequently,

$$\sigma_\theta = 0 \quad . \tag{5.22}$$

This result could also be obtained by use of the similarly derived expression (Timoshenko and Woinowsky-Krieger (38)),

$$N_\phi/R_\phi + N_\theta/R_\theta = Z \quad , \tag{5.23}$$

where R_ϕ and R_θ are radii of curvature of the shell, and Z is the intensity of the load per unit area in a direction perpendicular to the middle plane of the shell. In this case, $R_\phi = \infty$ and $Z = 0$.

Now consider the stiffening ring at the top of the shell. The requirement for the ring can be recognized by referring to the free-body

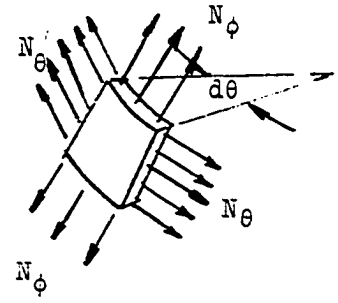

Fig. 5.6. Small element of the shell.

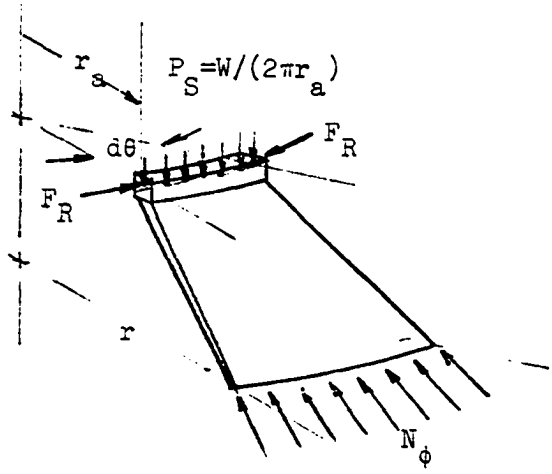

Fig. 5.7. Free-body diagram of structural element.

diagram of the structural element shown in Fig. 5.7. In that diagram the forces are shown in the actual directions in which they act and not in accordance with any sign convention.

For equilibrium, the radial component of F_R (the force in the ring) must equal the horizontal component of N_ϕ . (In Fig. 5.6, N_θ is not shown since, as derived above, it is everywhere equal to zero).

Summing forces in the radial direction,

$$2 F_R \sin \frac{d\theta}{2} = (N_\phi \cos \phi) r \, d\theta$$

or, since $d\theta$ can be taken as small as desired,

$$F_R = (N_\phi \cos \phi) r \quad . \tag{5.24}$$

Using expression 5.20 in equation 5.24, and noting that $\phi = \Phi$,

$$F_R = \frac{W}{2\pi \tan \Phi} \tag{5.25}$$

or, expressing $\tan \Phi$ in terms of r_a, r_b and z,

$$F_R = \frac{W(r_b - r_a)}{2\pi z} \quad . \tag{5.26}$$

To complete the demonstration of the correspondence of bar forces and shell traction resultants, it now needs to be shown that T_R, the lattice ring member force, is equal to F_R. To compute T_R, refer to the lattice element shown in Fig. 5.5. Summing forces in the radial direction,

$$2 T_R \sin (\frac{\pi}{2n}) = T_L \cos \Phi \quad , \tag{5.27}$$

or,

$$2 T_R \sin (\frac{\pi}{2n}) = \frac{W \cos \Phi}{2n \sin \Phi} = \frac{W}{2n \tan \Phi} \quad , \tag{5.28}$$

and, upon expressing $\tan \Phi$ in terms of r_a, r_b and z,

$$2\, T_R \sin\left(\frac{\pi}{2n}\right) = \frac{W(r_b - r_a)}{2nz} \quad . \tag{5.29}$$

If $\pi/(2n)$ is small (i.e. n is large), equation 5.29 reduces to

$$T_R = \frac{W(r_b - r_a)}{2\pi z} \quad , \tag{5.30}$$

which, by comparison with equation 5.26, demonstrates that $T_R = F_R$. Thus, the lattice and the shell differ in that the shell is loaded by a linearly distributed load, while the lattice is loaded discontinuously at 2n points. The larger 2n is, the closer the shell and lattice approximate one another.

Compatibility of deformations for this system of loads need not be considered in the shell analogy since the geometry of both the lattice and the shell are described in their respective deformed states (at which time they are defined to be geometrically similar). Compatibility of deformations would have to be considered in the analogy, if it were desired to use the analogy to determine the stresses due to other loads, or due to the removal of the design load system. (For example, if the residual stresses due to the removal of the loads on the lattice were to be determined by analysis of the residual stresses on the shell-ring structure.) In such a case, additional requirements on the correspondence of the shell-ring and lattice material properties would have to be introduced. For examples of such requirements see Benjamin (3) or Parikh and Norris (26).

Applicability of theorem to the shell

The theorem of zero absolute potential energy, equation 2.10, for this structure, can be written as,

$$\int_S \sigma_\phi \, dV_S + \int_S \sigma_\theta \, dV_S + \int_R \sigma_R \, dV_R = \sum \bar{F}_i . \bar{r}_i \quad , \tag{5.31}$$

where the subscripts S and R refer to the shell and the compressive ring respectively, and other symbols are as previously defined.

Considering the result of equation 5.22 ($\sigma_\theta = 0$), it is obvious that $\sigma_\phi > \sigma_\theta$ and that for least volume within this class of structures, t_r should be proportioned by use of equation 5.21 such that $\sigma_\phi \equiv f_c$ everywhere. Therefore, for use in equation 5.31,

$$\sigma_\phi = \frac{N_\phi}{t_r} \quad ,$$

$$\sigma_\theta = 0 \quad ,$$

and

$$\sigma_R = \frac{F_R}{A_R}$$

where A_R is the cross-sectional area of the ring. With these substitutions, equation 5.31 becomes,

$$\int_S \frac{N_\phi}{t_r} \, dV_S + \int_R \frac{F_R}{A_R} \, dV_R = \sum \bar{F}_i . \bar{r}_i \quad . \tag{5.32}$$

Using equations 5.25 and 5.20,

$$\int_S \frac{W}{2\pi r \, t_r \sin \phi} dV_S + \int_R \frac{W}{2\pi A_R \tan \phi} dV_R = \sum \bar{F}_i . \bar{r}_i \quad . \tag{5.33}$$

The integration of the second term of the left hand side can be easily

made, noting that all terms are constant and that,

$$\int_R dV_R = A_R \, 2\pi r_a \quad . \tag{5.34}$$

The integration of the first term can be carried out if dV_S is expressed in terms of r, t_r and ϕ. This can be done, referring to Fig. 5.8, by noting that,

$$\int_S dV_S = \int_\ell 2\pi r \, t_r \, d\ell \quad ,$$

and,

$$d\ell = \frac{dr}{\cos \phi}$$

or,

$$\int_S dV_S = \int_{r_a}^{r_b} \frac{2\pi r \, t_r}{\cos \phi} \, dr \quad . \tag{5.35}$$

Using equations 5.34 and 5.35 in equation 5.33, this latter one becomes

$$\int_{r_a}^{r_b} \left\{ \frac{W \, dr}{(\cos \phi)\sin \phi} \right\} + \frac{Wr_a}{\tan \phi} = \sum \bar{F}_i . \bar{r}_i \quad .$$

Integrating,

$$\frac{Wr_b}{(\cos \phi)\sin \phi} - \frac{Wr_a}{(\cos \phi)\sin \phi} + \frac{Wr_a}{\tan \phi} = \sum \bar{F}_i . \bar{r}_i \quad . \tag{5.36}$$

But, from geometry, since $\phi = \Phi$,

$$\tan \phi = \frac{z}{r_b - r_a} \quad ,$$

and,

$$(\cos \phi)\sin \phi = \frac{(r_b - r_a)z}{(r_b - r_a)^2 + z^2} \quad .$$

Therefore, equation 5.36 can be rewritten as

$$\frac{W[(r_b - r_a)^2 + z^2]}{(r_b - r_a)z} (r_b - r_a) + \frac{Wr_a(r_b - r_a)}{z} = \sum \bar{F}_i . \bar{r}_i \quad .$$

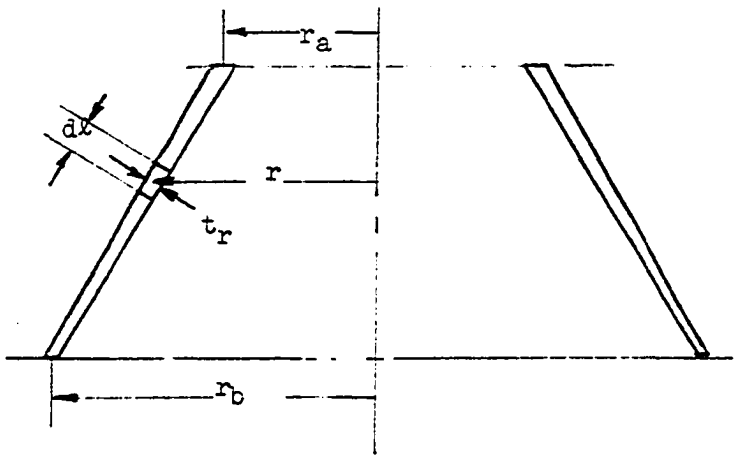

Fig. 5.8. Element of integration.

Collecting terms and simplifying, this last expression becomes,

$$W\left\{\frac{(r_b - r_a)r_b}{z} + z\right\} = \sum \bar{F}_i.\bar{r}_i \quad , \tag{5.37}$$

which can be seen to be an identity by comparison with equation 5.15.

It is thus demonstrated that the theorem of zero absolute potential energy (equation 2.10, or its equivalent, equation 5.31) holds. It is noteworthy that the derivation of equation 5.37 did not assume any particular value for σ_ϕ or σ_R and thus, the applicability of equation 2.10 is demonstrated regardless of whether or not t_r and A_R are designed so that σ_ϕ and σ_R are constant and equal to f_c.

Volume of analogous shell

It is possible to make σ_ϕ and σ_R constant and equal to f_c by letting

$$A_R = F_R/f_c \quad , \qquad \text{and} \qquad t_r = N_\phi/f_c$$

where F_R and N_ϕ can be expressed in terms of W by the use of equations 5.26 and 5.20, respectively. In such a case,

$$f_c\int_S dV_S + f_c\int_R dV_R = \sum \bar{F}_i.\bar{r}_i \quad ,$$

and, since the total volume, V_T, of the structure is,

$$V_T = \int_S dV_S + \int_R dV_R \quad ,$$

it follows that,

$$V_T = \frac{1}{f_c}\sum \bar{F}_i.\bar{r}_i \quad .$$

Thus, it is apparent that, since the entire shell-ring structure is uniaxially stressed to f_c, the shape that minimizes $\sum \bar{F}_i.\bar{r}_i$ will also

minimize the volume of the shell-ring. Furthermore, the volume of such a shell-ring structure will be identical to that of the lattice. Consequently, for the shell, as for the lattice, if V_{min} is to be achieved,

$$\left.\begin{aligned} z &= \sqrt{(r_b - r_a)r_b} \quad , \\ \text{or,} \qquad z &= r_a\sqrt{(r_b/r_a)^2 - (r_b/r_a)} \quad , \end{aligned}\right\} \tag{5.38}$$

$$\text{and,} \qquad V_{min} = \frac{2W}{f_c}\sqrt{(r_b - r_a)r_b} \quad , \tag{5.39}$$

$$\text{or} \qquad V_{min} = \frac{Wr_a}{f_c}\left[\frac{r_b/r_a}{\tan\Phi} + z/r_a\right] \quad , \tag{5.40}$$

with the proper values used for Φ and z.

Shell with plate in lieu of compression ring

If the compression ring of the shell-ring structure is replaced with a biaxially stressed circular plate, then, according to the theorem of zero absolute potential energy, if the subscript P is used to denote the plate, and if V_{S+P} is the total volume of the shell-plate structure,

$$V_{S+P} = \frac{1}{f_c}\sum \bar{F}_i.\bar{r}_i - \frac{1}{f_c}\int_P \sigma_P \, dV_P \quad . \tag{5.41}$$

This last equation indicates that the total volume of the structure is reduced by the second term of the right hand side when the plate is used, or,

$$V_{S+P} = V_{S+R} - \frac{1}{f_c}\int_P \sigma_P \, dV_P \quad ,$$

since $\sum \bar{F}_i.\bar{r}_i$ is not changed by the use of the plate.

To demonstrate this, let the plate also be designed so that $\sigma_P = f_c$, in which case, the second term of the right hand side is simply the volume

of the plate, or $V_{S+P} = V_{S+R} - V_P$,

and $V_S + V_P = V_S + V_R - V_P$,

and therefore, $V_P = \frac{1}{2} V_R$.

Thus, to demonstrate the applicability of equation 5.41, it is sufficient to show that when $\sigma_R = \sigma_P$, $V_P = \frac{1}{2} V_R$.

If a ring and a plate are subjected to the same distributed compressive load per unit length, N_H, then, for the ring,

$$V_R = 2\pi r_a A_R$$

where $A_R = F_R/\sigma_R$,

and, since $F_R = N_H r_a$,

$$V_R = 2\pi r_a^2 (N_H/\sigma_R) \quad . \tag{5.42}$$

For the plate, $V_P = \pi r_a^2 (t_P)$

where $t_P = N_H/\sigma_P$,

and therefore, $V_P = \pi r_a^2 (N_H/\sigma_P)$. (5.43)

Comparison of equations 5.42 and 5.43 shows that $V_P = \frac{1}{2} V_R$, as expected, when $\sigma_R = \sigma_P$.

It is to be noted that minimization of $\sum \bar{F}_i . \bar{r}_i$ alone would not yield the shape for minimum volume of this shell-plate structure. The entire right hand side of equation 5.41 should be minimized for that purpose. If this shell-plate structure had been chosen as the analogous shell for the lattice, minimization of $\sum \bar{F}_i . \bar{r}_i$ would still have given the shape for minimum lattice volume.

Second Lattice Alternative - Hyperboloidal

Geometry of the lattice

The global minimum volume lattice for the system of loads of this chapter is given by the conoidal lattice of the first alternative synthesis. Such a structure, however, may not be acceptable because of the long unsupported legs, and it may be desirable to explore another class of structures.

A different class of structures is shown in Fig. 5.9, where only some of the members are shown for clarity. The class depicted therein is one with clockwise and counterclockwise inclined legs that meet in pairs at the top and bottom levels, as well as at points in between. The structures can be characterized by r_a, r_b and z, as before, plus n and m, where n is the number of nodes around the top level (or the number of supports), and m is the number of spaces between the two nodes of a pair of legs. If α is the angle subtended by radii drawn to adjacent nodes, and β is the angle subtended by two radii drawn to the two nodes of a pair of legs (see Fig. 5.9), then

$$\left.\begin{aligned} \alpha &= \frac{2\pi}{n} , \\ \alpha &= \frac{\beta}{m} , \\ \text{and} \qquad \beta &= \frac{2\pi m}{n} . \end{aligned}\right\} \tag{5.44}$$

One limitation of this class of structures is that, if an all compression structure is sought, then,

$$\gamma \leq \pi/2,$$

where γ , as shown in Fig. 5.9, is the angle between the extension of the radius through one of the top nodes and the horizontal projection of the

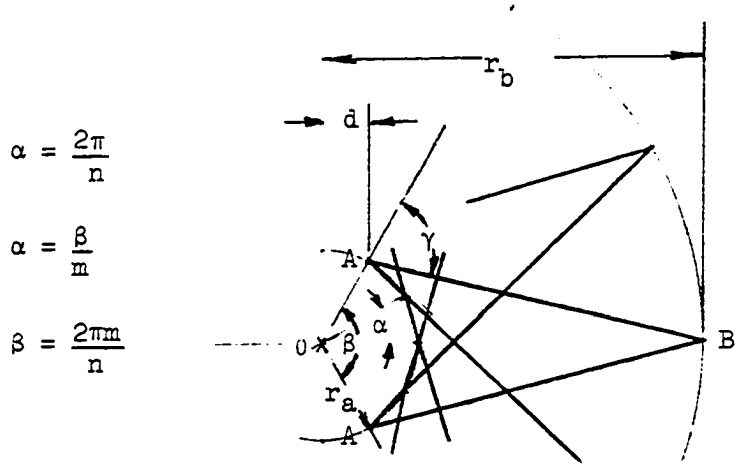

a. Top view.

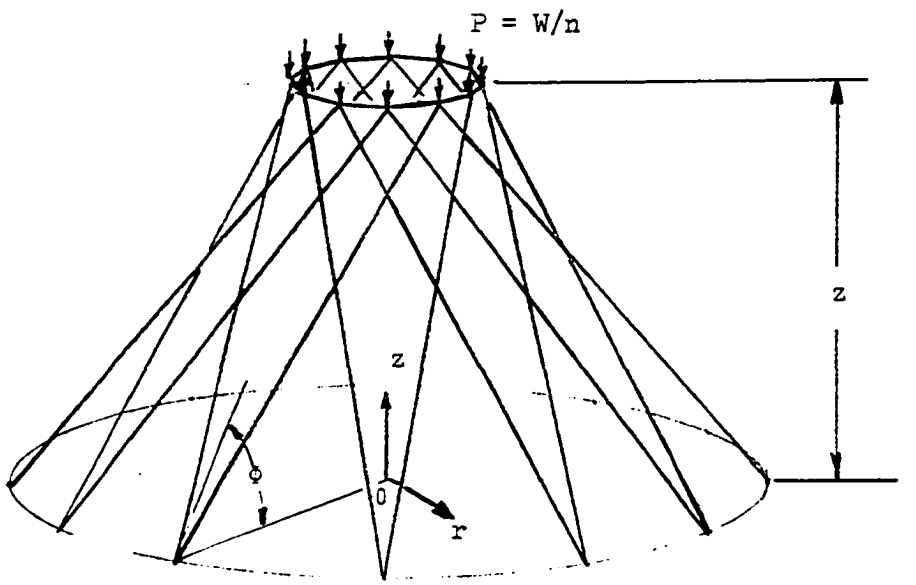

b. Side view.

Fig. 5.9. Another class of latticed structures.

legs which start at that node. (If $\gamma > \pi/2$ were allowed, the legs would pass under the circle with r_a as the radius and the top ring would be in tension).

$$\left.\begin{aligned} &\text{From geometry,} && d = r_a \cos \beta/2 \ , \\ &\text{or,} && d = r_a \cos \frac{\pi m}{n} \ , \\ &\text{and} && \tan \phi = \frac{z}{r_b - d} \ , \end{aligned}\right\} \qquad (5.45)$$

where d and ϕ are defined in Fig. 5.9.

Classical method

Using the generalized expressions developed in chapter three (equations 3.7 through 3.10),

$$V_{min} = \frac{1}{f_c} \left\{ \sum \frac{Z\, r_b}{\tan \phi} + \sum Pz \right\}_{min} \ ,$$

and, since from equilibrium of vertical forces, $Z = P$, while $\sum P = W$,

using equation 5.45, $V_{min} = \frac{W}{f_c} \left\{ \frac{r_b(r_b - d)}{z} + z \right\}_{min}$.

For V_{min}, letting $\frac{\partial V_{min}}{\partial z} = 0$,

$$\left.\begin{aligned} z &= \sqrt{(r_b - d) r_b} \ , \\ \text{and,} \qquad V_{min} &= \frac{2W}{f_c} \sqrt{(r_b - d) r_b} \ . \end{aligned}\right\} \qquad (5.46)$$

Note that V_{min} is a function of m and n by virtue of equation 5.45. If this class is preferable, it would probably be because of the shorter lengths of the portions of the legs between intersections. For the maximum number of intersections with a given n, m should be as large as possible. The magnitude of m is restricted by the requirement that

$\gamma \leq \pi/2$, as mentioned previously. If m and n are properly related (or if n is very large), then γ can be made equal to $\pi/2$. In that case,

$$\cos \beta/2 = r_a/r_b \quad ,$$

and

$$d = \frac{r_a^2}{r_b} \quad .$$

Then, for V_{min},

$$\left.\begin{aligned} \tan \Phi &= \frac{1}{\sqrt{1 - (r_a/r_b)^2}} \quad , \\ z &= \sqrt{r_b^2 - r_a^2} \quad , \\ \text{and} \qquad V_{min} &= \frac{2W}{f_c}\sqrt{r_b^2 - r_a^2} \quad . \end{aligned}\right\} \tag{5.47}$$

In terms of r_a and r_b/r_a,

$$\left.\begin{aligned} \tan \Phi &= \frac{r_b/r_a}{\sqrt{(r_b/r_a)^2 - 1}} \quad , \\ z &= r_a\sqrt{(r_b/r_a)^2 - 1} \quad , \\ \text{and} \qquad V_{min} &= \frac{Wr_a}{f_c}\left\{\frac{r_b/r_a}{\tan \Phi} + z/r_a\right\}. \end{aligned}\right\} \tag{5.48}$$

Shell analogy

The general equation for the hyperboloidal shell of Fig 5.10 is,

$$\frac{x^2}{a^2} + \frac{y^2}{b^2} - \frac{z^2}{c^2} = 1 \quad .$$

If $a \neq b$, the surface is a elliptical hyperboloid since for any constant z, x and y describe an ellipse. If $a = b = r_a$, then the equation of the hyperboloid of one sheet becomes,

$$\frac{x^2}{r_a^2} + \frac{y^2}{r_a^2} - \frac{z^2}{c^2} = 1 \quad .$$

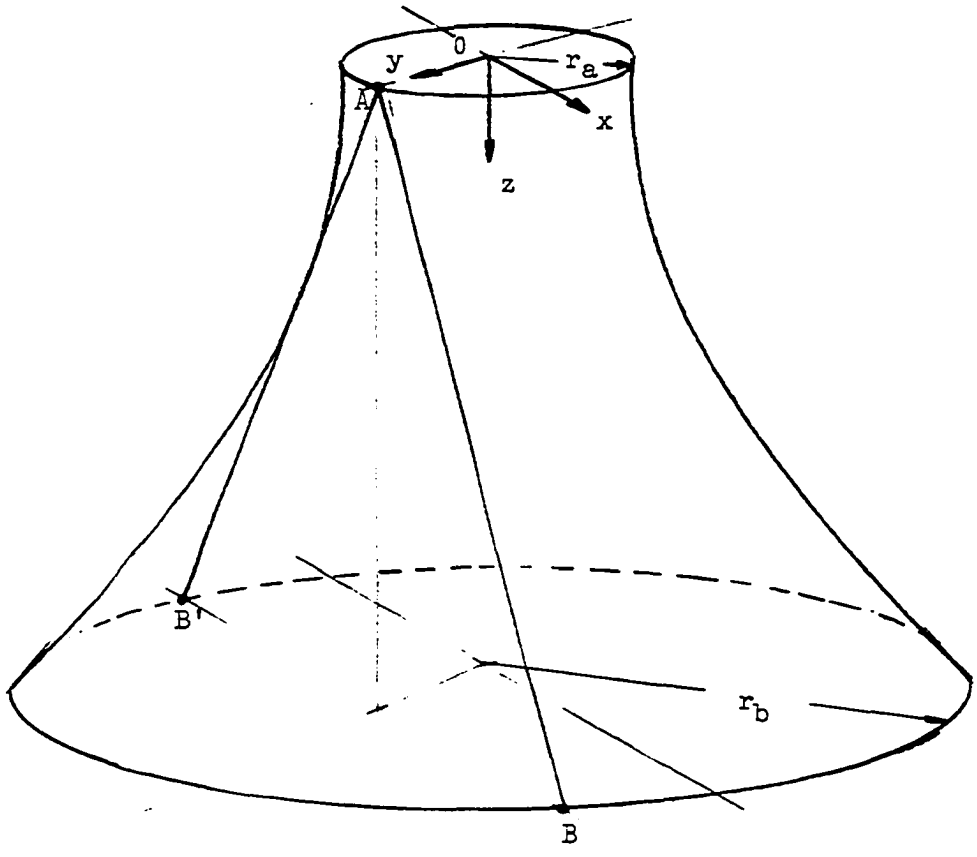

Fig. 5.10. Hyperboloidal shell.

When $y = r_a$, this expression reduces to

$$\frac{x^2}{r_a^2} = \frac{z^2}{c^2} \quad ,$$

from which, $$z = \pm \frac{c}{r_a}(x) \quad .$$

This last expression is the equation of two straight lines, shown as AB and AB' in Fig. 5.10, with slopes of c/r_a and $-c/r_a$. Consequently, the surface of Fig. 5.10, a circular hyperboloid of one sheet, can be generated by rotating a straight generatrix around a circle with radius r_a at $z = 0$; the generatrix being tangent to the circle and inclined at a slope of c/r_a or $-c/r_a$ in the vertical plane in which it lies. This, then, is the surface which would be occupied by all the inclined legs of the hyperboloidal latticed structure as $n \to \infty$. This hyperboloidal shell is geometrically similar to the lattice and can be used as the analogous shell to the hyperboloidal lattice.

In circular cylindrical coordinates, independent of θ, the equation for the shell is

$$\left.\begin{aligned} \frac{r^2}{r_a^2} - \frac{z^2}{c^2} &= 1 \quad , \\ \text{or,} \qquad z &= c\sqrt{(r/r_a)^2 - 1} \quad . \\ \text{Furthermore,} \qquad \frac{dz}{dr} &= \frac{c(r/r_a)}{r\sqrt{(r/r_a)^2 - 1}} \quad . \end{aligned}\right\} \qquad (5.49)$$

For load analogy, the shell is to be loaded with a ring load of P_S, per unit length, and acting down at $z = 0$, of such intensity that,

$$P_S = \frac{W}{2\pi r_a} \quad .$$

That this shell satisfies the conditions for it to be analogous to the lattice can be verified by comparing the shell analogy solution to be

obtained, with the one already obtained by direct consideration of the lattice. Thus, the correspondence of bar forces and shell traction resultants will not be explored.

Considering a free-body diagram as shown in Fig. 5.11, and summing forces in the vertical direction,

$$N_\phi = \frac{W}{2\pi r \sin \phi} \quad . \tag{5.50}$$

At the supports, using Z to denote the vertical component of N_ϕ, since $r = r_b$,

$$Z = \frac{W}{2\pi r_b} \quad ;$$

while the horizontal component, X, acting in the radial direction, is

$$X = \frac{W}{2\pi r_b \tan \phi} \quad .$$

Using the generalized expression developed in chapter three (equations 3.7 through 3.10),

$$\sum \bar{F}_i . \bar{r}_i = \left\{ \frac{W(2\pi r_b) r_b}{2\pi r \tan \phi} + W z_b \right\} \quad ,$$

or,

$$\sum \bar{F}_i . \bar{r}_i = W \left\{ \frac{r_b}{\tan \phi} + z_b \right\} .$$

But ,

$$\tan \phi = \left. \frac{dz}{dr} \right|_{r_b} \quad ,$$

thus, using the expression for dz/dr from equations 5.49, and substituting its estimated value at $r = r_b$ in the last expression for $\sum \bar{F}_i . \bar{r}_i$, the latter one becomes,

$$\sum \bar{F}_i . \bar{r}_i = W \left\{ \frac{r_a r_b \sqrt{(r_b/r_a)^2 - 1}}{c(r_b/r_a)} + z_b \right\} .$$

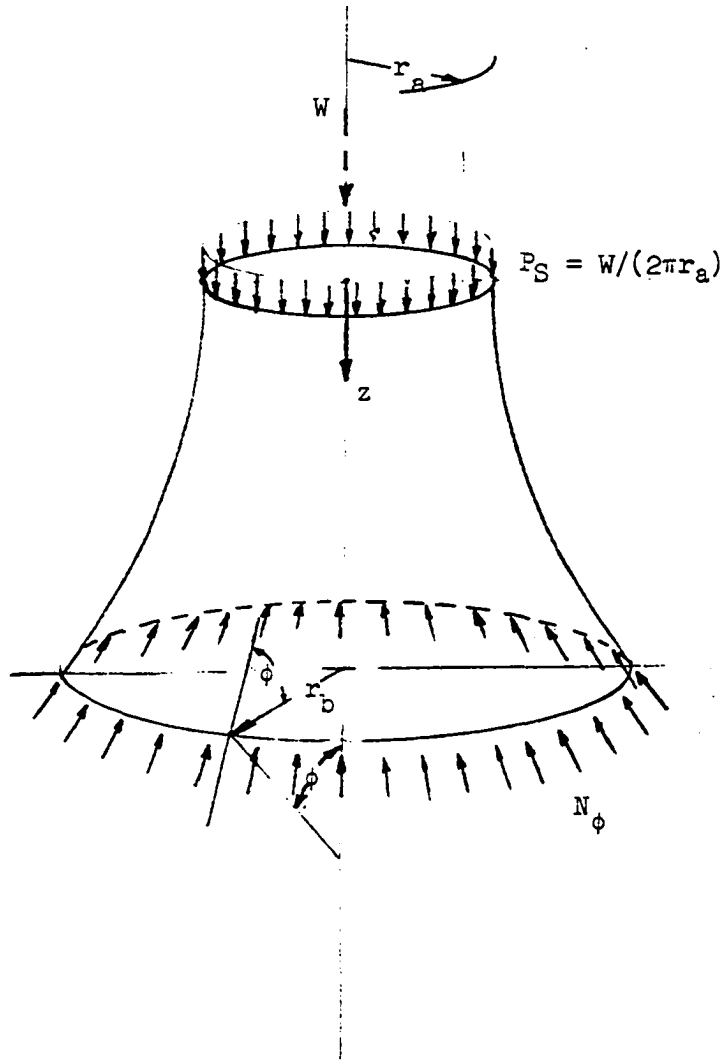

Fig. 5.11. Free-body diagram of the analogous hyperboloidal shell.

But, using the expression for z_b, also from equations 5.49 (evaluated at $r = r_b$), this can be further reduced to,

$$\sum \bar{F}_i.\bar{r}_i = W \left\{ \frac{r_b^2 - r_a^2}{z_b} + z_b \right\} . \qquad (5.51)$$

For minimum $\sum \bar{F}_i.\bar{r}_i$,

letting $$\frac{\partial(\sum \bar{F}_i.\bar{r}_i)}{\partial z_b} = 0 ,$$

yields $$z_b = \sqrt{r_b^2 - r_a^2} . \qquad (5.52)$$

Expression 5.52 can be seen to be identical to equation 5.47 for the latticed hyperboloid.

Note also, that when z_b is given by equation 5.52, then from equations 5.49, $c = r_a$, (5.53)
and therefore, the slope of the inclined legs of the latticed hyperboloid is either 1 or -1, and they make an angle of 45° with their horizontal projections.

Applicability of theorem to the shell

For the hyperboloidal shell described in the previous section, the theorem of zero absolute potential energy (equation 2.10) can take the form,

$$\int_S \sigma_\phi \, dV_S + \int_S \sigma_\theta \, dV_S = \sum \bar{F}_i.\bar{r}_i . \qquad (5.54)$$

Its applicability will be demonstrated. However, it is convenient to first develop some expressions to be used.

It can be shown that $\sigma_\phi \geq \sigma_\theta$. Thus, by properly defining the thickness of the shell, t_r, it is possible to make $\sigma_\phi = f_c$ and $\sigma_\theta \leq f_c$ everywhere.

From equation 5.50, letting $\sigma_\phi = f_c$,

$$t_r = \frac{W}{2\pi r f_c \sin \phi} \quad . \tag{5.55}$$

To obtain an expression for σ_θ, it is first necessary to obtain N_θ

and then, $$\sigma_\theta = \frac{N_\theta}{t_r} \quad . \tag{5.56}$$

The value of N_θ can be evaluated from consideration of the equilibrium of a small element of the shell. Since there is no load perpendicular to the surface of the shell,

$$\frac{N_\phi}{R_\phi} + \frac{N_\theta}{R_\theta} = 0 \quad . \tag{5.57}$$

Since the radii of curvature, R_ϕ and R_θ, are of opposite signs, (a hyperboloidal surface is anticlastically curved) it can be seen that both N_ϕ and N_θ, and hence σ_ϕ and σ_θ will be of the same sign (i.e. both compressive).

For this shell, $$R_\theta = \frac{r}{\sin \phi} \quad , \tag{5.58}$$

and R_ϕ can be evaluated from

$$R_\phi = \frac{\left[1 + \left(\frac{dz}{dr}\right)^2 \right]^{3/2}}{\frac{d^2z}{dr^2}} \quad . \tag{5.59}$$

Upon using the proper expressions for the derivatives in equation 5.59, R_ϕ can be expressed as,

$$R_\phi = - \frac{z^3 r_a^2}{c^4 \cos^3 \phi} \quad . \tag{5.60}$$

Substituting expressions 5.58 and 5.60 into equation 5.57, and solving for N_θ,

$$N_\theta = N_\phi\left[\frac{r_a^2(\cos\phi)\sin\phi}{z\,r}\right] . \qquad (5.61)$$

Noting that $(\cos\phi)\sin\phi = \frac{1}{2}\sin 2\phi$, it is verified that the ratio N_θ/N_ϕ (and hence $\sigma_\theta/\sigma_\phi$) decreases as ϕ decreases and z and r increase (i.e. as r increases from its minimum value of r_a). If equation 5.50 is used in equation 5.61, the latter becomes,

$$N_\theta = \frac{W\,(r_a/r)^2\cos\phi}{2\pi z} . \qquad (5.62)$$

(At $z = 0$, expression 5.62 becomes indefinite since $\phi = \pi/2$ and $\cos\phi = 0$. However, by the proper substitutions it can be shown that $N_\theta = N_\phi$, and consequently, $\sigma_\theta = \sigma_\phi$ at $r = r_a$.)

With t_r defined by expression 5.55, $\sigma_\phi = f_c$ everywhere. Then, to demonstrate the applicability of equation 5.54, it may be first rewritten as,

$$V_S = \frac{1}{f_c}\sum \bar{F}_i.\bar{r}_i - \frac{1}{f_c}\int_S \sigma_\theta\, dV_S . \qquad (5.63)$$

The volume of the shell will be computed directly and compared with $\sum \bar{F}_i.\bar{r}_i$. Then, by computation of $\frac{1}{f_c}\int_S \sigma_\theta\, dV_S$ it will be shown that equation 5.63 is an identity.

The volume of the shell, V_S, can be computed as,

$$V_S = \int 2\pi r\, t_r\, d\ell ,$$

where $d\ell$ is a differential element of length of a meridian. Using expression 5.55 for t_r,

$$V_S = \frac{W}{f_c}\int \frac{d\ell}{\sin\phi} .$$

After a change of variables, and entering the limits of integration, V_S can be expressed as,

$$V_S = \frac{W}{f_c} \left\{ \int_{r_a}^{r_b} \frac{dr}{(dz/dr)} + \int_{r_a}^{r_b} (dz/dr)dr \right\} . \qquad (5.64)$$

The second integral is simply z_b. Then, using the expression for dz/dr from equations 5.49, equation 5.64 becomes,

$$V_S = \frac{W}{f_c} \left\{ z_b + \frac{r_a}{c} \int_{r_a}^{r_b} \frac{\sqrt{(r/r_a)^2 - 1}}{(r/r_a)} dr \right\} . \qquad (5.65)$$

The integral in equation 5.65 can be integrated by a change of variables. Then,

$$V_S = \frac{W}{f_c} \left(z_b + \frac{r_b^2 - r_a^2}{z_b} - \left\{\frac{\sqrt{r_b^2 - r_a^2}}{z_b}\right\} r_a \tan^{-1}[\sqrt{(r_b/r_a)^2 - 1}] \right) . \qquad (5.66)$$

Comparing equations 5.51 and 5.66, it is obvious that,

$$V_S = \frac{1}{f_c} \sum \bar{F}_i . \bar{r}_i - \frac{W}{f_c} \left\{\frac{\sqrt{r_b^2 - r_a^2}}{z_b}\right\} r_a \tan^{-1}[\sqrt{(r_b/r_a)^2 - 1}] .$$

Thus, considering equation 5.63, it must now be shown that,

$$\frac{1}{f_c} \int \sigma_\theta \, dV_S = \frac{W}{f_c} \left\{\frac{\sqrt{r_b^2 - r_a^2}}{z_b}\right\} r_a \tan^{-1}[\sqrt{(r_b/r_a)^2 - 1}] . \qquad (5.67)$$

To evaluate the integral and verify the validity of equation 5.67, use the same differential element for dV_S as was used before, then,

$$\frac{1}{f_c} \int \sigma_\theta \, dV_S = \frac{1}{f_c} \int \frac{N_\theta}{t_r} 2\pi r \, t_r \, d\ell .$$

Cancelling t_r, and using equation 5.62,

$$\frac{1}{f_c} \int \sigma_\theta \, dV_S = \frac{W}{f_c} \int \frac{r_a^2 \cos \phi}{zr} \, d\ell .$$

However, noting that $(\cos \phi)d\ell = dr$, and replacing z by its equivalent from equation 5.49,

$$\frac{1}{f_c}\int \sigma_\theta \, dV_S = \frac{W}{f_c}\int_{r_a}^{r_b} \frac{r_a}{c(r/r_a)\sqrt{(r/r_a)^2 - 1}}\, dr \quad . \tag{5.68}$$

where the limits of integration have been added. Integrating,

$$\frac{1}{f_c}\int \sigma_\theta \, dV_S = \frac{Wr_a^2}{cf_c} \tan^{-1}[\sqrt{(r_b/r_a)^2 - 1}] \quad . \tag{5.69}$$

In equation 5.69, c can be expressed in terms of r_a, r_b and z_b by using equation 5.49. Making such substitution, equation 5.69 yields,

$$\frac{1}{f_c}\int \sigma_\theta \, dV_S = \frac{W}{f_c}\left\{\frac{\sqrt{r_b^2 - r_a^2}}{z_b}\right\} r_a \tan^{-1}[\sqrt{(r_b/r_a)^2 - 1}]. \tag{5.70}$$

Equation 5.70 is exactly as predicted by equation 5.67, and thus completes the demonstration of the applicability of the theorem of zero absolute potential energy.

It is to be noted that this demonstration was made for the general shell of this class, and thus not only for the one that minimizes $\sum \bar{F}_i.\bar{r}_i$.

If $\sum \bar{F}_i.\bar{r}_i$ is to be minimized (for minimum volume of the lattice to which this shell is analogous), then, as shown by equation 5.52,

$$z_b = \sqrt{r_b^2 - r_a^2} \quad .$$

With that substitution, $\sum \bar{F}_i.\bar{r}_i$ for the shell (equation 5.51) and for the lattice are identical, as they should be, while equations 5.66 and 5.70 are somewhat simplified.

Volume of analogous shell

In the process of demonstrating the applicability of the theorem of zero absolute potential energy, the volume of the analogous shell was computed as shown in equation 5.66. In the comparison of volumes which is the last section in this chapter, the numerical values for the volumes of the hyperboloidal shells were computed by subtracting the quantity,

$$\frac{1}{f_c} \int \sigma_\theta \, dV_S$$

from the corresponding volumes of the lattices. The quantity to be subtracted was computed using equation 5.67 and the known value for z_b (equation 5.52).

Third Lattice Alternative - Free Form by Shell Analogy

Lattice with constant slenderness ratio

The second latticed alternative (hyperboloidal) has shorter unsupported lengths between intersections than the first (conoidal), and does provide greater lateral stability by its inherent lateral bracing. Yet, all segments of the legs in either of those two designs carry equal axial loads. The second alternative has legs subdivided into segments of different lengths. Therefore, the different segments have different slenderness ratios. This variable load-to-length (T/L) ratio is a disadvantage since those portions or segments with the lesser T/L ratios (longer lengths) are more susceptible to buckling. Thus, it is desirable to explore the minimum volume of a lattice to support the same system of loads, but with constant T/L ratios. The form of the lattice to fulfill such requirement will be obtained by a shell analogy.

Correspondence of bar forces and shell traction resultants

Consider a typical bar of such a structure, as shown in Fig. 5.12. The bar is shown as it would appear projected on the plane which is tangent to the analogous shell at a point midway between the ends of the bar. If it is assumed that the lattice pattern will include only such typically inclined members, and no ring members (except perhaps at the top if required), then such typical bar must carry the membrane forces present in the element of the analogous shell whose projection on the tangent plane is also shown, dotted, in Fig. 5.12 . The bar field distances, which define the portion of the shell whose membrane forces migrate to the bar, can be approximated by the average height, and width, of the trapezoidal shell element. The equivalent dimensions are labeled b_ϕ and b_θ in Fig. 5.12 to denote the bar field to be used for N_ϕ and N_θ of the shell, respectively.

Then, using T_ϕ and T_θ to denote the components of the bar force in the ϕ and θ directions, respectively,

$$T_\phi = T\frac{b_\theta}{L},$$

and

$$T_\theta = T\frac{b_\phi}{L}.$$

It then follows that,

$$\left.\begin{aligned} N_\phi &= \frac{T}{L}\left\{\frac{b_\theta}{b_\phi}\right\}, \\ \text{and,}\quad N_\theta &= \frac{T}{L}\left\{\frac{b_\phi}{b_\theta}\right\}. \end{aligned}\right\} \qquad (5.71)$$

Thus,

$$\frac{N_\theta}{N_\phi} = \left(\frac{b_\phi}{b_\theta}\right)^2 = \tan^2\alpha \qquad (5.72)$$

where α is the angle measuring the inclination of the bar (at the point

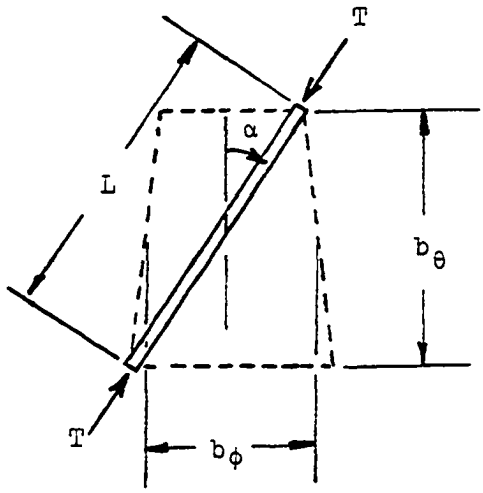

Fig. 5.12. Typical bar.

where N_θ/N_ϕ is being computed) with respect to the meridian passing through the midpoint of the bar.

Observing equations 5.71 and 5.72, it is obvious that many shell classes (or lattices) are possible. The conoidal lattice and shell represent the class wherein $\alpha = 0$, and consequently $N_\theta = 0$. (Of course in the conoidal lattice, $\alpha = 0$ implies, by the geometry of Fig. 5.12, that b_ϕ is equal to the width of the legs. The legs are then touching each other, and thus the analogous lattice and shell are one and the same.) The constancy of the T/L ratio from point to point in the lattice can be achieved by insuring that N_ϕ, N_θ and α be related as indicated by equations 5.71 and 5.72. If α varies from bar to bar, then the ratio N_θ/N_ϕ will have to vary also from point to point in the analogous shell.

The class selected for this illustrative example will be the one in which α is constant and equal to 45° for all bars. Then N_ϕ and N_θ will everywhere be constant and,

$$N_\phi = N_\theta = \frac{T}{L} = S \qquad (5.73)$$

where S is used to denote constant shell traction in all directions. Thus, although the lengths of the bars will vary, the ratio T/L will be constant throughout.

Shell analogy solution

Shells in a membrane state of stress with constant traction in all directions (and of course constant stress with constant thickness, t) have been of interest to many investigators, as was already mentioned in previous chapters. In some cases, recourse was made to soap film analogies to determine their shape, since a soap film membrane, not being able to resist

shear, assumes a shape such that the membrane traction is constant, and equal to twice the surface tension of the particular soap solution used (since the film has two surfaces), regardless of the load imposed on the membrane. Harrenstien (15) used a system of loads exactly the reverse of that being considered here (the soap film is tension stressed). He also derived the analytical equation for the membrane shape. It is his work that inspired the use of this conceptual system of loads to illustrate the theory developed in this dissertation. Unfortunately, Harrenstien's membrane shape was uniquely determined by the surface tension properties of the soap solution he used (and, of course, by the weights and dimensions of his models) and was not the least volume membrane of its class.

The general equations describing the geometry of this class of shell (constant S) will be independently developed here. The least volume shape will then be obtained by minimization of $\sum \bar{F}_i.\bar{r}_i$. All the equations of equilibrium must be used in developing the equations describing the general form for the class of the shell, and to express $\sum \bar{F}_i.\bar{r}_i$ in terms of only one variable (one degree of freedom) prior to optimizing it.

A typical shell element is shown in Fig. 5.13. The analogous lattice element is shown, dotted, in the same figure. The center node, and one-quarter of the corner nodes of the analogous lattice lie within the shell, with their centers on the middle surface of the shell. Denote by the subscripts V, R and T the vertical, radial and tangential components of S, respectively.

The total load, W, on the shell is applied as before, at $r = r_a$, as a ring load of intensity, P_S, per unit length as follows,

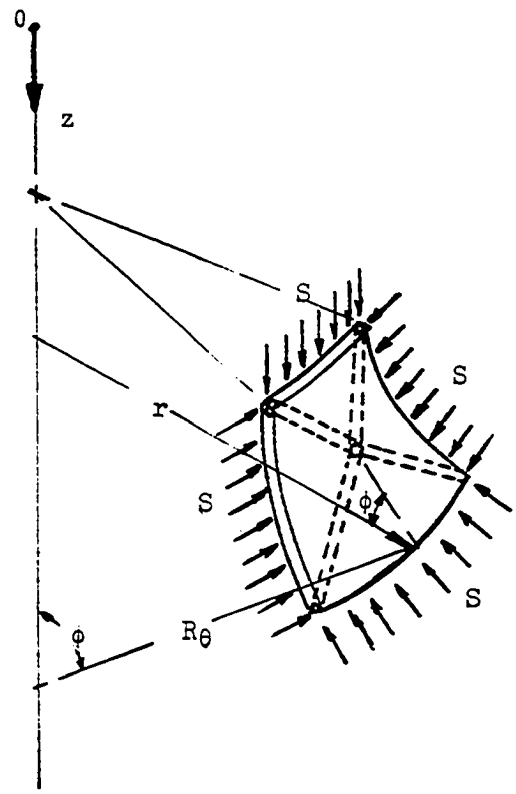

Fig. 5.13. Shell element.

$$P_S = \frac{W}{2\pi r_a} \quad . \tag{5.74}$$

Vertical equilibrium of a portion of the shell above an arbitrary r demands that S_V, the vertical component of S be,

$$S_V = \frac{W}{2\pi r} \quad . \tag{5.75}$$

Furthermore, since no bending is present, if S_H is the horizontal component of S,

$$\left.\begin{aligned} &\frac{S_V}{S_H} = \tan\phi \quad , \\ &\text{while} \qquad \tan\phi = \frac{dz}{dr} \quad , \\ &\text{and} \qquad S = \sqrt{S_V^2 + S_H^2} \quad . \end{aligned}\right\} \tag{5.76}$$

Expressions 5.75 and 5.76 can be used to yield

$$\frac{dz}{dr} = \sqrt{\frac{1}{\left\{\frac{2S\pi r}{W}\right\}^2 - 1}} \quad . \tag{5.77}$$

Equation 5.77 is equivalent to Harrenstien's corresponding expression to which it can be reduced by the appropriate notation adjustments. Expression 5.77 is positive while Harrenstien's is negative, because he chose his origin at the lower level so that z decreases as r increases. The opposite is true here, with the origin as shown in Fig. 5.13.

Then,

$$\sum \bar{F}_i . \bar{r}_i = \sum S_{H_b} r_b + \sum S_{V_b} z_b \quad , \tag{5.78}$$

where the subscript b indicates that the quantity subscripted must be evaluated at $r = r_b$ prior to the symbolic summation.

From equations 5.75, 5.76 and 5.77,

$$\left.\begin{aligned} S_{V_b} &= \frac{W}{2\pi r_b} \ , \\ S_{H_b} &= \frac{W}{2\pi r_b}\sqrt{\left\{\frac{2S\pi r_b}{W}\right\}^2 - 1} \ , \\ \text{and,} \qquad z_b &= \int_{r_a}^{r_b} \frac{dr}{\sqrt{\left\{\frac{2S\pi r}{W}\right\}^2 - 1}} \ . \end{aligned}\right\} \tag{5.79}$$

Since r_b and z_b are constant for the purposes of evaluating equation 5.78, the summations of S_{V_b} and S_{H_b} can be carried out separately. Then,

$$\sum \bar{F}_i.\bar{r}_i = Wr_b\sqrt{\left\{\frac{2S\pi r_b}{W}\right\}^2 - 1} + W\int_{r_a}^{r_b} \frac{dr}{\sqrt{\left\{\frac{2S\pi r}{W}\right\}^2 - 1}} \ . \tag{5.80}$$

The integral can be evaluated noting that ,

$$\frac{d}{dx}\cosh^{-1}u = \frac{1}{\sqrt{u^2 - 1}}\cdot\frac{du}{dx} \ , \quad u>1 \ .$$

Performing the integration and collecting terms,

$$\sum \bar{F}_i.\bar{r}_i = W\left\{ r_b\sqrt{\left\{\frac{2S\pi r_b}{W}\right\}^2 - 1} + \frac{1}{(S/W)2\pi}\left[\cosh^{-1}\left\{\frac{2S\pi r_b}{W}\right\} - \cosh^{-1}\left\{\frac{2S\pi r_a}{W}\right\}\right] \right\} . \tag{5.81}$$

If all members of the latticed structure are designed to be stressed to f_c, and if they conform to the requirements to be met for this shell to be analogous (i.e. pattern as shown in Fig. 5.13, $\alpha = 45°$ for all members, and all nodes lying in the middle surface of the shell when the lattice is under the design load), then the lattice volume, V_L, is

$$V_L = \frac{1}{f_c} \sum \bar{F}_i . \bar{r}_i \quad , \tag{5.82}$$

where $\sum \bar{F}_i . \bar{r}_i$ is given by equation 5.81. It is interesting to note that it has been possible to arrive at a general design for the lattice, and to a statement for its volume, prior to a definitive design, by means of the theorem of zero absolute potential energy.

The variable in equation 5.81 is the S/W ratio. When the desired S/W ratio is selected, then the shape of the lattice (and shell) is defined by the second term of the right hand side of equation 5.81, which, with r_b replaced by r, is the equation for z. That is,

$$z = \frac{1}{(S/W)2\pi}\left[\cosh^{-1}\left\{\frac{2S\pi r}{W}\right\} - \cosh^{-1}\left\{\frac{2S\pi r_a}{W}\right\}\right] \quad . \tag{5.83}$$

In addition, the lattice members can be designed directly from the previouly developed expression (equation 5.73), that

$$S = T/L \quad .$$

The lengths of the lattice members can be found once n, the number of nodes around the periphery, is known. It may be necessary to adjust n (or conversely, r_a or r_b) to insure that a layer of nodes will correspond to r_a, r_b and z_b. This is so because, since $\alpha = 45°$, as soon as n (and consequently the spacing between adjacent nodes) is chosen, then the vertical distance between levels of nodes is also determined.

Note that,

$$\frac{S}{W} \geq \frac{1}{2\pi r_a} \quad , \tag{5.84}$$

since lesser values yield imaginary solutions. When the "greater than" sign applies, the tangent to a meridian at $r = r_a$, makes an angle, ϕ_a,

with the horizontal plane such that,

$$\phi_a < \pi/2 \quad ,$$

and in that case the lattice needs a ring at $r = r_a$ to equilibrate the radial component of S. For the shell, it is best to use a diaphragm or compression cap plate, rather than a ring, since then the entire shell, including such a plate, can be biaxially stressed to f_c by properly selecting the thicknesses of the shell (constant) and of the diaphragm (also constant but not necessarily equal to that of the shell). It can be verified, by direct evaluation of the volume of such shell-plate structure that its volume, V_S, is,

$$V_S = \frac{1}{2f_c} \sum \bar{F}_i . \bar{r}_i \quad ,$$

or one half the volume of the lattice, as it must be in accordance with the theorem of zero absolute potential energy.

When the "equal" sign of equation 5.84 applies, then the tangent at $r = r_a$ is vertical and no ring is needed (for equilibrium) in the lattice. In the shell, the volume of the diaphragm can be shown to vanish in that case as the required thickness of the diaphragm becomes zero. There is an infinitesimally small discontinuity in N_θ in that case at r_a since it must be zero there and equal to S as soon as $r > r_a$ by an infinitesimal amount.

Minimization of the lattice volume

To obtain the S/W ratio that minimizes $\sum \bar{F}_i . \bar{r}_i$, and consequently V_L and V_S, is a complicated task not amenable to analytical treatment for all values of r_a and r_b since both equations 5.81 and its derivative are transcendental equations. In an actual numerical example it would be

necessary to use the actual values of r_a and r_b and minimize equation 5.81 by numerical methods, or by obtaining a graphical solution to the equation which is obtained by equating to zero the first derivative of $\sum \bar{F}_i.\bar{r}_i$ with respect to S/W.

To gain an insight into the range of S/W ratios that may yield a minimum volume structure of this class, equation 5.81 will be rewritten in a slightly different form. It will then be plotted.

Assume that,

$$\frac{S}{W} = \frac{1}{2\pi c} \quad ,$$

where, to rule out imaginary solutions (equation 5.84),

$$c \leq r_a \quad .$$

Then, equations 5.81 and 5.82 can be combined, and the resulting equation can be written as,

$$V_L = \frac{Wr_b}{f_c}\left\{ \frac{r_b}{c}\sqrt{1-(c/r_b)^2} + \frac{c}{r_b}\ln\frac{r_b}{c}\left[1+\sqrt{1-(c/r_b)^2}\right] - \frac{c}{r_b}\ln\frac{r_a}{c}\left[1+\sqrt{1-(c/r_a)^2}\right] \right\} \quad . \tag{5.85}$$

The three terms of the right hand side of equation 5.85 are separately plotted (signs included), and also added together, in Fig. 5.14. A ratio of r_a to r_b of 5/8 was selected to show in greater detail the significant portion of the plot. Other plots of the third term (the only one affected by the value of r_a/r_b) are shown in dotted lines.

To the right of the hashed boundary lies the region forbidden by the requirement that $c \leq r_a$. The minimum volume is obtained by a c value close to but less than r_a. For the given r_a/r_b ratio (5/8), the optimum c is graphically estimated to be $0.93(r_a)$. Such a reduction of c from

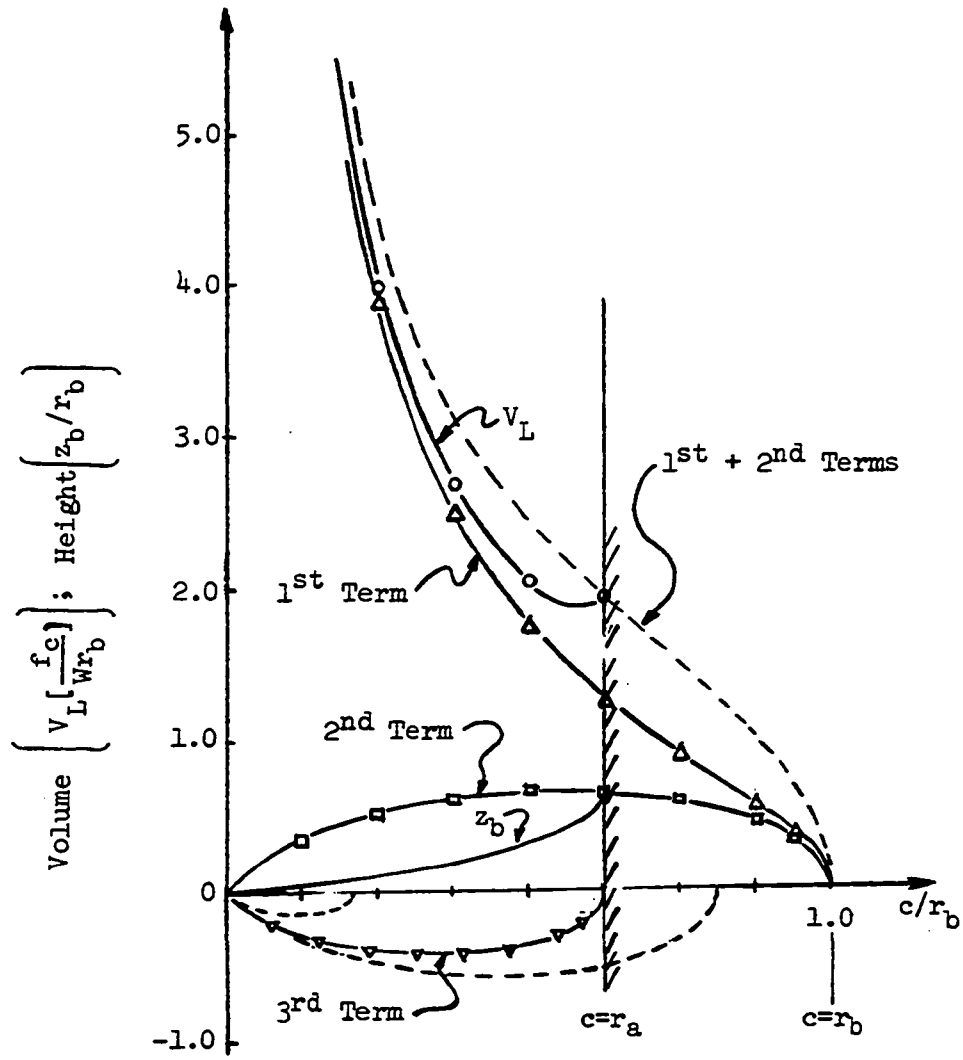

Fig. 5.14. Plot of equation 5.85.

$c = r_a$ achieves only a small reduction in the volume (less than 3%), but a drastic reduction in the overall height, z_b, of the structure (about 39% reduction based on the z_b corresponding to $c = r_a$). (A nondimensional plot of z_b is also shown in Fig. 5.14.) Furthermore, c could be as small as $0.88(r_a)$ and the volume would still be equal to or less than that of the structure with $c = r_a$. (With $c = 0.88(r_a)$, z_b is only 47% of its value when $c = r_a$.) Thus, if the height of the structure is an important factor, then the choice of c, and consequently of S/W, should be carefully investigated. The latitude on the choice of c is less, and its effect on z_b much reduced at much lesser values of r_a/r_b.

For the volume comparisons of the section that follows, it is assumed, for ease of computations, that the minimum volume of this class of structures corresponds to $c = r_a$. In that case, z_b can be expressed, using equation 5.83 evaluated at $r = r_a$ and with $S/W = 1/(2\pi r_a)$, in the equivalent form,

$$z_b = r_a \ln[\, r_b/r_a + \sqrt{(r_b/r_a)^2 - 1}\,] \quad . \qquad (5.86)$$

Similarly, from equation 5.77,

$$\tan \Phi = \frac{r_a/r_b}{\sqrt{1 - (r_a/r_b)^2}} \quad , \qquad (5.87)$$

where, as before, $\Phi = \phi_b$.

Volume Comparisons and Observations

Using equations 3.7 through 3.10, the volumes of the three latticed alternatives considered can be expressed as,

$$V_{min} = \frac{Wr_a}{f_c} \left\{ \frac{r_b/r_a}{\tan \Phi} + z/r_a \right\}_{min} , \qquad (5.88)$$

where $\tan \Phi$ is the tangent to a meridian in the analogous shell at $r = r_b$,

and z is the overall height, that correspond to V_{min}.

The corresponding expressions for tan Φ and z, as developed earlier, are collected below using the original equation numbers for reference purposes.

1. Conoidal lattice:

$$\tan \Phi = \frac{1}{\sqrt{1 - r_a/r_b}} \quad , \tag{5.7}$$

and,

$$z = r_a\sqrt{(r_b/r_a)^2 - r_b/r_a} \quad . \tag{5.9}$$

2. Hyperboloidal lattice:

$$\tan \Phi = \frac{1}{\sqrt{1 - (r_a/r_b)^2}} \quad , \tag{5.47}$$

and,

$$z = r_a\sqrt{(r_b/r_a)^2 - 1} \quad . \tag{5.48}$$

3. Lattice of constant slenderness ratio, for c = r (not for V_{min}):

$$\tan \Phi = \frac{r_a/r_b}{\sqrt{1 - (r_a/r_b)^2}} \quad , \tag{5.87}$$

and,

$$z = r_a \ln[\, r_b/r_a + \sqrt{(r_b/r_a)^2 - 1}\,] \quad . \tag{5.86}$$

The heights of the structures, z, and the corresponding volumes are plotted in Fig. 5.15 for varying r_b/r_a ratios.

In Fig. 5.15, the hyperboloidal and conoidal lines approach each other for higher r_b/r_a values. This is as should be expected, since $r_b/r_a = \infty$ implies that r_a is zero and then, the hyperboloidal lattice is indistinguishable from the conoidal. Then, tan Φ = 1, and z = r_b for both.

It is to be noted, as predicted by the first alternative design, that the volume of the conoidal lattice is a global minimum for the lattices. As additional restraints are placed on the geometries of the lattices (i.e. hyperboloidal, lattice of constant slenderness ratio) the minimum volume

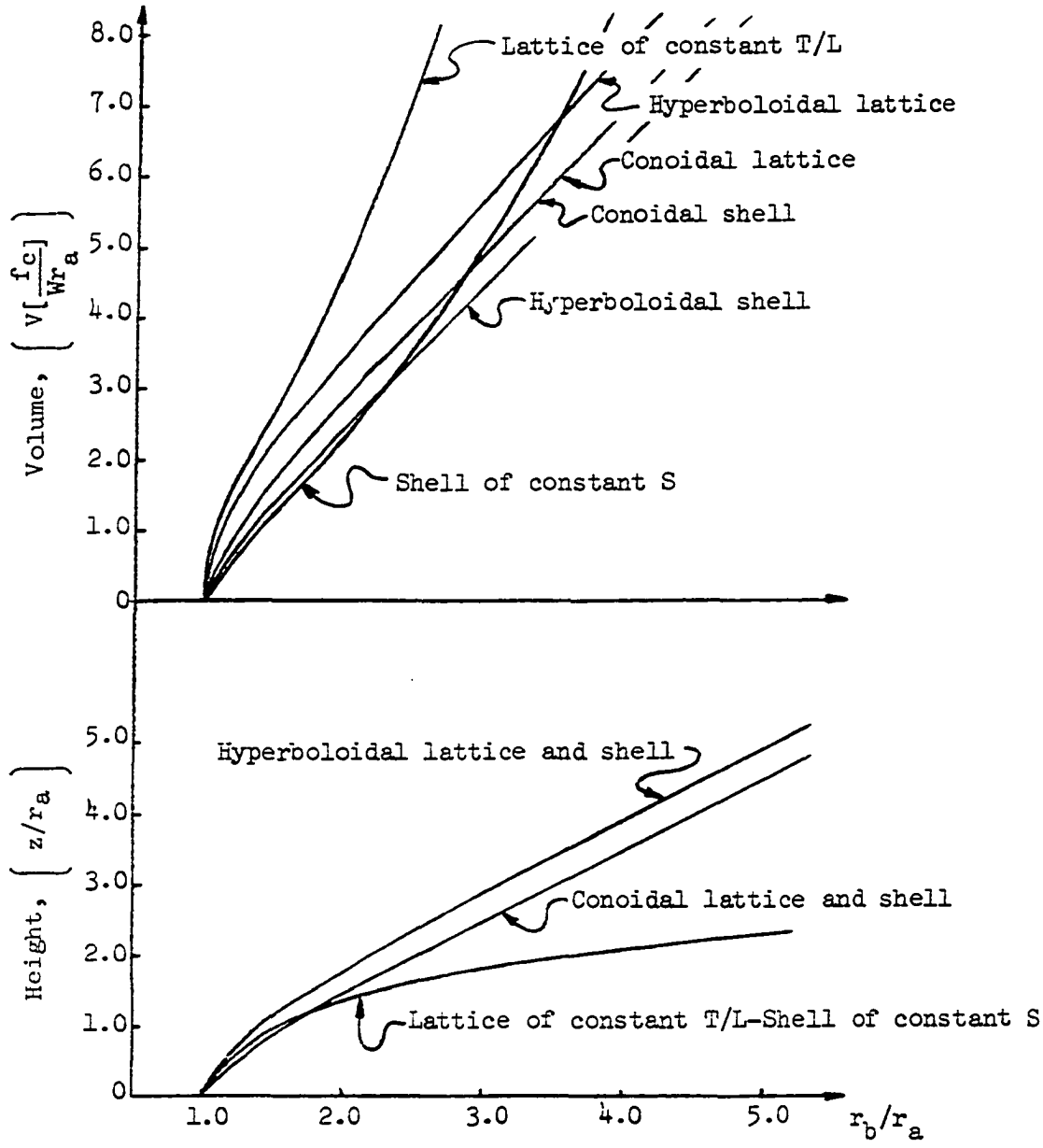

Fig. 5.15. Heights and volumes of alternative structures.

increases. For low r_b/r_a ratios (up to about 1.8), the lattices of constant slenderness ratios have an optimum z greater than the conoidal lattices but less than for hyperboloidal lattices.

The volumes of the analogous shells are also shown. The conoidal shell volume is the same as that of the conoidal lattice. The volume of the shell of constant traction (constant S) is one-half that of the lattice of constant slenderness ratio. (Since $c = r_a$ for the volumes shown, the shell does not have a plate, and the lattice does not have a compression ring. If $c \neq r_a$, then the ring and plate would have to be provided, but the volume of the shell would still be one-half that of the lattice since the shell-plate structure would be entirely biaxially stressed to f_c.) The volume of the hyperboloidal shell is less than that of the hyperboloidal lattice by the amount $\frac{1}{f_c}\int\sigma_\theta \, dV_S$ which was computed using equation 5.67.

The hierarchy for the shells is the reverse of that of the lattices. That is, the conoidal shell, which is uniaxially stressed, always has a minimum volume larger than that of the hyperboloidal shell, which has some stress in the tangential direction in addition to being fully stressed in the meridional direction. The shell of constant traction, being biaxially stressed to f_c (and thus of constant stress, f_c), is capable of providing a minimum volume less than that of either of the other two alternatives for r_b/r_a ratios of up to about 2.2. For larger r_b/r_a ratios, the least volume structure of constant S has a volume larger than the other two.

It is felt that the volume of the fully stressed (constant S) shell is greater than that of the others at the greater r_b/r_a ratios because it represents a class of structures so different from that of the other two,

that the load systems (including the reactions) are no longer comparable.

The conoidal and the hyperboloidal shells can be considered to be two sub-classes of a larger class of shells, i.e. those that can be generated by straight lines generatrices. That they become one and the same when r_a is zero, has already been pointed out. Note also that the conoidal lattice (or shell) can be generated by letting m = 0 in the expressions mathematically defining the hyperboloidal lattice (equations 5.44), in which case, $d = r_a$ (equation 5.45). Comparing equations 5.38 and 5.39 with equations 5.46 it can be seen that then the volumes for both sub-classes become identical for all r_a. Furthermore, note the similarity of expression of $\sum \bar{F}_i.\bar{r}_i$ in that, for minimum $\sum \bar{F}_i.\bar{r}_i$,

$$\sum \bar{F}_i.\bar{r}_i = 2Wz \qquad (5.89)$$

for both. The contribution of the horizontal forces and the vertical forces are equal to each other in each of the two structural sub-classes. They differ only in the expression found for z in each shell. Thus, the load systems of both represent generally comparable systems in the sense implied in the hierarchy of structural levels of chapter two. Since the conoidal lattice is a global optimum for the larger class, it follows that the volume of the hyperboloidal lattice would never be less. Furthermore, it also follows that, since the hyperboloidal shell is also stressed in the tangential direction (albeit not to f_c), then the volume of the conoidal shell, which is always stressed uniaxially, should never be less than that of the hyperboloidal shell.

In contrast, the constant S shell cannot be generated by straight lines, and could never be made to occupy the same space of either of the other two by adjusting the variables which define it. Furthermore, its load system cannot be considered fully comparable to either of the other two. Note that when $\sum \bar{F}_i . \bar{r}_i$ is a minimum for this shell (or lattice) it does not fulfill the condition expressed by equation 5.89. In addition, the contribution of the horizontal forces (to $\sum \bar{F}_i . \bar{r}_i$) is much larger than that of the vertical forces, the disparity becoming more pronounced with larger r_b/r_a ratios. Thus, this class is more efficient (yields a lesser volume) for some r_b/r_a values, and less efficient for the higher r_b/r_a ratios when the horizontal thrusts must increase greatly to keep the stress trajectories within the shell. In those cases (the larger r_b/r_a ratios), it is felt that the condition of constant S becomes a constraint which requires greater material energy than that needed to support the loads. That is, the tangential stress is needed to bend the stress trajectories and force them to remain within the structure. (In the same vein, the most efficient of all classes of structures for this system of loads would be one in which it is permissible to make $r_b = r_a$, a trivial solution resulting in a requirement for zero volume and zero stresses in a non-existent structure.)

In summary, this series of examples illustrates the method of application of the theorem (classical and shell analogy); it shows the correspondence of $\sum \bar{F}_i . \bar{r}_i$, volume and geometry for shells and lattices; and, it demonstrates the general applicability of the hierarchy of structures of chapter two. It is cautioned that in searching for a superior class

of structures, a check on the magnitude of $\sum \bar{F}_i . \bar{r}_i$ should be made so that it is not unduly increased in order to force the new structural class to apply.

SUMMARY AND CONCLUSIONS

This dissertation developed a new theorem named the theorem of zero absolute potential energy whose mathematical expression is

$$\sum_{j}^{m} \{ \int \sigma_1 dV_j + \int \sigma_2 dV_j + \int \sigma_3 dV_j \} - \sum_{i}^{n} \bar{F}_i . \bar{r}_i = 0 .$$

The mathematical expression is valid for all three-dimensional structures in internal and external static equilibrium under any system of loads. The expression is a generalized form of Maxwell's theorem for frameworks.

The theorem was used to develop a hierarchy of structural levels arranged in order of increasing material efficiency according to the state of stress existing in the structures belonging to each level. From this, it is concluded that the most efficient structures to support a given system of loads would be those which are fully and homogeneously stressed (all in tension, or all in compression). The least volume structure among those fully and homogeneously stressed will be the one with the least numerical value for $\sum \bar{F}_i . \bar{r}_i$. Triaxially stressed structures fulfilling the above requirements have lesser volume than biaxially stressed structures, which, in turn, have lesser volume than uniaxially stressed structures. Least volume statically determinate and statically indeterminate structures, if they are possible, provide the same volume when optimized with respect to a single system of loads and if their respective $\sum \bar{F}_i . \bar{r}_i$ values are of the same magnitude.

The above observations and conclusions led to a concept of optimization by variation of $\sum \bar{F}_i . \bar{r}_i$ wherein the points of application of the loads are allowed to vary along the line of action of the loads as the configuration

of the structure is varied.

A sequence of examples of the synthesis of alternate structures for the support of the same loads was presented. These examples illustrate the observations made above, as well as the transitions from one hierarchical level to other more efficient levels.

The theorem, when coupled with the concept of variation of $\sum \bar{F}_i.\bar{r}_i$ in the structural synthesis of least volume structures, results in significant simplifications of the optimization process. The number of variables is greatly reduced in the case of statically determinate structures. As a result, only the constraints of statical equilibrium need be considered. In general, the detailed design of the structure need not be addressed until after the optimum form of the structure is determined from the optimization process.

Three optimization methods utilizing the above concepts were developed (classical, nonlinear programming, and shell analogy) for application to three-dimensional nonplanar lattices. These were illustrated in the optimization of rectangular grid lattices, network domes, and Schwedler-like domes. A means to consider the volume of the tension ring, if present, was also illustrated.

The classical method is also directly applicable to shells in a membrane state of stress (the most efficient state of stress for shells) if their shape is restricted to a specific class (hyperboloidal, paraboloidal, etc.) expressible in a closed-form, integrable function. In general, these shapes will allow the shells to be fully stressed in only one direction. The optimization of a paraboloidal shell is presented as an illustration.

Possible ways are indicated for the extension of the method to the optimization of more general shapes. These include the use of numerical integration methods, or the incorporation of the minimization of $\sum \bar{F}_i . \bar{r}_i$ into the method developed by Smith and Wilson (32) for the synthesis of membrane stressed shells.

LITERATURE CITED

1. Anderheggen, E. and Thurlimann, B. Optimum design using linear programming. International Association for Bridge and Structural Engineers, Journal 26: 555-571. 1966.

2. Barnett, Ralph L. Survey of optimum structural design. Experimental Mechanics 6, No. 12: 19A-26A. Dec. 1966.

3. Benjamin, B. S. The analysis of braced domes. New York, N.Y., Asia Publishing House. c1963.

4. Borrego, John. Space grid structures. Cambridge, Massachusetts, The MIT Press. c1968.

5. Brotchie, John F. Direct design of plate and shell structures. American Society of Civil Engineers Proceedings, Journal of the Structural Division 88, No. ST6: 127-148. Dec. 1962.

6. Brown, D. M. and Ang, A. H.-S. Structural optimization by nonlinear programming. American Society of Civil Engineers Proceedings, Journal of the Structural Division 92, No. ST6: 319-340. Dec. 1966.

7. Burington, Richard Stevens. Handbook of mathematical tables and formulas. 3rd ed. Sandusky, Ohio, Handbook Publishers, Inc. 1954.

8. Castigliano, Carlo Alberto Pio. The theory of equilibrium of elastic systems and its applications (Translated title). Turin, Auguste Frederic Negro, Editeur. 1879. Original not available; translated by Ewart S. Andrews. New York, N.Y., Dover Publications, Inc. c1966.

9. Charlton, Thomas Malcolm. Energy principles in applied statics. London, Blackie and Son, Ltd. 1959.

10. Cox, H. L. The design of structures of least weight. New York, N.Y., Pergamon Press. 1965.

11. Crockett, William Arthur. Optimal design of trussed structures. Microfiche copy. Unpublished M.S. thesis. Monterrey, California, Library, Naval Postgraduate School. U.S. Dept. Commerce, National Technical Information Service Report AD 705 093. Oct. 1968.

12. Dobbs, Michael W. and Felton, Lewis P. Optimization of truss geometry. American Society of Civil Engineers Proceedings, Journal of the Structural Division 95, No. ST10: 2105-2118. Oct. 1969.

13. Fiacco, Anthony V. and McCormick, Garth P. The sequential unconstrained minimization technique for non linear programming, a primal-dual method. Management Science 10, No. 2: 360-366. Jan. 1964.

14. Gerard, G. Minimum weight analysis of orthotropic plates under compressive loading. Aerospace Science Journal 27, No. 1: 21-26 and 64. Jan. 1960.

15. Harrenstien, Howard Paul. Configuration of shell structures for optimum stresses. Unpublished Ph.D. Thesis. Ames, Iowa, Library, Iowa State University. 1959.

16. Kicher, T. P. Optimum design-Minimum weight versus fully stressed. American Society of Civil Engineers Proceedings, Journal of the Structural Division 92, No. ST6: 265-279. Dec. 1966.

17. Lin, T. Y. Load balancing method for design and analysis of prestressed concrete structures. Journal of the American Concrete Institute, Proceedings 60, No. 6: 719-742. June 1963.

18. Makowski, Z. S. Braced domes, their history, modern trends and recent developments. Architectural Science Review 5, No. 2: 62-79. July 1962.

19. Maxwell, James Clerk. On reciprocal figures, frames, and diagrams of forces. Transactions of the Royal Society of Edinburgh XXVI. 1869. Original not available; reprinted in Niven, W. D., ed. The scientific papers of James Clerk Maxwell. Vol. II. Pp. 161-207. New York, N.Y., D. Van Nostrand Company. 1927.

20. Michell, A. G. M. The limit of economy of material in frame structures. Philosophical Magazine, Ser. 6, 8, No. 47: 589-597. Nov. 1904.

21. Moses, Fred. Optimum structural design using linear programming. American Society of Civil Engineers Proceedings, Journal of the Structural Division 90, No. ST6: 89-104. Dec. 1964.

22. Neal, B. G. Structural theorems and their applications. New York, N.Y., The Macmillan Company. c1964.

23. Otto, Frei. Shells and membranes. In World Conference on Shell Structures. Publication No. 1187. Pp. 3-20. Washington, D.C., National Academy of Sciences-National Research Council. 1964.

24. Otto, Frei and Stromeyer, Peter. Pneumatic structures (Translated title). Deutsche Verlagsanstalt GmbH. July 1961: 518-527. 1961. Original not available; translated in American Institute of Architects Journal 37, No. 4: 101-111. April 1962.

25. Owen, J. B. B. The analysis and design of light structures. New York, N.Y., American Elsevier Publishing Company, Inc. 1965.

26. Parikh, Kirit S. and Norris, Charles H. Analysis of shells using framework analogy. In World Conference on Shell Structures. Publication No. 1187. Pp. 213-222. Washington, D.C., National Academy of Sciences-National Research Council. 1964.

27. Prager, William. Optimization of structural design. Presented at Symposium on Optimization, National Meeting, Society for Industrial and Applied Mathematics, June 11-14, 1968. U.S. Dept. Commerce, National Technical Information Service Report AD 716 136. 1968.

28. Romstad, K. M. and Wang, A. K. Optimum design of framed structures. American Society of Civil Engineers Proceedings, Journal of the Structural Division 94, No. ST12: 2817-2845. Dec. 1968.

29. Rozvani, George I. N. Optimum synthesis of prestressed structures. American Society of Civil Engineers Proceedings, Journal of the Structural Division 90, No. ST6: 189-211. Dec. 1964.

30. Schmit, Lucien A. Structural design by systematic synthesis. American Society of Civil Engineers, National Conference on Electronic Computation Proceedings, 2nd: 105-132. 1960.

31. Schmit, Lucien A. and Kicher, Thomas P. Synthesis of material and configuration selection. American Society of Civil Engineers Proceedings, Journal of the Structural Division 88, No. ST3: 79-102. June 1962.

32. Smith, Peter G. and Wilson, Edward L. Automatic design of shell structures. American Society of Civil Engineers Proceedings, Journal of the Structural Division 97, No. ST1: 191-201. Jan. 1971.

33. Soosaar, Keto. Optimization of topology and geometry of structural frames. Microfilm copy. Unpublished Ph.D. thesis. Cambridge, Massachusetts, Library, Massachusetts Institute of Technology. 1967.

34. Soosaar, Keto and Cornell, C. Allin. Optimization of topology and geometry of structural frames. (Abstract) American Society of Civil Engineers Joint Specialty Conference on Optimization and Nonlinear Problems, 18-20 April, 1968. Pp. 113-116. 1968.

35. Sposito, V. A. and Soults, D. J. AUKLET: Reference Manual. Iowa State University, Statistical Laboratory, Numerical Analysis-Programming Series, No. 6. 1968.

36. Templeman, A. B. A note on light structures of the Maxwell/Michell type. Institution of Civil Engineers Proceedings 35: 111-120. Sept. 1966.

37. Timoshenko, S. and Goodier, J. N. Theory of elasticity. 2nd ed. New York, N.Y., McGraw-Hill Book Company, Inc. 1951.

38. Timoshenko, S. and Woinowsky-Krieger, S. Theory of plates and shells. 2nd ed. New York, N.Y., McGraw-Hill Book Company, Inc. 1959.

39. Torroja, Eduardo. Philosophy of structures. English version by J. J. Polivka and Milos Polivka. Berkeley, California, University of California Press. 1958.

40. Wasiutynski, Zbigniew and Brandt, Andrzej. The present state of knowledge in the field of optimum design of structures. Applied Mechanics Reviews 16, No. 5: 341-350. May 1963.

41. Zetlin, Lev. Steel cable creates novel structural space systems. American Institute of Steel Construction, Engineering Journal 1, No. 1: 1-11. Jan. 1964.

ACKNOWLEDGEMENTS

The author is indebted to many others who assisted during the investigation and the writing of the dissertation. Dr. Ti-ta Lee, under whose guidance the work was carried out, provided continuous encouragement and valuable suggestions, among them, the form of the derivation of the theorem which appears in the appendix. Dr. Vince A. Sposito undertook the task of modifying and assembling the subroutines and programs used in the nonlinear programming solutions, and of modifying the constraint equations as necessary. The automatic data processing work was funded by the Department of Civil Engineering. Supplemental funds were provided by the Computation Center. The preparation and assembly of the master copy for reproduction of the manuscript was done by Joan Wicht, U.S. Army Engineer District, New York. Many thanks and unending appreciation goes to all the above, as well as to the writer's wife, Ann, for her devotion and understanding particularly during the period of the investigation.

APPENDIX - ALTERNATE DERIVATION OF THE THEOREM OF ZERO ABSOLUTE POTENTIAL ENERGY

The equations of equilibrium of a differential element of a structure (Fig. 3.1) are

$$\left.\begin{aligned} \frac{\partial \sigma_x}{\partial x} + \frac{\partial \tau_{xy}}{\partial y} + \frac{\partial \tau_{xz}}{\partial z} &= 0 \ , \\ \frac{\partial \sigma_y}{\partial y} + \frac{\partial \tau_{xy}}{\partial x} + \frac{\partial \tau_{yz}}{\partial z} &= 0 \ , \\ \text{and} \qquad \frac{\partial \sigma_z}{\partial z} + \frac{\partial \tau_{yz}}{\partial y} + \frac{\partial \tau_{xz}}{\partial x} &= 0 \ . \end{aligned}\right\} \tag{A.1}$$

Equations A.1 can be arbitrarily multiplied as follows,

$$\left.\begin{aligned} \int_z \int_y \int_x \left[\frac{\partial \sigma_x}{\partial x} + \frac{\partial \tau_{xy}}{\partial y} + \frac{\partial \tau_{xz}}{\partial z} \right] x \, dx \, dy \, dz &= 0 \ , \\ \int_z \int_y \int_x \left[\frac{\partial \sigma_y}{\partial y} + \frac{\partial \tau_{xy}}{\partial x} + \frac{\partial \tau_{yz}}{\partial z} \right] y \, dx \, dy \, dz &= 0 \ , \\ \text{and} \qquad \int_z \int_y \int_x \left[\frac{\partial \sigma_z}{\partial z} + \frac{\partial \tau_{yz}}{\partial y} + \frac{\partial \tau_{xz}}{\partial x} \right] z \, dx \, dy \, dz &= 0 \ , \end{aligned}\right\} \tag{A.2}$$

without altering their validity.

Each of the three equations A.2 results in the addition of three integrals of which the following expression is typical.

$$\int_z \int_y \int_x \frac{\partial \sigma_x}{\partial x} x \, dx \, dy \, dz + \int_z \int_y \int_x \frac{\partial \tau_{xy}}{\partial y} x \, dx \, dy \, dz + \int_z \int_y \int_x \frac{\partial \tau_{xz}}{\partial z} x \, dx \, dy \, dz = 0 \ . \tag{A.3}$$

In general, using integration by parts,

$$\int g'(x)\, k(x)\, dx = g(x)\, k(x) - \int g(x)\, k'(x)\, dx \quad . \tag{A.4}$$

The integrations indicated in equations A.2 will be carried out over the entire structure (or over the entire range of x, y and z in the structure) of which the element is a part.

Applying equation A.4 to the first term of equation A.3,

$$\iiint \frac{\partial \sigma_x}{\partial x}\, x\, dx\, dy\, dz = \iint [x\, \sigma_x] \Big|_{x_1}^{x_2} dy\, dz - \iiint \sigma_x dx\, dy\, dz \quad . \tag{A.5}$$

The second term of equation A.3 becomes,

$$\iiint \frac{\partial \tau_{xy}}{\partial y}\, dy\, x\, dx\, dz = \iint [\tau_{xy}] \Big|_{y_1}^{y_2} x\, dx\, dz - \iiint \tau_{xy}\, (0)\, x\, dx\, dy\, dz \quad . \tag{A.6}$$

Similarly, the third term of equation A.3 can be written as,

$$\iiint \frac{\partial \tau_{xz}}{\partial z}\, dz\, x\, dx\, dy = \iint [\tau_{xz}] \Big|_{z_1}^{z_2} x\, dx\, dy - \iiint \tau_{xz}\, (0)\, x\, dx\, dy\, dz \quad . \tag{A.7}$$

Thus, considering equations A.5, A.6 and A.7, equation A.3 becomes,

$$\iint [x\, \sigma_x] \Big|_{x_1}^{x_2} dy\, dz + \iint [\tau_{xy}] \Big|_{y_1}^{y_2} x\, dx\, dz + \iint [\tau_{xz}] \Big|_{z_1}^{z_2} x\, dx\, dy - \iiint \sigma_x \; dx\, dy\, dz = 0 \tag{A.8}$$

Similarly, the other two of equations A.2 would give rise to expressions,

$$\iint[y\ \sigma_y]\Big|_{y_1}^{y_2} dx\ dz + \iint[\tau_{xy}]\Big|_{x_1}^{x_2} y\ dy\ dz + \iint[\tau_{yz}]\Big|_{z_1}^{z_2} y\ dy\ dx - \iiint\sigma_y\ dx\ dy\ dz = 0\ , \tag{A.9}$$

and,

$$\iint[z\ \sigma_z]\Big|_{z_1}^{z_2} dx\ dy + \iint[\tau_{yz}]\Big|_{y_1}^{y_2} z\ dz\ dx + \iint[\tau_{xz}]\Big|_{x_1}^{x_2} z\ dz\ dy - \iiint\sigma_z\ dx\ dy\ dz = 0\ . \tag{A.10}$$

Note that in expression A.8 the double integration terms represent the sum of "magnitude of force component in x-direction multiplied by the x-coordinate of its point of application" for all external boundary forces. Defining this sum by $\sum_i X_i\ x_i$, the expression A.8 can be rewritten as,

$$\sum_i X_i\ x_i - \int_V \sigma_x\ dV = 0\ . \tag{A.11}$$

Similarly, from expressions A.9 and A.10,

$$\sum_i Y_i\ y_i - \int_V \sigma_y\ dV = 0\ , \tag{A.12}$$

and,

$$\sum_i Z_i\ z_i - \int_V \sigma_z\ dV = 0\ . \tag{A.13}$$

Although equations A.11, A.12 and A.13 could be useful in some cases, it is more useful, for the purposes at hand, to add them to yield,

$$\int_V \sigma_x\ dV + \int_V \sigma_y\ dV + \int_V \sigma_y\ dV = \sum_i X_i\ x_i + \sum_i Y_i\ y_i + \sum_i Z_i\ z_i \tag{A.14}$$

An arbitrarily oriented boundary force could have x, y and z components present in three terms of the right hand side of equation A.14. The right hand side could be expressed in the statically equivalent form

$\sum \bar{F}_i . \bar{r}_i$ where $\bar{F}_i$ is the force vector at point i, and $\bar{r}_i$ is its respective position vector. Then, equation A.14 can be expressed as,

$$\int \sigma_x \, dV + \int \sigma_y \, dV + \int \sigma_z \, dV = \sum_i \bar{F}_i . \bar{r}_i \qquad (A.15)$$

In equations A.1 body forces were assumed to be zero for clarity. If body forces are present, the terms to be added to equations A.8, A.9 and A.10 would be, respectively,

$$\iiint \bar{X} \, x \, dx \, dy \, dz \quad ,$$

$$\iiint \bar{Y} \, y \, dx \, dy \, dz \quad ,$$

and $$\iiint \bar{Z} \, z \, dx \, dy \, dz \quad ,$$

where $\bar{X}$, $\bar{Y}$ and $\bar{Z}$ are the body forces per unit volume in the x, y and z directions, respectively. These terms are directly analogous to those of the boundary forces to which they could be added. Thus, the right hand side of equation A.15, $\sum \bar{F}_i . \bar{r}_i$, must include the contributions of the body forces if they are present.

Equation A.15, identical to equation 2.10, is a mathematical expression of the theorem of zero absolute potential energy.